How to cite: *Angew. Chem. Int. Ed.* **2023,** *62,* e202218000
International Edition: doi.org/10.1002/anie.202218000
German Edition: doi.org/10.1002/ange.202218000

Metals in Medicine

Gold Complexes in Anticancer Therapy: From New Design Principles to Particle-Based Delivery Systems

Guillermo Moreno-Alcántar, Pierre Picchetti,* and Angela Casini**

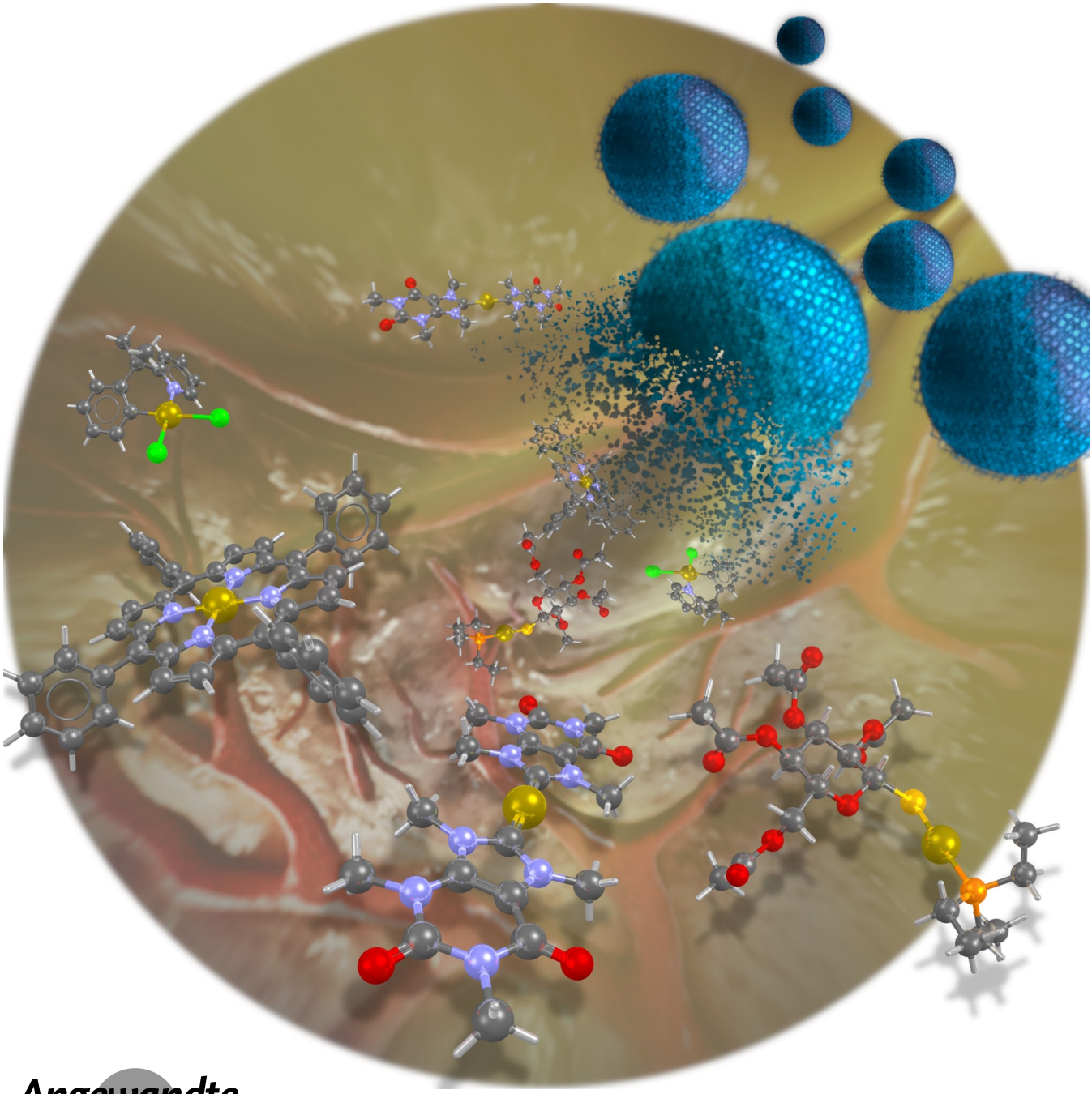

Abstract: The discovery of the medicinal properties of gold complexes has fuelled the design and synthesis of new anticancer metallodrugs, which have received special attention due to their unique modes of action. Current research in the development of gold compounds with therapeutic properties is predominantly focused on the molecular design of drug leads with superior pharmacological activities, e.g., by introducing targeting features. Moreover, intensive research aims at improving the physicochemical properties of gold compounds, such as chemical stability and solubility in the physiological environment. In this regard, the encapsulation of gold compounds in nanocarriers or their chemical grafting onto targeted delivery vectors could lead to new nanomedicines that eventually reach clinical applications. Herein, we provide an overview of the state-of-the-art progress of gold anticancer compounds, andmore importantly we thoroughly revise the development of nanoparticle-based delivery systems for gold chemotherapeutics.

1. Introduction

Cancer is one of the leading causes of death worldwide, besides other chronic non-communicable diseases, such as cardiovascular or respiratory diseases.[1] The number of cancer cases worldwide is expected to increase rapidly, first due to an increasingly ageing population,[2] and second due to new socioeconomically dependent lifestyles, which are associated with a higher incidence of cancer.[3] Therefore, the prevention and treatment of cancer is a leading priority pursued by the World Health Organization (WHO).[4]

Among the anticancer chemotherapeutic agents, small organic molecules and biologics predominate, but the use of transition metal-based drugs has proven to be very effective. For instance, cisplatin and related platinum-based chemotherapeutics are used to treat a variety of cancers.[5,6] However, platinum complexes cause severe side effects such as nephrotoxicity, neurotoxicity, gastrointestinal toxicity, peripheral neuropathy, ototoxicity, asthenia, and hematologic toxicity, which limits their therapeutic efficacy.[7,8] Moreover, the development of platinum resistance in cancer represents a central problem and results in poor prognosis due to the lack of alternative treatments.[9,10] Therefore, research into new chemotherapeutic agents based on transition metals, such as ruthenium- or osmium-based metal complexes, has attracted considerable interest.[11–14]

Gold-based compounds have demonstrated promising potential for the design of new chemotherapeutic agents.[15–20] Historically, the use of gold complexes for the treatment of disease arose from the observation that dicyanoaurate(I) potassium salts, originally proposed by Robert Koch for the treatment of tuberculosis, exhibited instead anti-inflammatory effect.[21] Since then gold-based anti-arthritic therapeutics, such as aurothiomalate, aurothioglucose, and auranofin (AF), to mention the most prominent examples, have received FDA approval (Figure 1).[22] In addition to anti-inflammatory activity, gold compounds show acute toxicity to cells and even platinum-resistant cancer cell lines *in vitro*. One of the major reasons hindering the current FDA approval of Au^{I}- and Au^{III}-based compounds for the treatment of cancer is their limited solubility and chemical stability in the physiological milieu - responsible not only for reduced cytotoxic activity but also for the undesirable accumulation of the heavy metal in vital organs. While in some cases the so-called *speciation* of cytotoxic Au^{I}/Au^{III} compounds is responsible for their bioactivity, in most cases this phenomenon not only results in rapid ligand exchange reactions with biological nucleophiles but, especially for Au^{III} complexes, favours the reduction to Au^{I} or

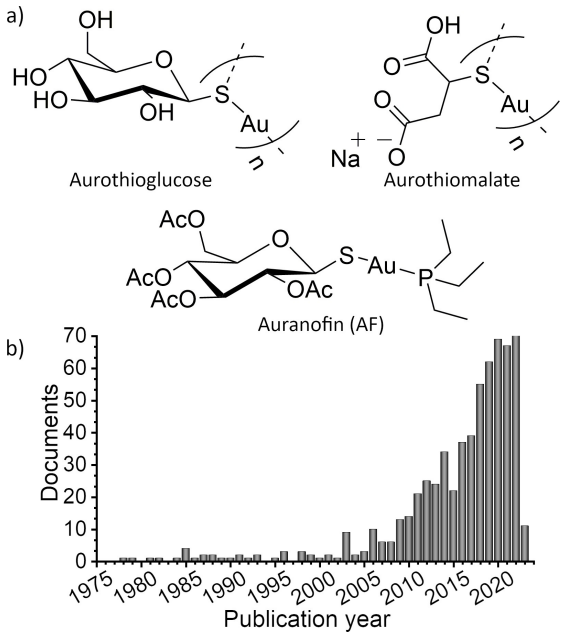

Figure 1. a) Chemical structure of antiarthritic Au^{I}-based compounds. b) Trend in the number of publications indexed in Scopus on cancer-inhibiting gold compounds from 1975 to 2023 ($n = 636$).

[*] Dr. G. Moreno-Alcántar, Prof. Dr. A. Casini
Chair of Medicinal and Bioinorganic Chemistry, School of Natural Sciences, Department of Chemistry, Technical University of Munich (TUM)
Lichtenbergstr. 4, 85748 Garching b. München (Germany)
E-mail: g.moreno-alcantar@tum.de
angela.casini@tum.de
Dr. P. Picchetti
Karlsruhe Institute of Technology (KIT), Institute of Nanotechnology
Hermann-von-Helmholtz-Platz 1, 76344 Eggenstein-Leopoldshafen (Germany)
E-mail: pierre.picchetti@kit.edu

Au^0,[23] resulting in loss of activity and possible side-effects, arising from the release of either the free ligands or the metal. Therefore, for gold compounds to be viable in cancer treatment, nano-formulation strategies may be essential to improve delivery and stability problems.

The advent of nanomedicine,[24,25] which by definition applies the tools and knowledge of nanotechnology to medicine, such as the use of nanoparticles (NPs) for drug delivery and/or imaging applications, has led to the development of innovative therapies. This has recently been impressively demonstrated by the approval of the liposomal-based drug Onpattro[26] or the recently approved anti-SARS-CoV-2 mRNA vaccines.[27] NPs are defined as having at least one of their external dimensions in the range of 1 to 100 nm.[28,29] Many authors, especially in the field of nanomedicine, often extend the term "nanoparticle" to particles bigger than 100 nm, provided that novel biological or physicochemical properties are observed that are otherwise not obtained from the bulk material.[30] Approval of transition metal-based nanomedicines for the treatment of cancer by the FDA and EMA is still pending – a fact that is in striking contrast to other approved non-metal-based nanomedicines (e.g., drug delivery systems based on doxorubicin, vincristine, irinotecan, or paclitaxel).[31–35] Transition metal-based nanomedicines for the treatment of cancer that are currently in clinical trials are limited to liposomal or polymeric formulations of cisplatin (lipoplatin and stealth cisplatin).[36–38]

The development of gold-based nanomedicines can be based on a variety of different NPs, but to make real progress, it is important to consider the lessons of the past. For example, the NPs themselves and their components must be biocompatible, and their toxicological profiles must be evaluated to avoid otherwise predictable pitfalls. In this context, we would like to refer to the recently published critical assessment by the Nanotechnology Characterization Laboratory (NCL),[39] which lists typical challenges faced by newly researched NPs for use in biomedical applications.

In 2014 Che and co-workers[40] summarized the few examples available in the literature dealing with particle-based delivery systems for gold compounds. Since then, much progress has been made in developing particle-based delivery for anticancer treatment using gold compounds. Both supramolecular encapsulation and chemical tethering strategies have been used to load nanomaterials with gold compounds, and both strategies are reviewed and critically discussed here. The use of Au^0 nanoclusters or NPs for cancer therapy/imaging is beyond the scope of this review, and we refer the reader to other literature reviews on this topic.[41–49]

To provide an overview of the state-of-the-art of gold-based anticancer compounds, as well as currently available particle-based delivery systems, we first recapitulate the main chemical and biological properties of this class of compounds in Section 2. In Section 3, we review the types of micro- and nanoparticles that have been investigated for the delivery of gold compounds for cancer therapy and discuss their main advantages and disadvantages. We hope that the reader will find the overview provided here an incentive to

Guillermo Moreno-Alcántar completed his PhD at Universidad Nacional Autónoma de México (UNAM), Mexico, in 2018 under the supervision of Prof. Hugo Torrens. From 2018 to 2020 he was a postdoctoral fellow at the University of Strasbourg, where he studied the control of self-assembly processes of luminescent coordination compounds. Since 2021, he is a Research Fellow of the Alexander von Humboldt Foundation at the Technical University of Munich (TUM). His current research is focused on the development of smart materials based on supramolecular coordination complexes containing gold for biomedical applications.

Pierre Picchetti completed his PhD in chemistry in 2020 at the University of Strasbourg under the supervision of Prof. Luisa De Cola, with a focus on functional and photonic materials. He is currently a postdoctoral fellow in the group of Dr. Frank Biedermann at the Institute of Nanotechnology (INT) at the Karlsruhe Institute of Technology (KIT) in Germany. His research interests include supramolecular chemistry and materials chemistry with a special focus on smart (nano)materials for biomedical applications.

Angela Casini is Chair of Medicinal and Bioinorganic Chemistry and Liesel Beckmann Distinguished professor at the Technical University of Munich (TUM) since 2019. Her research interests are in Medicinal Inorganic and Bioinorganic Chemistry. Specifically, she focuses on the study of the role of metal ions in biological systems and of the mechanisms of action of organometallic anticancer agents, as well as on novel applications for metal-based compounds and supramolecular coordination complexes/materials in various domains of chemical biology, drug delivery, and medicine.

undertake much-needed work in the development of better metallodrug delivery systems for nanomedicine.

2. Gold Complexes as Anticancer Agents

Gold compounds have received much attention for biomedical applications since the FDA approval of aurothiomalate, aurothioglucose, and AF for the treatment of arthritis in the 1980s (Figure 1).[12,16,17,50–55] In this regard, the anticancer properties and applications of coordination or organometallic gold compounds of phosphines,[56] dithiocarbamates,[57–59] cyclometalates,[60] porphyrins,[61] N-heterocyclic carbenes (NHCs),[61–66] alkynyls,[67] Schiff bases,[68] arenes,[69] and biologically relevant molecules[70,71] have been reviewed.[72]

In addition, detailed up-to-date literature reviews regarding the mechanisms underlying the anticancer activity of gold complexes are available.[19,72–80] Therefore, this section is not intended to be a comprehensive summary of these topics, but rather a general overview of the most important aspects of the medicinal chemistry of anticancer gold compounds, their chemical properties, and mechanisms of action.

The most common oxidation states of gold at standard conditions, besides Au^0, are $1+$ and $3+$. Au^I has a closed-shell $[Xe]4f^{14}5d^{10}$ electron configuration and its complexes are characterized by a predominant coordination number of 2 and a linear geometry due to the relativistic contraction of valence orbitals.[81,82] Further oxidation to Au^{III} is possible giving the $[Xe]4f^{14}5d^8$ configuration, which is isoelectronic to that of Pt^{II}. Therefore, it is not surprising that Au^{III} complexes have a square-planar coordination geometry. Moreover, auric derivatives display a strong oxidant character due to the higher oxidation state and enhanced electronegativity of the Au^{III} centre.[82] An important aspect when considering the different chemistry of gold complexes is that Au^I is *soft* and Au^{III} centres are *hard* Lewis acids according to Pearson's acid-base concept.[82,83] The relevance of these differences for the bioactivity of the various families of gold compounds will be discussed in the next sections.

Most of the known active gold compounds have been found to induce apoptosis via protein-targeting pathways. However, some remarkable examples of gold complexes that bind DNA targets have also been discovered in recent times. In the next sections, some of the main molecular targets for gold-based chemotherapeutics are introduced.

2.1. Mode of Action (MoA)

2.1.1. Gold(I) Complexes

The anticancer activity of AF[22,84,85] and the potent *in vitro* cytotoxic properties of numerous Au^I phosphine- and thiolate-related coordination complexes are often not observed *in vivo*.[8] This is mainly due to the prompt ligand substitution by intracellular nucleophiles, including cysteine thiolates, which are abundant in serum proteins, and within cells.[23] Further, in many cases Au^I is reduced to Au^0, resulting in the deactivation of the pharmacological activity. To increase the stability of Au^I compounds in biological media ligands that harvest the stability of gold by sulfur coordination, such as thioureas[86–88] or dithiocarbamates[89] have gained much attention for use in anticancer therapy.

Numerous studies have revealed that the MoA of linear Au^I coordination compounds is often driven by their binding to the catalytic centres of disulfide reductases.[90] In fact, Au^I compounds have a high affinity for thiol and selenol moieties present in these enzymes. Amongst the reductase enzymes, thioredoxin reductases (TrxRs) are essential to maintain redox homeostasis in cells. In particular, TrxRs mediate the reduction of thioredoxins (Trx) by NADPH (reduced nicotinamide adenine dinucleotide phosphate). Mammals have three types of TrxRs: the cytosolic (TrxR1, Figure 2a), the mitochondrial (TrxR2) and the hybrid Trx-glutathione reductase (TrxR3 or TGR).[91] The affinity of Au^I complexes for binding to TrxRs is well known, and crystal structures of TrxR-Au complexes have been reported.[73,90,92] The active sites of TrxR1 consist of a redox-active selenocysteine residue (Sec-498) in a ligand-accessible region that allows Trx binding (Figure 2b). Au^I centres, which are soft acids, can reach this region of TrxR, resulting in strong binding to selenolate (a soft base) and displacement of a ligand from the gold compound. The so-formed gold-selenide complex cannot function as a disulfide redox-active centre and the enzyme's activity is lost. Inhibition of TrxR leads to an increase in the concentration of oxidants, particularly reactive oxygen species (ROS) in the cell lumen, causing oxidative stress and inducing apoptosis. Many Au^I compounds that tend to undergo ligand exchange reactions have shown TrxR inhibition properties,[73,84,93–95] and AF, in particular, is known to be a potent inhibitor of human TrxR2.[96] In this way, Au^I compounds affect the redox activity of the mitochondria increasing the likelihood of induction of oxidative stress and membrane pore transition (MPT), eventually leading to cell death.[73,97] Recent advances in Au^I TrxRs inhibitors include, for example, the study of polymetallic systems,[98,99] or the hybridization with photoactive[100,101] or targeting moieties.[102,103]

The chemical structure of the ligands used is relevant to the pharmacological activity of Au^I coordination compounds, as the MoA is often associated with ligand displacement reactions, as well as non-covalent interactions established by the compounds with their targets along with (or alternatively to) coordinative adduct formation. Moreover, the balance between the kinetics of ligand substitution with target proteins (i.e., reductases, membrane proteins, transcription factors, etc.) and the stability required to avoid serum protein-mediated deactivation is an important aspect that has to be considered when designing new Au^I compounds.[93]

Although trigonal coordination is not the most common in Au^I compounds, recently such complexes have been used in the development of anticancer agents, showing important differences compared to linear compounds. Mertens et al. have studied the effect of the modification of the picnogenic ligand (phosphine or arsine) on the activity of a family of N^N (bipyridine or phenanthroline) chelated Au^I com-

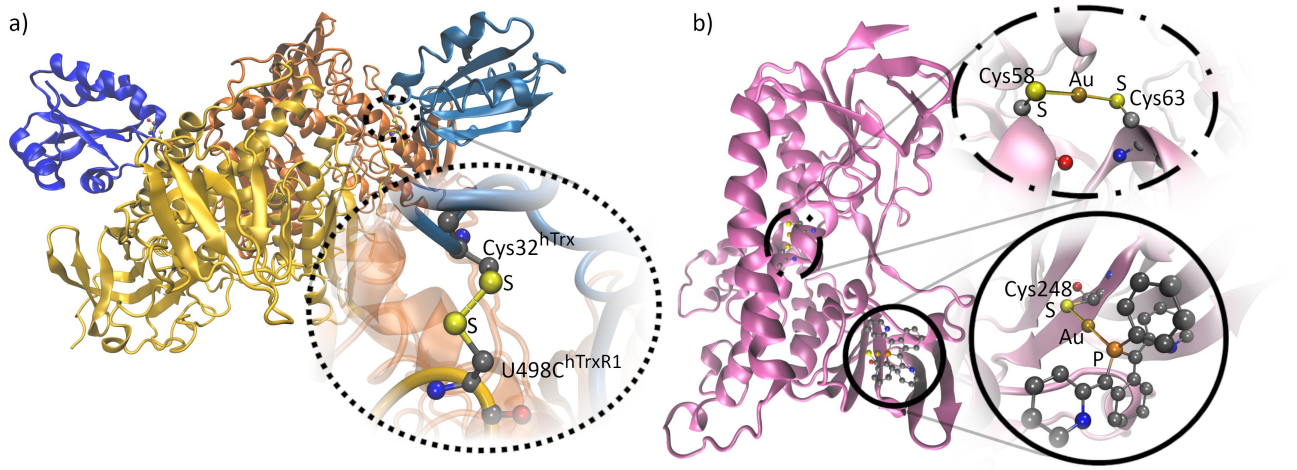

Figure 2. a) Crystal structure of the human homodimeric TrxR1 (yellow/orange)-Trx (blue) complex. The inset shows the Se(S)–S bond formed during Trx reduction. The interacting Sec-498 (U498C) in TrxR is the exposed target site proposed for Au^{I} compounds (to enable the isolation of the reactive intermediate, a hybrid TrxR was used in which Sec-498 was replaced by Cys, labelled as -U498C-, PDB code 3QFA).[91] b) Crystal structure of the binding sites of LAu(I) (L = 2,2′-(2-phenyl-4,5,6,7-tetrahydro-2H-isophosphindole-1,3-diyl)dipyridine) with glutathione reductase (PDB 2AAQ). The insets show the S_{Cys58}-Au-S_{Cys63} (top) and L-Au-S_{Cys248} (bottom).[90] The images were generated using the VMD software.[313] Colour code for the explicit atoms: C, grey; N, blue; O, red; P, orange; S, yellow; Au, golden. Hydrogen atoms, water molecules, and additional ligands present in the structures have been omitted for clarity.

pounds (Figure 3a).[104] An initial assessment of the toxicity of ten compounds showed promising efficacy against the triple negative breast cancer (TNBC) cell line MDA-MB-231, with three derivatives being superior to cisplatin and AF and selective for cancerous cells.[104] Proteomic studies suggest that the lead compound [Au(PhPhen)(Sphos)]SbF_6 (**AuTri-9**, PhPhen = 4,7-diphenyl-1,10-phenanthroline, and Sphos = 2-dicyclohexylphosphino-2′,6′-dimethoxybiphenyl) disrupts the mitochondria. Indeed, transmission electron microscopy (TEM, Figure 3b) shows pronounced rupture of mitochondrial membranes and fragmentation of cristae. In addition, a preliminary *in vivo* evaluation in mice showed that the compound was well tolerated in the short term, with no noticeable change in body weight or behaviour, suggesting good biocompatibility.[104]

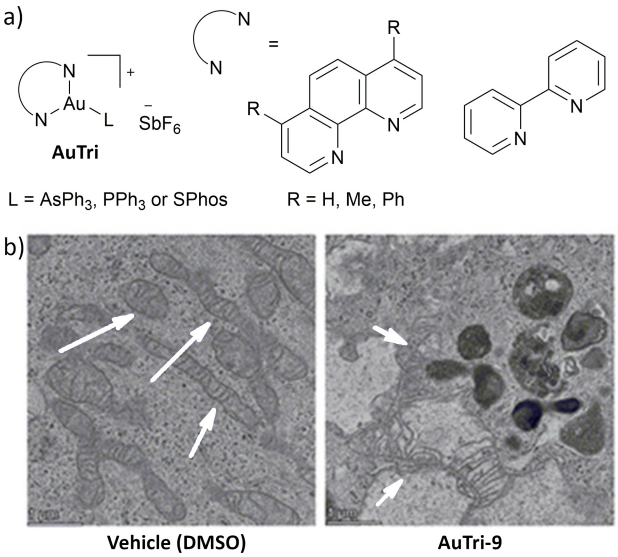

Figure 3. a) Chemical structures of tricoordinate Au^{I} compounds that disrupt the mitochondrial structure.[104] b) Electron microscopy images showing mitochondrial damage in MDA-MB-231 cells treated with **AuTri-9** (10 μM). Healthy mitochondria are pointed by arrows in the control DMSO (1%) treated cells. Arrows show the fragmented cristae in the compound treated cells. Panel b) was adapted from ref. [104]. CC-BY-NC-ND the authors 2021, published by American Chemical Society.

To stabilize the Au^{I} centre against reduction, N-heterocyclic carbenes (NHCs) are among the most suitable ligands due to their pronounced σ-donor character, providing stable Au–C bonds.[61–64,66,105] The anticancer activity of NHC Au^{I} compounds was first reported in 2004 by the group of Berners-Price and Day[106] when testing the mitochondrial swelling capabilities of a series of bis-NHC Au^{I} derivatives. This initial discovery, combined with the relative ease of functionalization of NHCs, prompted more research into this type of organometallics.[107] For example, by combining NHC and phosphane ligands, Che and co-workers reported on dinuclear Au^{I} complexes featuring not only important anticancer effects *in vivo* but also anti-angiogenesis effects in tumour models and inhibition of sphere formation of cancer stem cells *in vitro*. Via the judicious combination of the aforementioned ligands, the dinuclear complex displayed favourable stability in the presence of blood thiols, which did not prevent its inhibition of TrxR.[108]

An important task for chemists in gold drug development is to design strategies for the post-synthetic functionalization of hit compounds, e.g., to optimize their lipophilicity or to conjugate them with targeting or imaging components. For instance, Arambula, Sessler, and co-workers introduced the use of alcohol-to-carbonate[109] and alcohol-to-carbamate[110] functionalization of heteroleptic bis-NHC Au^{I}

complexes (Supporting Information, Scheme S1). For example, heteroleptic bis-NHC–Au^{I} complexes featuring a fluorescent naphthalimide ancillary ligand were cytotoxic ($IC_{50}=72\pm4$ nM in A549 lung cancer cells), and their cellular uptake was followed by fluorescence microscopy. The same compound was shown to interact also with bovine serum albumin (BSA) without being deactivated, resulting in a water-soluble and active formulation ($IC_{50}=59\pm3$ nM in the same cell line). The latter example again demonstrated how ligand design can significantly contribute to improved pharmacological properties (i.e., aqueous solubility with simultaneous biological activity).

Within this framework, NHC ligand design has taken several directions and has proven to be important for fine-tuning the activity, mechanism, and selectivity of gold compounds.[111] For example, modification of the aryl group substituents in 4,5-diarylimidazole-based ligands is a suitable strategy to modulate the activity of the resulting NHC–Au^{I} compounds, as shown by the change in cytotoxicity against MCF-7 breast cancer cells (IC_{50} ca. 2.8 μM) by the 4-H derivative (Figure 4a).[112] Kühn and collaborators[113] showed that even small changes such as conformational isomerism can have important effects on compound activity. For the *syn/anti* isomers of dinuclear NHC compounds that were studied (Figure 4b), a 10-fold increase in TrxR inhibitory activity was reported when the *anti* isomer ($IC_{50}=14$ nM) was used when compared to the *syn* derivative ($IC_{50}=146$ nM). This activity was associated with the lack of reactivity of the *syn* isomer with cysteine, which was explained by density functional theory (DFT) simulations showing that this conformation prevents nucleophilic attack on the gold centre by the cysteine thiols (Figure 4c).[113] To improve water solubility, Jakob et al.[114] reported bis-NHC–Au^{I} complexes derived from histidine that were synthesized with different end groups (ester, acid, amide), and their cellular uptake and distribution were studied in PC-3 prostate adenocarcinoma cells. The results show that although the benzyl ester and benzyl amide derivatives feature similar Au uptake, they differ in their intracellular distribution. For instance, proton-induced X-ray emission showed negligible retention of gold within the cells treated with the ester, indicating that it acts mainly by binding to the cell membrane. On the other hand, Au was localized within the cells when the amide compound was used. This structure-dependent behaviour can be further exploited for targeting purposes (Scheme S2a).[114]

A prominent strategy to prepare biologically active organometallic compounds is to use ligands of biomolecules or compounds that also have known pharmacological activity that can be potentiated by the inclusion of the metal.[71] Recently, the structure of lepidilin A, a bioactive alkaloid from maca root, was also taken as inspiration for the design of NHC ligands for gold complexes.[115] The effects of various ancillary ligands—acetylides, phosphines, halogens and even double NHC coordination to Au^{I}—were evaluated and showed that the cationic bis-NHC complexes were the most active compounds from the series achieving submicromolar IC_{50}-value *in vitro*.[115]

Immunogenic cell death (ICD) was first reported in 2005 by Casares, Kroemer, et al. as a strategy for the treatment of cancer and consists of reactivating the immune response against tumour cells.[116] In general, chemotherapy has

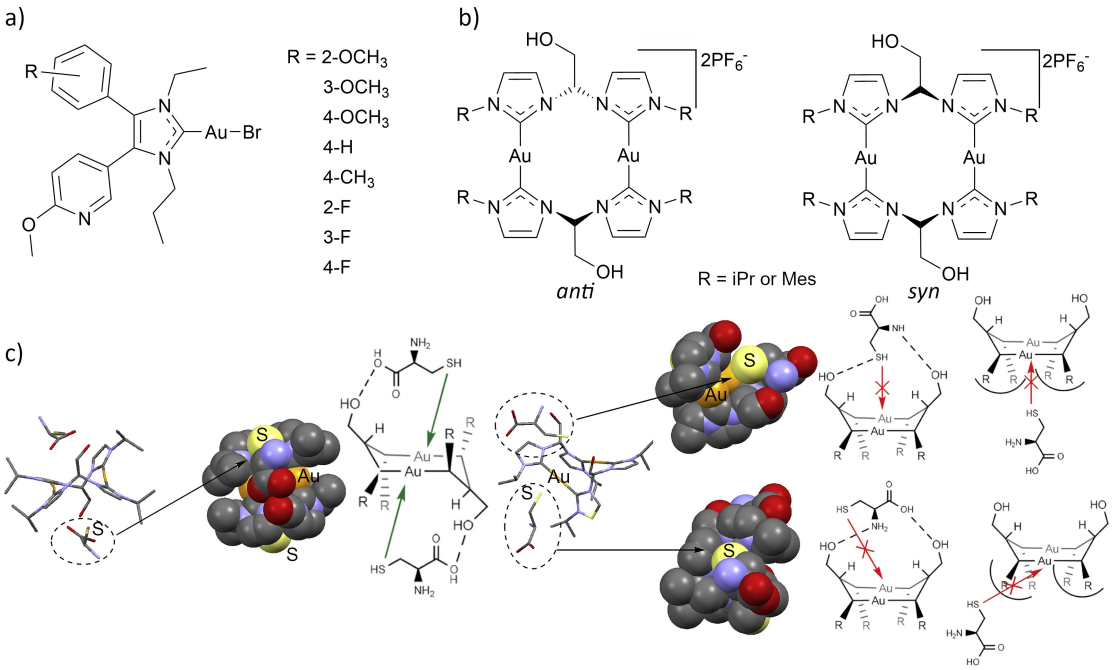

Figure 4. a) Chemical structure of phenyl substituted NHC–Au compounds .[112] b) *Anti*- and *syn*-NHC Au^{I} derivatives that exhibit different TrxR inhibitory activity .[113] c) DFT simulation of the possible interaction of cysteine thiol with the gold centre in the *anti* isomer of the compound (left) and the excluded interactions of Cys with the *syn*-isomer (right). Panel c) was adapted from ref. [113] Copyright 2020, with permission from Elsevier.

immunosuppressive effects and few anticancer drugs have been shown to induce ICD.[117] Very recently, the activity of NHC–Au^{I} compounds as ICD inducers has been described by the group led by Cui, Arambula, and Sessler.[118] In their work, a redox-active naphthoquinone NHC complex (Figure 5a) generates endoplasmic reticulum stress by generating ROS – all prerequisites for the induction of ICD. In detail, the Au^{I} NHC complex has sub-micromolar IC_{50} values *in vitro* against A549, CT116, and CT26 cell lines.[118] *In vivo* tumour depletion by ICD was tested by subcutaneous injection of the Au^{I} NHC complex in the right flank of syngeneic immunocompetent mice (BALB/c) with CT26 cells previously treated ex vivo with the drug or with oxaliplatin as a positive ICD induction control.[118] After 7 days, the left flank was challenged with tumourigenic functional CT26 cells (Figure 5c). It was found that the gold-based treatment successfully reduced tumour growth and was more effective (anti-tumour activity was observed at lower doses) than the same treatment with oxaliplatin (Figure 5b).[118]

Although NHCs dominate the carbene-type ligands used in Au^{I} anticancer compounds, Proetto et al.[119] have very recently introduced the use of cyclic (alkyl)(amino)carbenes (CAACs) in gold-based chemotherapeutics. These ligands are stronger σ-donors and have a more pronounced π-acceptor character than the NHCs. Promisingly, these different electronic features reduce nonspecific binding to non-cancer-related proteins such as BSA (55 ± 10 % binding vs. 79 6 % for AF) while maintaining a strong affinity for TrxR, showing $IC_{50} = 0.9 \pm 0.1$ μM vs. 0.015 ± 5 μM for AF in rat TrxR inhibition.[119] For comparison, a structurally related NHC-gold compound (Scheme S2b) has an IC_{50} of over 50 μM vs. HeLa,[120] while the CAAC equivalent has an $IC_{50} = 0.6$ μM,[119] which highlights the advantage of this type of compound over the related NHCs.

In addition to carbenes, the formation of stable Au–C bonds involving alkynyls is possible. The first report on the anticancer activity of Au^{I} alkynyls was published in 2009 by Wong and collaborators.[121] The relative ease of incorporating terminal alkynes into chemical structures has encouraged the use of acetylide ligands in the search for new anticancer complexes. Among the latest advances in this direction, Erlotinib, a commonly used and approved anticancer drug, bears a terminal alkyne that was used by Ruiz's group to coordinate triphenylphosphine Au^{I}, resulting in a 68-fold increase in toxicity compared with the original Erlotinib.[122] In this case, the MoA of the Au^{I}-Erlotinib conjugate was not relying on the typical EGFR tyrosine kinase inhibition but involved multiple pathways, including the increase in ROS production, mitochondrial dysfunction, and DNA

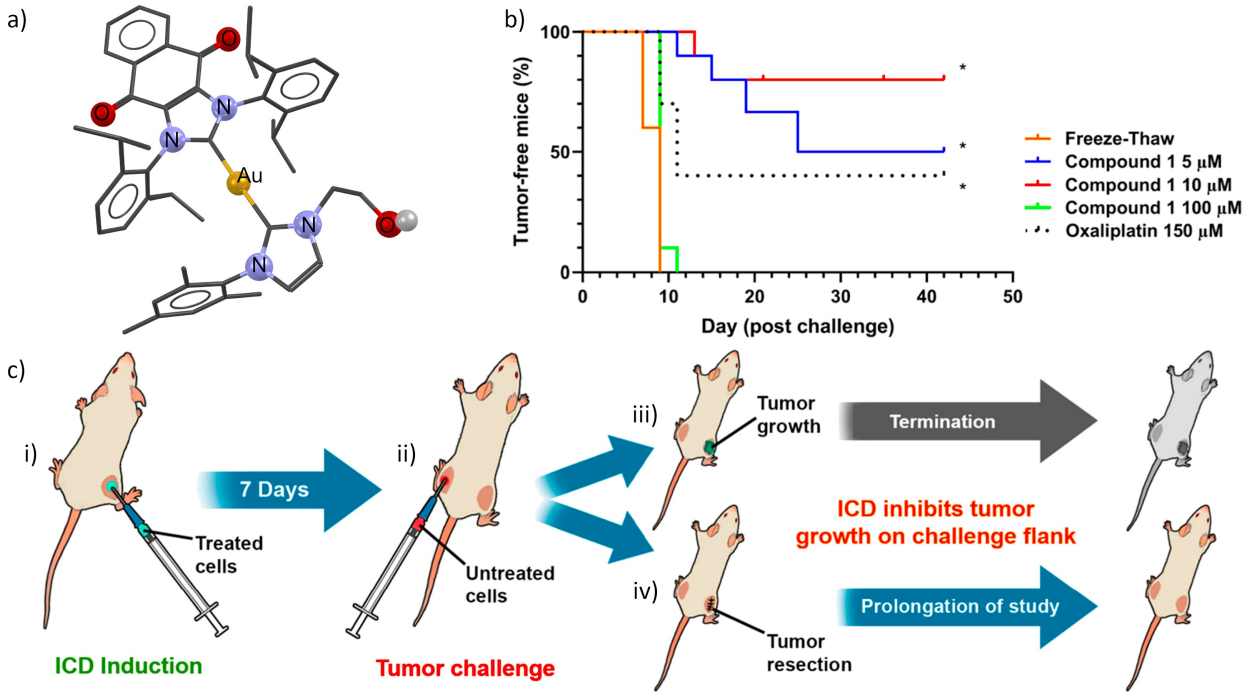

Figure 5. a) Single-crystal molecular structure of the naphthoquinone-containing bis-NHC Au^{I} compound studied as an ICD inducer.[118] The image was generated with Mercury.[314] Colour code: C, grey; N, blue; O, red; H, white; Au, golden. C-based hydrogen atoms and the chloride counterion are omitted for clarity (CCDC 1951804). b) Tumour development in the challenged side on the mice model stimulated previously with cancer cells that have been treated with the gold ICD-inducer.[118] c) Experimental design followed for the testing of ICD activity: i) BALB/c mice were subcutaneously injected on the right flank with CT26 cells that were pre-treated with varying concentrations (5, 10, or 100 μM) of the bis-NHC Au^{I}. Untreated CT26 cells subjected to three freeze-thaw cycles to induce necrosis were injected as a negative control. ii) Seven days later, the mice were challenged subcutaneously in the left flank with lCT26 cells, and the tumour growth was monitored on tis flank. iii) In some cases, tumour development is observed in the right flank, forcing the premature termination of the experiment.[118] iv) Depicted is an alternative strategy which includes the right-flank tumour resection to allow the long-term observation of the left-flank. Adapted with permission from ref. [118]. copyright 2020 American Chemical Society.

damage. In another work, Humphrey and co-workers synthesized gold-alkynyl complexes with phenanthrene units. These complexes show moderate cytotoxicity against several cancer cell lines *in vitro*, similar to that of cisplatin.[123] Furthermore, in silico studies suggested the potential binding of these complexes to DNA.[123]

Thang's group has reported an interesting system that combines the anticarcinogenic activity of a pentafluorophenyl Au^{I} complex with an aggregation-induced emission chromophore (TBP, Figure 6) that also acts as a sensitizer for photodynamic therapy (PDT).[124] By using the **TBP-Au** system, it is possible to take advantage of the simultaneous generation of ROS by PDT and the suppression of the antioxidant mechanisms to kill cancer cells. **TBP-Au** showed concentration-dependent TrxR inhibition, which was not shown by TBP alone. Furthermore, **TBP-Au** features preferential lysosome over lipid droplet localization, which is also desired for effective PDT. With the synergistic effect from PDT and the chemotherapeutic effect of the gold compound, TBP-Au showed good tumour ablation in xenografts carrying the HeLa tumour subcutaneously compared with different control groups.[124] This multifunctional approach has shown great promise for the design of organometallic gold compounds given the rich synergy between AIE-based imaging, PDT, and gold chemotherapeutic agents.

2.1.2. Gold(III) Complexes

As mentioned earlier, Au^{3+} ions are not stable under physiological conditions and the use of chelating ligands is required. Diverse chelated Au^{III} compounds are under investigation to be used as potential anticancer drugs, including bidentate ligands as dithiolates,[125,126] dithiocarbamates,[127] diamines,[128,129] or diphosphines.[56] Moreover, the use of tri- and tetra-dentated ligands as Schiff bases,[68] pincer ligands,[130] and porphyrins[61] have shown promising results, in some cases uncovering unexpected and diverse mechanisms of action. Similarly, Au^{III} corroles have been studied and found to be cytotoxic and cytostatic to cisplatin-resistant cancer cell lines.[131]

Many Au^{III} anticancer agents act mainly as prodrugs that, in physiological conditions, undergo redox reactions to form active Au^{I} compounds. However, in 2006, Messori and collaborators[132] reported a family of bipyridyl Au^{III} dinuclear oxo complexes (Auoxo) from which **Auoxo6** ($[Au_2(\mu\text{-}O)_2(6,6'\text{-dimethyl-}2,2'\text{-bipyridine})_2]^{2+}$, Figure 7a) showed the most promising properties.[132] Further studies have shown that these compounds present complex mechanisms of action that may involve concomitantly i) the oxidant character of the compounds, ii) the formation of Au^{I} adducts, and iii) the liberation of pyridyl ligands. Yet, the targets of these compounds are only partially known and involve, among others, the histone acetylase, and the protein kinase C.[133]

Inspired by the potential of dithiocarbamates as inhibitors of cisplatin-induced nephrotoxicity, the group of Fregona[134] developed a family of Au^{III} dithiocarbamates that display promising anticancer activity. The chelating effect displayed by these type of ligands prevents nonspecific ligand substitution, avoiding deactivation and increasing the effective cytotoxicity.[135,136] These compounds have been shown to inhibit TrxR as well as the UB proteasome activity.[135–137] In particular, **AuL12** (Figure 7a) is one of the

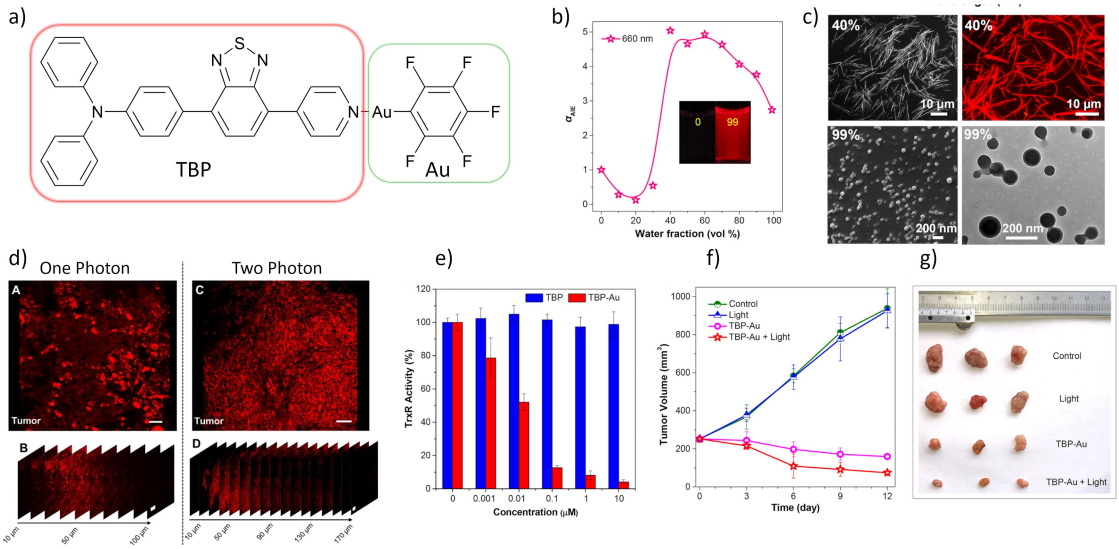

Figure 6. a) Chemical structure of **TBP-Au**. b) Plot of the increase in emission intensity at 660 nm for TBP-Au as a function of water content (%w): the addition of water causes aggregation and increased emission at 99% water content. c) Morphology, as observed in electron microscopy and emission microscopy, of aggregates of **TBP-Au** formed at 40%w (fibres) and 99%w (spheres). d) Confocal microscopy single-photon image (A, $\lambda_{ex}=488$ nm) and two-photon (C, $\lambda_{ex}=870$ nm) of ex vivo tumour tissue stained with **TBP-Au** showing penetration (B, D) through Z-stack images (ca.100 and 170 μm, respectively). e) *In vitro* TrxR inhibition by **TBP-Au**. f) Plot showing *in vivo* tumour depletion as a result of simultaneous photothermal and cytotoxic activity of **TBP-Au**. g) Reduction in tumour size observed after combined photothermal treatment with administration of TBP-Au. Adapted with permission from ref. [124] copyright 2021 American Chemical Society.

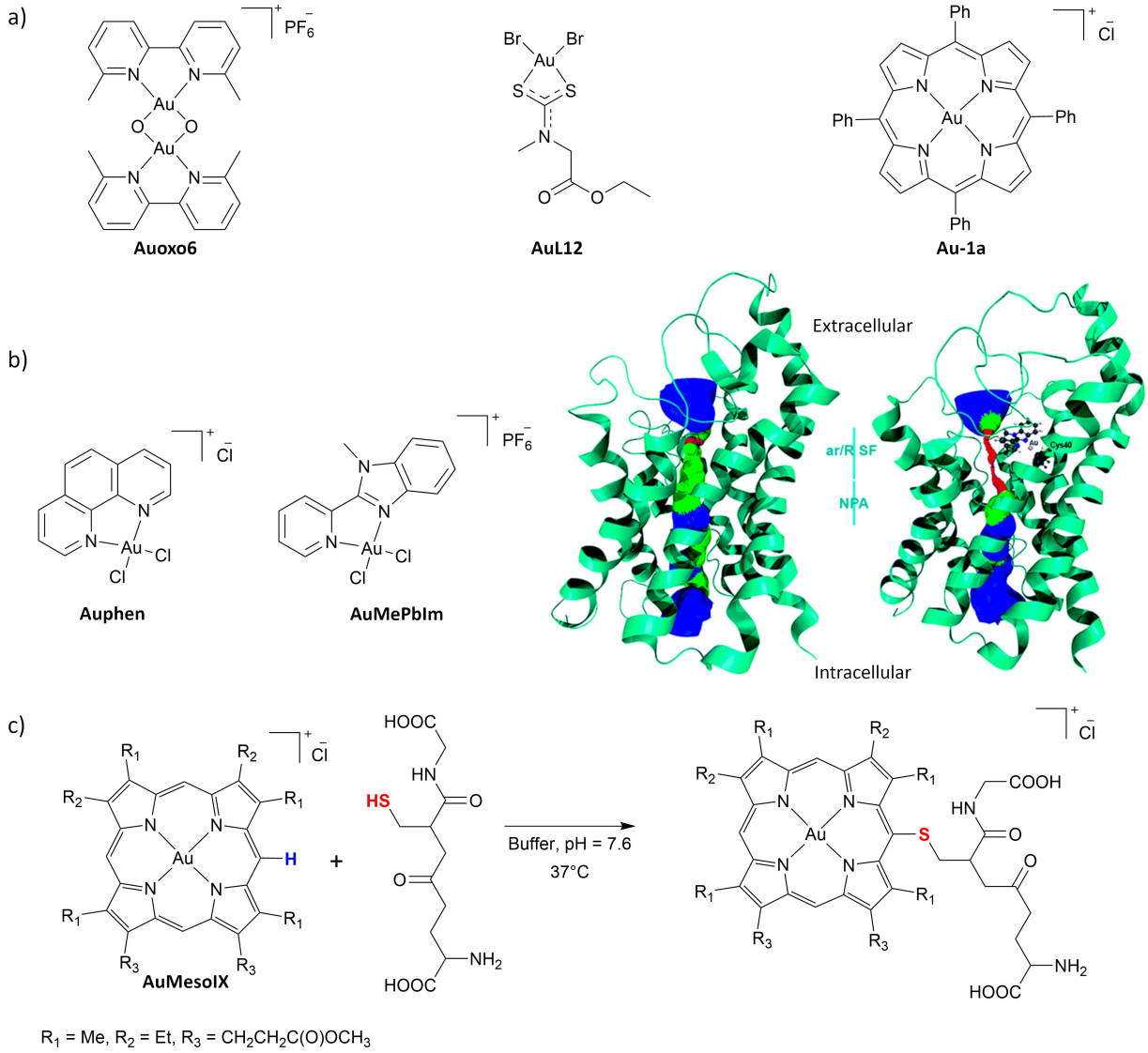

Figure 7. a) Benchmark anticancer Au^{III} coordination compounds. b) The Au^{III} complexes **Auphen** and **AuMePbIm** (MePbIm = 1-methyl-2-(2-pyridyl)benzimidazole) are potent human AQP3 inhibitors. **AuMePbIm** binds to Cys40 in the AQP3 channel. The red volume represents size constraints (shrinkage with respect to the unbound AQP3 monomer) which would block the passage of glycerol molecules.[140] c) Reaction Scheme showing coordination-activated nucleophilic substitution in the meso-position of Au^{III} porphyrins. This mechanism was identified for cysteine-containing protein-targeted MoA.[145] Panel b) was adapted with permission from ref. [140]. copyright Royal Society of Chemistry 2020.

more promising compounds of this type, showing outstanding *in vitro* and *in vivo* antitumour properties and reduced systemic and nephrotic toxicity when compared to cisplatin.[137] One of the major drawbacks of **AuL12** and other Au^{III} dithiocarbamates is the low solubility, resulting in their low bioavailability and speciation in physiological environment; thus, cyclodextrin formulations have been used to address these issues.[138]

In 2012, Martins et al.[139] reported the first aquaporin-inhibiting Au^{III} compound, **Auphen** ([$AuCl_2$(1,10-phenanthroline)]), featuring selective inhibition of human aquaglyceroporin 3 (AQP3) channels via a mechanism that induces shrinkage of the channel upon metal binding to a cysteine residue (Figure 7b).[140] Aquaporins (AQPs) are water/glycerol channels over-expressed in certain cancer types and postulated as anticancer drug targets.[141] Interestingly, the Au^{I} complex aurothiomalate does not inhibit AQPs. The substitution of phenanthroline by 1-methyl-2-(2-pyridyl)benzimidazole to give the cationic Au^{III} compound **AuMePbIm** (Figure 7b) improves the AQP3 inhibitory potency.[140,142]

Porphyrin-Au^{III} complexes are important therapeutic agents as porphyrin ligands are capable of stabilizing Au^{III} and remain metalated in biological environments. In particular, the benchmark compound, meso-tetraphenylporphyringold(III) (**Au-1a**, Figure 7a), reported by Che et al.[143] in 2003, has demonstrated higher activity than cisplatin against a wide range of cancer cell lines, both *in vitro* and *in vivo* (in xenograft tumour bearing mice).[61] **Au-1a** has been shown to cause apoptosis by disrupting

mitochondrial function, in particular, its activity has been linked to the interaction with a mitochondria chaperon, i.e., the heat shock protein 60 (Hsp60).[144] Recently, a new MoA for the meso-unsubstituted porphyrin derivatives has been identified. Che and co-workers have demonstrated the reactivity of such derivatives toward thiol proteins.[145] Coordination of gold was found to activate the porphyrin scaffold to nucleophilic aromatic substitutions in the meso position (Figure 7c). Cysteine-thiol conjugation has been proposed to deactivate cysteine-dependent redox enzymes, as an alternative to the direct coordination of gold observed mainly in Au^{I} compounds. Considering that porphyrin gold derivatives are known for their significant activity as DNA and G-quadruplex (G4) binders,[61] and that they often lack protein binding-related MoA due to stabilization of the gold centre by the chelating porphyrin, this new reactivity involving protein targets sheds light on the potential use of such systems as multimodal therapeutics.

Cyclometallation is one of the main strategies to stabilize Au^{III} centres towards reduction so that these compounds become stable enough to serve as useful anticancer agents.[60,61] The interest in these types of organometallic compounds was revived by the discovery of the anticancer potential of $[Au(damp)(CH_3COO)_2]$ (damp = 2-((dimethylamino)methyl)phenyl), which exhibits similar cytotoxicity to cisplatin.[146] Recent studies have shown that cyclometalated gold compounds act simultaneously as DNA binders and TrxR inhibitors.[147,148]

Moreover, Au^{III} compounds of this family have shown interesting activity as inhibitors of zinc fingers (ZFs). ZFs are structural motifs of proteins that function as recognition domains for DNA, RNA, and other proteins.[149] Many ZF-proteins have been observed to be associated with cancer progression, although the general mechanisms are subject of current research.[150,151] Within the ZFs family, there are several zinc-binding domains, including Cys_2His_2 (CCHH), Cys_3His (CCHC), and Cys_4 (CCCC) as the most common, while several other non-classical families of ZFs exist.[149,150] ZFs are interesting target proteins for the treatment of cancer as they are involved in DNA transcription, translation, and repair.[149] Metallodrugs can displace Zn^{2+} and alter the structure of ZFs, disrupting or inhibiting their function, as is the case of gold compounds.[151] The displacement of Zn^{2+} by Au^{I} or Au^{III} in the ZF domain yields the so-called "gold fingers".[152–154] The facile reduction of Au^{III} in physiological conditions normally leads to formation of Au^{I}-adducts with ZF-proteins.[154,155]

Targeting poly(adenosine diphosphate ribose)polymerases (PARPs), sometimes referred to as "*the guardian angle of DNA*",[156] is of particular interest in the treatment of cancer, because the survival of many tumours is supported by PARP-mediated DNA repair. In addition to the active catalytic site of PARP-1, which can serve as a pharmacological target, the enzyme features two N-terminal ZF domains for DNA binding that can be targeted by metallodrugs to indirectly inhibit the function of the protein (Figure 8a).[157] In particular, inhibition of PARP-1 by Au^{I} and Au^{III} complexes, following the removal of Zn^{II} with the formation of the aforementioned "gold finger" structure, has been reported.[156,158] The current challenges are to increase selectivity by understanding the factors that control PARP-ZF targeting. A recent study has provided some insights into the structural design of PARP-1-targeted Au^{III} compounds, showing that cyclometalated C^N, C^N^C, and chelated N^N Au^{III} compounds (Figure 8b) exhibit a strong affinity for PARP-1 ZFs and avoid the reduction to Au^{I}.[159] The increased stability of cyclometalated Au^{III} C^N adducts favours PARP-ZF targeting, suggesting cyclometallation as a strategy to achieve selectivity.[159]

Noteworthy, further investigation of the binding mode of the **$[Au(py^b)Cl_2]$** complex (py^b = 2-benzylpyridine) with different ZF domains and model peptides, enabled the observation of a peculiar reactivity towards cysteine residues.[160] In detail, following **Aupy^b**-peptide adduct formation, the reaction progressed towards cysteine arylation (Figure 8c).[160] Combined mass spectrometry and density functional theory (DFT) calculations showed that the formation of the C–S bond is templated by the Au^{III} centre via reductive elimination.[161] With the idea of exploiting metal-templated C–S bond-forming reactions to achieve modification of cysteines in bacterial proteins, an analogue of the cyclometalated Au^{III} compound was studied in a competitive chemoproteomic approach in *S. aureus* cell extracts.[162] The obtained results showed that of ca. 100 cysteines that were liganded by the gold complex, 27 of them were found in proteins encoded by essential genes and, of those, 10 were assigned to be close to the respective functional protein sites. Of note, Cys-134 of the bacterial TrxR was amongst the highlighted residues.[162]

Recently, Martens et al. demonstrated how to enhance the activity of dithiocarbamate derivatives by tuning the structure of the C^N ligand.[148] The use of cell transcriptomics allowed the identification of the global effects of the lead compound (**2a**, Figure 9a) on MDA-MB-231 cells ($IC_{50} = 0.773 \pm 0.117$ μM, 72 h), revealing interference with mitochondrial processes related to oxidative phosphorylation, cell cycle, and organelle fission processes. Further, a drop in mitochondrial membrane potential was observed by JC-1 staining confocal microscopy (Figure 9b,c).[148] Following their interest in biphosphine-based cytotoxic Au^{III} compounds,[98,163] a detailed study of a series of compounds containing 1,2-bis(diphenylphosphino)benzene (dppBz) was recently published by the same group.[164] The compounds were obtained by the reaction of cyclometalated C^N adducts with dppBz, (Figure 9d). This family of compounds, termed AuPhos, was tested on the US National Cancer Institute reference series of cancer cell lines (NCI-60) and showed promising cytotoxicity.[165] The most potent compound $[Au(dppBz)(2\text{-phenylpyridine})]Cl_2$ (**AuPhos-89**, Figure 9d) was subjected to differential gene expression assays to gain insight into the MoA. The modulation of oxidative phosphorylation by **AuPhos-89** was suggested as a possible MoA.[164] In addition, the *in vitro* increase in mitochondrial oxygen consumption rate and proteomic studies support mitochondrial targeting. To overcome the low solubility and dosage problems, a formulation containing the non-ionic surfactant Kolliphor® was used as a vehicle to perform *in vivo* studies. The results showed a reduction of tumour

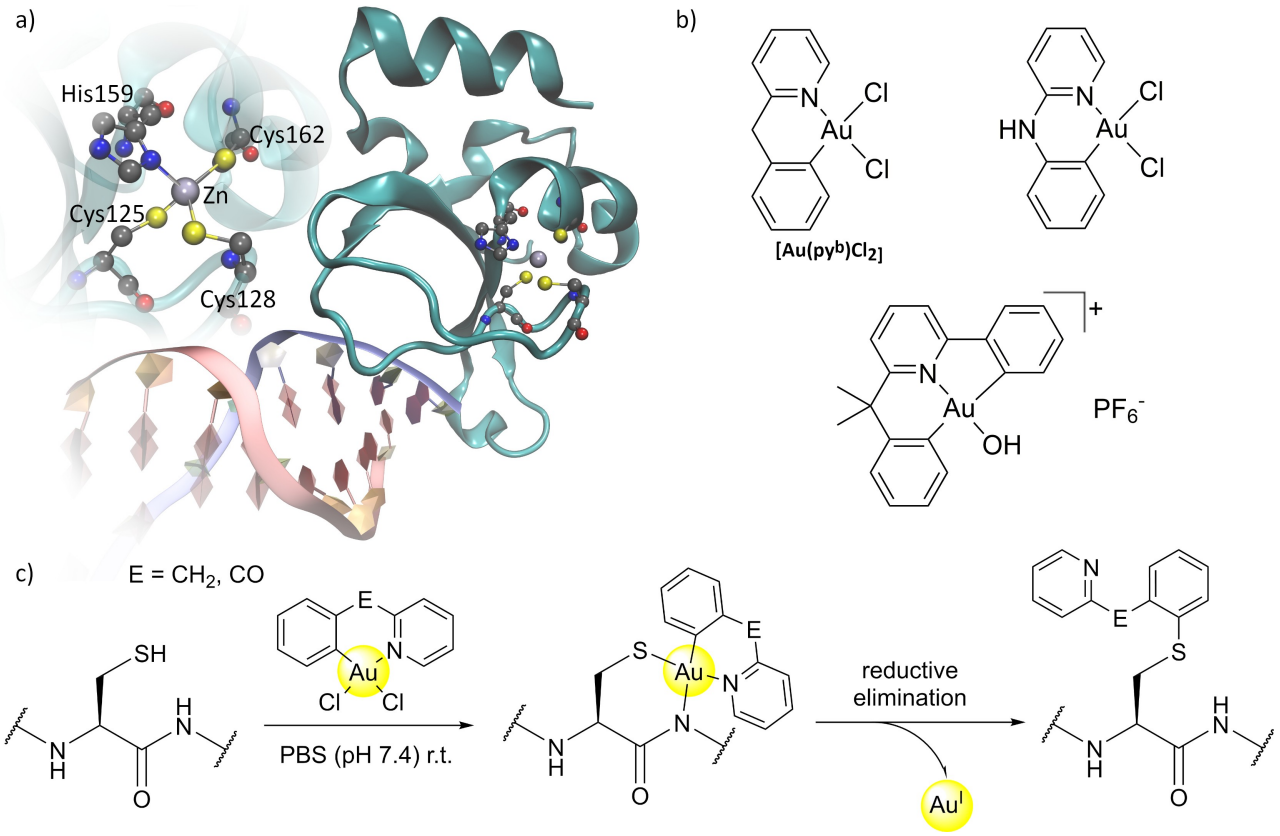

Figure 8. a) X-Ray structure of the PARP-1(ZF2) DNA recognition fragment showing the localization of the ZF shaping the binding site. The inset displays the Zn^{II} tetrahedral CCHC environment (PDB 3ODE). The image was generated using the VMD software.[313] Colour code for the explicit atoms: C, grey; N, blue; O, red; Zn, silver; S, yellow. Hydrogen atoms and water molecules present in the structure have been omitted for clarity. b) Gold(III) compounds studied for targeting PARP-1 ZF moieties.[159] c) Mechanism of cysteine arylation templated by cyclometalated C^N Au^{III} compounds via reductive elimination.[160]

growth in 4T1 triple-negative breast cancer with an intraperitoneal dose of 10 mg kg^{-1} (Figure 9e). This reduction was comparable to that observed with cisplatin (dose 3 mg kg^{-1}). Additionally, **AuPhos-89** showed inhibition in metastasis to the liver, which was histologically detected in the control systems.[164] These promising results exemplify the need of developing smart delivery vehicles for the optimal usage of these types of metallodrugs.

In 2006 Che and collaborators reported a family of dicyclometalated C^N^C Au^{III} compounds bearing deprotonated 2,6-diphenylpyridine (diPhPy) as ligand, the studied compounds were found to be cytotoxic and act as DNA intercalators and TrxR inhibitors.[166] They also observed that the auxiliary ligands, a family of phosphines are released and can exert concomitant anticancer effects.[166] In particular, the dinuclear compound $[Au_2(diPhPy)_2(\mu\text{-dppp})](CF_3SO_3)$ has been shown to inhibit hepatocellular carcinoma at a dosage of 0.5 mg kg^{-1} in rat models.[167] The same group has lately used NHCs as complementary ligands together with C^N^C cyclometalates, exploiting the ease of functionalization of NHCs to generate multifunctional compounds with photoactivable binders and "clickable" moieties.[168] These systems where then used to identify—by photoactivated-bonding—the compounds' protein targets using copper-catalysed fluorescent click labelling of the protein-compound adducts. Importantly, all six identified targets were oncogenic proteins.[168]

Au^{III} C^N^N cyclometalates were reported in 2004 by Cinellu, Messori, and co-workers, which highlighted the stability of these compounds in physiological conditions and showed the cytotoxic activity of $[Au(bipy^{dmb})(4\text{-}(CH_3)C_6H_4\text{-}NH)]PF_6$ ($bipy^{dmb}$ = C-deprotonated 6-(2-phenylpropan-2-yl)-2,2′-bipyridine).[169] Recent proteomic studies suggest that the related hydroxo complex $[Au(bipy^{dmb})OH]PF_6$ causes mitochondrial damage and disrupts the glycolytic pathway of ovarian cancer cells.[170]

Recently, Au^{III} C^N^C hydride complexes have been investigated by the group of Zou, exhibiting selective photoactivable thiol reactivity.[171] The possibility of light-triggered cytotoxic activity enables the reduction of side effects, as shown by the reduction of compounds' cytotoxicity (400-fold) in the dark. The MoA is related to the inhibition of TrxR, and not to the photoinduced generation of $^1O_2$. In addition, the previously observed anti-angiogenesis effect of gold complexes,[108,172,173] treatment with these Au^{III}-C^N^C compounds was also shown to have light-induced toxic effects in zebrafish embryos (Figure 10).

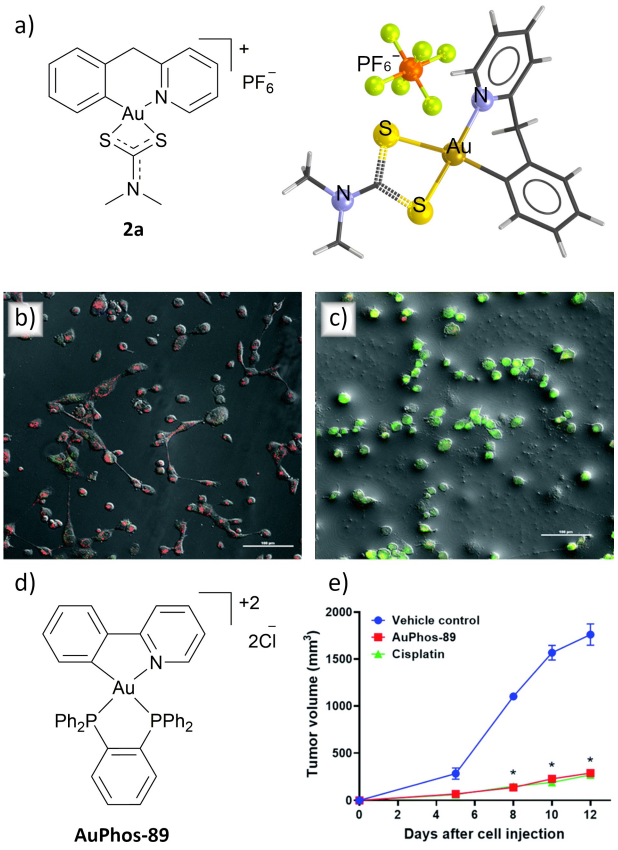

Figure 9. a) Chemical structure of the carbamate C^N cyclometalated Au^{III} (**2a**) complex and its single-crystal X-ray diffraction structure (CCDC 1889819). b) Confocal bright field image showing JC-1 staining in MDA-MB-231 cells with normal mitochondrial function. c) Confocal bright field image of JC-1 stained MDA-MB-231 cells treated with compound **2a** (10 μM). The change from aggregate red-emitting to monomeric green-emitting form is associated with a drop in MMP. d) Chemical structure of compound **AuPhos-89**. e) *In vivo* 4T1 tumour growth suppression observed with **AuPhos-89** (10 μM) when combined with Kolliphor as the vehicle. Panels b) and c) adapted with permission from ref. [148] CC BY the authors, published by The Royal Society of Chemistry. Panel e) was adapted with permission from ref. [164] CC BY 2021 the authors, published by The Royal Society of Chemistry.

Cycloaurated triphenyl sulfides Au^{III} complexes with anti-angiogenesis and cytotoxic activity were also recently reported by Bhargava's group.[174,175] In one example, cytotoxicity and anti-angiogenesis activity were maximal when a dithiocarbamate was used as a ligand compared with chlorido or biphosphine ligands, highlighting the structural fine-tuning involved in regulating activity in this type of compound.[174]

Overall, the effect of a particular chelating ligand on the activity of Au^{III} complexes remains elusive, as changes in the number of N and C donors lead to changes in the charge and general reactivity of the resulting compound, which in turn strongly affects their anticancer activity.

2.1.3. DNA Targeting

A common strategy in anticancer therapy is the inhibition of DNA replication by chemotherapeutic agents, including metallodrugs.[176] While most cytotoxic gold complexes seem to act via protein-related MoAs as discussed in the previous sections, some relevant examples of Au^{I} and Au^{III} complexes as nucleic acid binders need to be highlighted.

In addition to duplex DNA, other secondary nucleic acid structures have been disclosed and found to have key physiological roles. For example, G-quadruplexes (G4) are secondary DNA structures formed by stacked quartets of guanines, that are found usually in guanine-rich sequences and are known to play a role in vertebrate transcription processes.[177–179] G4s are found in mammalian DNA,[178,180] especially in abundance within the promoter regions of many oncogenes.[181,182] As such, targeting G4s becomes an important strategy as it has been demonstrated that stabilization of these structures downregulates transcription and prevents telomerase binding, indirectly inhibiting its activity, which in turn induces apoptosis.[183,184]

Che and co-workers reported the affinity of Au^{III} porphyrin derivatives for both double-stranded and G4 DNA structures. While most of the free porphyrins were able to inhibit telomerase activity, only **[AuTMPyP]Cl_5** (Figure 11a) has been shown to stabilize G4.[143]

Recent studies have also demonstrated that cationic Au^{I} xanthine-NHC homoleptic derivatives such as the cationic biscarbene $[Au(9\text{-methylcaffein-8-ylidene})_2]^+$ complex (**$AuTMX_2$**, Figure 11a–c) can bind effectively to G4 s[176,186] via π-stacking interactions.[187–189] Structural analysis of the gold-DNA adduct showed that the complex binds at both the 3′-3′ and 5′-5′ sites of the G4 structure, leading to the binding of three **$AuTMX_2$** units per G4 structure (2 units in the 5′-5′ site). More recently, the mechanism of action of **$AuTMX_2$**, particularly the effects of its G4 binding activity, has been investigated by a combination of mass spectrometry-based proteomics and pharmacological assays in A2780 ovarian cancer.[190] The results supported a multimodal MoA involving the non-covalent binding of **$AuTMX_2$** to nuclear and cytoplasmic components. In addition, stress indicators such as the upregulation of heat shock proteins, NRF2, and production of stress actin fibres (Figure 11d) support G4 stabilization as a possible major mechanism.[190] Recent efforts to tune the ligand structure have revealed the importance of an uncrowded xanthine structure for efficient binding to various G4 units, and it has been shown that functionalization of N9 or N1 reduces G4 affinities when compared to the methylated adduct **$AuTMX_2$**.[191] In another work, the use of dimeric cyclic analogues of **$AuTMX_2$** did not show stabilization improvements compared to the monomeric benchmark compound, but proved to be beneficial in the case of benzimidazole-based NHCs, although the obtained dimers are less selective than **$AuTMX_2$**.[192]

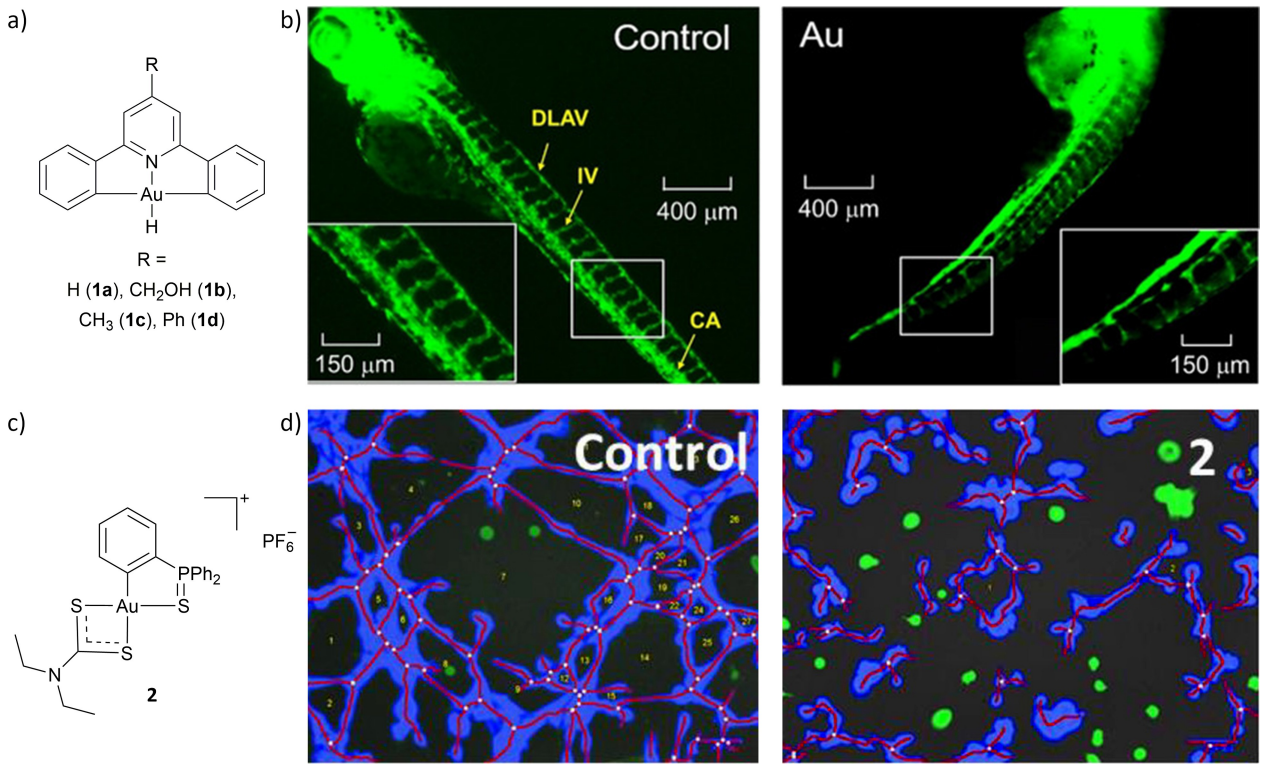

Figure 10. a) Chemical structures of Au^{III}C^N^C hydride compounds with light-activable cytotoxicity. b) Angiogenesis inhibition by compound **1a** (100 μg L^{-1}) in zebrafish embryos. The compound impairs the development of caudal artery (CA), intersegmental vessels (IV), and dorsal longitudinal anastomotic vessels (DLAV), when compared with the control. Adapted with permission from ref. [171] copyright 2020 Wiley-VCH GmbH 2020 c) Chemical structure of the C S cyclometalated thiocarbamate Au^{III} compound which shows cytotoxicity and antiangiogenic properties. d) *In vitro* anti-angiogenicity test in human umbilical vascular endothelial cells (HUVEC). The treated sample ($c = 3.89$ μM) showed reduced length, loops, covered area, and branching points than the control sample. Adapted with permission from ref. [174] copyright 2020 American Chemical Society.

3. Delivery of Gold Chemotherapeutics Based on Micro- and Nanocarriers.

Nanoparticle-based drug delivery systems have been shown to improve treatment outcomes by increasing therapeutic efficacy, reducing toxicity, improving patient compliance, and enabling entirely new medical treatments.[32,193] Recent design strategies for NPs attempt to improve pharmacological properties by taking advantage of the ability to introduce active targeting groups on their surface,[32,41,194] and to render NPs "labile" or "breakable" on demand, so that overall NPs can accumulate at diseased sites and be safely cleared from the body after the release of their payloads.[195,196] Generally, NPs and their degradation products are excreted through organs such as the liver, spleen, or kidneys.[197]

In general, the bioaccumulation of NPs depends on whether they are made of "soft" or "hard" materials, as well as their size, shape, and surface chemistry.[198–201] For example, surface functionalization of NPs with polyethylene glycol[202,203] or with proteins that reduce recognition by the mononuclear phagocyte system[204,205] has been shown to increase their blood-circulation lifetime and their *in vivo* stability. Surface functionalization of NPs can also provide active targeting, in which NPs are delivered to specific cells or tissues.[194] For example, the liposomal formulation SGT-53, which includes a transferrin antibody for targeted breast cancer therapy, has entered clinical trial (trial number: NCT05093387).[206] Concerning ways to precisely trigger the release of NPs payload,[207–209] this can be achieved by rendering NPs degradable once they reach their target site (e.g., by the presence of a specific stimulus) or, as in the case of porous NPs, by opening specific pore-blocking moieties ("gatekeepers").[210]

Of the various types of "soft" NPs that have also been studied for gold-based delivery, lipid-based nanoparticles (LbNPs) are the most successful nanocarriers when it comes to FDA approval.[211–213] LbNPs are biodegradable, biocompatible and have low immunogenicity; moreover, they can load a variety of drugs improving the therapeutic performance and minimizing their side effects. Given their now long secure history in biomedical research, LbNPs have an edge over other nanoparticles. However, their limited stability in biofluids is their main drawback.

Polymeric nanocarriers are composed of natural or synthetic polymers and can be more stable in biofluids compared to LbNPs.[214] Tuning their physicochemical properties is relatively easy, as there are numerous synthetic methods for preparing polymers and co-block polymers with well-defined chain lengths, chemical composition and

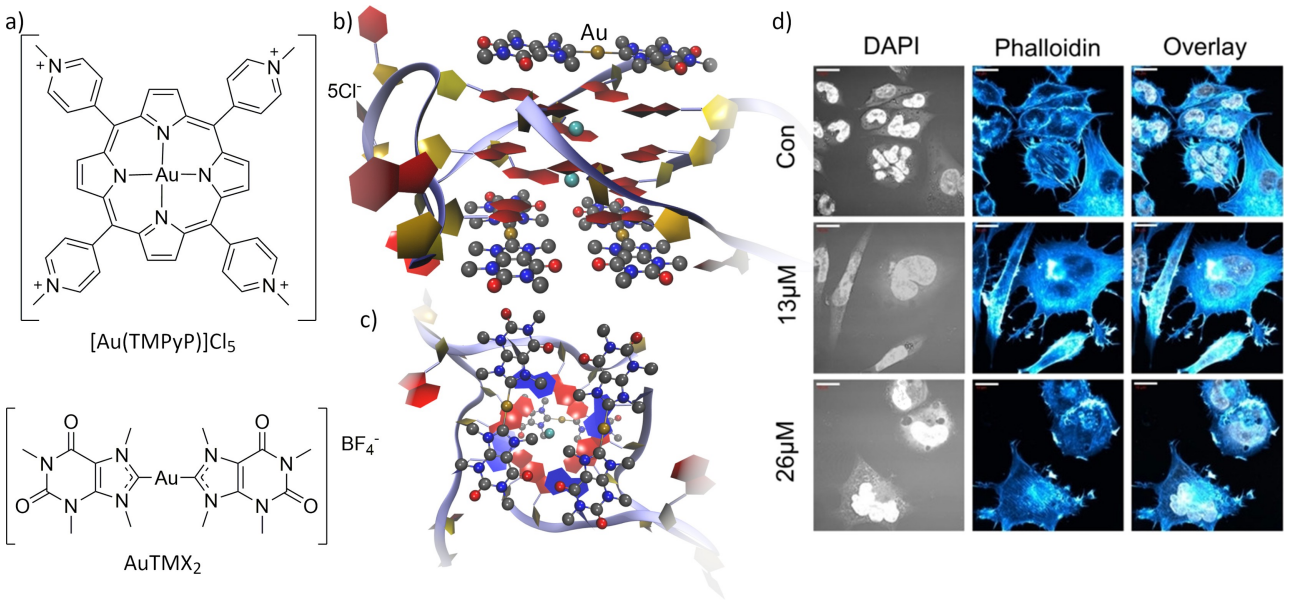

Figure 11. a) Chemical structures of Au^{III} (**[AuTMPyP]Cl_5**) and Au^{I} (**AuTMX_2**) compounds with G4 binding activity. b) Lateral view of the G4-**AuTMX_2** structure (PDB 5CCW) showing the binding of two molecules of **AuTMX_2** at the 5′-5′ site (bottom in the image) and one additional molecule at the 3′-3′site (upper part of the image). c) Projection of the G4-**AuTMX_2** adduct from the 5′-5′ side, showing the stacking of **AuTMX_2** with the G4; the first guanine tetrad is displayed in blue for clarity. Panels b) and c) were generated using the VMD software.[313] Colour code for the explicit atoms: C, grey; N, blue; O, red; K, cyan; Au, golden. Hydrogen atoms, water molecules, and additional ligands present in the structures have been omitted for clarity. d) Fluorescence microscopy images of A2780 cancer cells treated with different concentrations (13 and 26 μM) of **AuTMX_2**. The presence of stress actin fibres in the treated cells, observed as bright regions in the phalloidin staining particularly visible in the filopodia, supports a multimodal MoA of **AuTMX_2** that may also include G4-binding. Panel d) was adapted with permission from ref. [190] copyright 2020, The Authors, Published by Wiley-VCH GmbH.

morphologies.[214] The use of labile crosslinkers is an interesting approach to making degradable polymeric NPs. For example, the incorporation of acid-labile crosslinkers can trigger nanoparticle degradation in acidic environments, such as those found in some tumours or lysosomal cell compartments.[215,216]

The development of protein-based drug carriers is gaining importance in the targeted delivery of cancer therapy, particularly as a result of the market approval of the paclitaxel-loaded albumin nanoparticle, Abraxane®.[217] Albumin-binding is a general strategy for improving the pharmacokinetics, increasing the uptake in cancer cells or improving the clearance of drugs. Apoferritin is another appealing protein carrier. Its cage-like structure can encapsulate bioactive molecules in its cavity (8 nm in diameter) and exhibits dynamic assembly and disassembly behaviour.[218] Apoferritin is non-toxic and shows affinity for tumour cells due to its ability to bind human TfR1 receptors. However, when protein-based carriers are used, the integrity of Au-based complexes becomes a critical factor that is currently under investigation.[219,220]

Concerning "hard" nanomaterials, mesoporous silica nanoparticles (MSPs) can be prepared in a variety of sizes, shapes and porosities thanks to the various surfactant-templated synthesis methods.[221] The presence of a porous mesophase in MSP enables drug loading, while the outer surface of the nanoparticles can be further functionalized, e.g., by alkoxysilane-based chemistry, with additional performance enhancers such as polymers and dyes, targeting units, etc. Silica (SiO_2) is classified as "Generally Recognized as Safe" (GRAS) by the FDA and several clinical trials are currently underway involving the use of silica-based NPs.[222] Although MSPs are expected to hydrolyse in aqueous media, there are still biosafety issues related to the efficient clearance of these nanoparticles to be addressed before they can be used as nanomedicines. As an alternative to MSPs, mesoporous organosilica nanoparticles (MONPs) have received considerable attention in the generation of stimuli-responsive nanocarriers.[223,224] To date, redox-responsive (e.g., disulfide,[225–227] diselenide[228]) and hydrolyzable (e.g., amide,[229] oxamide,[230] carbamate[231] or imine groups[232]) groups have been used for the preparation of breakable MONPs. Undesired bioaccumulation of mesoporous silica, which leads to chronic toxicity, can be avoided as, in principle, the particles degrade once they have released their payload.[233]

Metal-organic frameworks (MOFs)[234] are microporous (nano)materials formed via self-assembly of metal ion nodes or clusters (e.g., Zr^{IV}, Fe^{III}, and Zn^{II}) and organic ligands (e.g., carboxylic acids or amines).[235] Due to their high porosity, they have recently attracted considerable interest as drug delivery carriers, as they allow for high loading capacity and controlled charge release.[235–237] Despite their advantages in terms of functionalizability and targeting capacity, applications of MOFs in the biomedical domain are still limited to pre-clinical studies due to issues with biocompatibility, toxicity and stability in the physiological environment.

Since we aim to showcase exclusively particle-based delivery systems involving gold complexes, we would like to draw the reader's attention to other excellent reviews that summarize in detail other NP-based systems for drug delivery and imaging.[198,238–241] In this section, we review the current status of existing nano- and microparticle-based systems for the delivery of anticancer gold compounds. To this aim, the particle systems are divided into two categories depending on whether the active gold compound is non-covalently adsorbed/entrapped in the nanocarrier or covalently tethered to it. The particles discussed here with their cargo drugs and main features are summarized in Table S1 (see Supporting Information).

3.1. Particle Formulations Based on Non-Covalent Loading Strategies of Gold Complexes

Non-covalent loading strategies rely on the supramolecular attractive interactions between the drug and the nanocarrier,[242] and can be regarded as "mild" methods, since the chemical structure of the drug, and thus, its intrinsic biological activity, is not altered.[242,243]

Two early examples reported by the groups of Wataha[244] and Che[245] described the use of particle-based delivery of gold complexes. In detail, Wataha and co-workers described the preparation of AF-loaded monosodium titanate (MST) and amorphous peroxo-titanate (APT) microparticles (**P1**) and characterized their biological activity *in vitro*.[244] The titanate particles have been previously synthesized and reported elsewhere.[246,247] The moderate loading efficiency with AF (**AF@P1**; 5.4×10^{-3} mmol Au g^{-1} APT) is most likely related to the impregnation method in aqueous media, where the solubility of the drug is limited. When **AF@P1** was incubated with fibroblasts at a dose of 5 μg mL^{-1}, significant succinate dehydrogenase (SDH) suppression was observed and was more pronounced compared with the use of free AF. In the case where fibroblast cells were treated with higher doses of **AF@P1** (100 μg mL^{-1}, corresponding to 0.540 μM AF), strong SDH activity suppression by 35–40 % was observed.[244] Interestingly, no significant SDH suppression was reported when monocytes (THP1) were treated with **AF@P1** even at 72 h of incubation time.[244]

In search of more robust delivery systems in which passive diffusion of the surface-adsorbed gold compound can be excluded, Che and co-workers[245] reported the encapsulation of their benchmark porphyrin-based Au^{III} complex, **Au-1a** ($IC_{50}=0.033\pm0.004$ μM against human nasopharyngeal carcinoma cells; Figure 7),[143] and the Schiff-base complex $[Au(dsc)]PF_6$ (dsc = N, N-bis-(4-diethylamino-salicylidene)-1,2-cyclohexanediamine) in micrometre-sized and pH-responsive gelatin-acacia capsules (**P2**, Figure 12). The anticancer activity of this particle-based delivery system was evaluated *in vitro* towards multiple cancer cell lines and *in vivo* in tumour-bearing mice.[245] **P2** formulations were prepared by mixing solutions of either **Au-1a** or $[Au(dsc)]PF_6$ in DMSO with aqueous mixtures containing poly(ethylene) glycol (MW ca. 2000 Da), acacia, and gelatin. Subsequent coacervation was triggered acidifying the solution (pH = 4), whereas subsequent covalent crosslinking of the gelatin with acacia was achieved by adding formaldehyde at pH 9. The microcapsules have a loading efficiency for compound **Au-1a** of up to 2 wt% (by UV/Vis absorption spectroscopy). No degradation of the gold compound was observed after addition of glutathione to the particles, as determined by UV/Vis absorption spectroscopy, which is most probably due to the shielding of the drug from the external environment through the formation of a protective shell by the NP. A slow and passive release of **Au-1a** (90 % drug release after 50 h) was observed in phosphate-buffered saline (PBS) at pH 7.0, while an enhanced release of the gold compound was observed at acidic pH (pH 5.0 and pH 3.0)[245] due to acid-catalysed hydrolysis of the acetal and imine crosslinking groups in the microcapsules. *In vitro* studies showed that **Au-1a@P2** (the dose was adjusted so that the concentration of **Au-1a** was 0.2 μM) has a pronounced time-dependent cytotoxicity towards HeLa cells, whereas free **Au-1a** (0.2 μM) showed acute toxicity. *In vivo* experiments with subcutaneous tumour-bearing mice (from the injection of HeLa cells) showed that intraperitoneal administration of **Au-1a@P2** (dose = 152.3 mg kg^{-1}; equivalent to 3.0 mg kg^{-1} of **Au-1a**) resulted in the survival of all mice after 28 days of treatment,

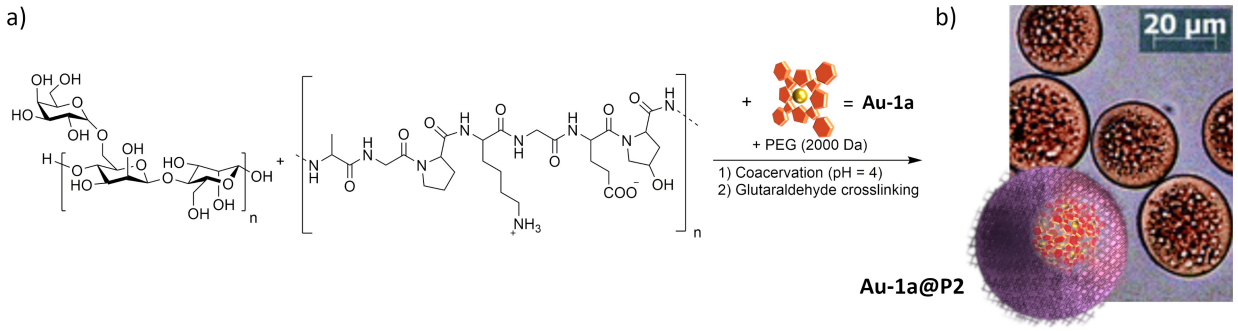

Figure 12. a) Schematic representation of the preparation of gold compound-loaded Acacia-PEG-gelatine-based microparticles (**P2**). b) Photographs of microcapsules prepared with a ratio of **Au-1a** to acacia (100 : 1000). Adapted with permission from ref. [245]. copyright 2010 The Royal Society of Chemistry.

whereas 75 % of mice treated with **Au-1a** were found dead 18 days after the first treatment.[245]

The seminal studies involving **P1** and **P2** demonstrated the benefits of particle-based delivery strategies. However, the use of microparticles is suboptimal. Rather, smaller nanoparticles (size <200 nm), are preferred for drug delivery applications due to potentially lower immunologic responses, facilitated clearance,[248] faster drug release.[249] and more efficient transcytosis into adjacent tissues.[250,251] A micellar nanometer-sized formulation (80 ± 30 nm) that encapsulates **Au-1a** (**P3**, Figure 13)[143] for the potential treatment of neuroblastoma was reported in 2010 by Wong and co-workers.[185] The loaded micelles were prepared by dissolving the gold compound in hexadecane-1-ol followed by the addition of the surfactant Brij 78 and deionized water. Systematic intraperitoneal injection of **Au-1a@P3** into the tumour of neuroblastoma-bearing mice at the dose of 0.08 mg (approx. 4 mg kg^{-1}) every 7 days, showed a substantial reduction in tumour growth (Figure 13b). Moreover, all mice survived the 21 days treatment (Figure 13c). In contrast, the survival rate of tumour-bearing mice treated with the free **Au-1a** (dose = 4 to 5 mg kg^{-1}) dropped to zero after the second day of treatment. Limitations for **P3** arise when high therapeutic doses of the drug are required, as doses of 0.1 mg resulted in acute toxicity, as the survival after the second week of the treatment dropped to 33 % (Figure 13c).[185] In a follow-up study, the same authors mentioned that **P3** is taken up by the liver macrophages after intravenous injection, which limits their use in cancer therapy.[252] However, PEGylation of **P3** resulted in decreased liver uptake in mice and an increased accumulation of **Au-1a** in the tumour. Nevertheless, the ability to inhibit tumour growth was not significantly improved when compared with non-PEGylated **P3**.[252]

In 2014, Accardo and co-workers[253] prepared functionalized sterically stabilized micelles (SSM) and sterically stabilized mixed micelles (SSMM) with a size of 20 nm for bombesin-targeted gold complex delivery by adapting a previously reported procedure (**P4** in Figure 14).[254] SSMs were composed of 1,2-distearoyl-sn-glycero-3-phosphoethanolamine-N-[amino(polyethylene glycol)-2000] (DSPE-PEG2000 amine), whereas SSMMs were composed of L-α-phosphatidylcholine (PC) and 1,2-dioleoyl-sn-glycero-3-phosphocholine (DOPC) phospholipids (5, 10 or 20 % mol/mol to DSPE-PEG2000) and loaded with the dithiocarbamate Au^{III} complex **AuL12** (Figure 14).[253] The use of a bombesin-derived peptide-based lipid (MonY-BN-AA1) enabled *in vitro* targeting of cells that overexpress the GRP/bombesin receptor - an autocrine growth factor receptor in tumour cells (Figure 14b).[255] The **P4** micelles efficiently encapsulate **AuL12** (30 %), the encapsulation efficiency depends on the PC to DOPC molar ratios used for the preparation of the micelles. Stability studies of **AuL12@P4** showed that only a low release of the cargo occurred in serum (Figure 14c), indicating a robust encapsulation of the gold complex. Importantly, prolonged stability of **AuL12** within the micelles (up to 72 h in 0.9 wt% NaCl saline) was observed and confirmed by UV/Vis spectroscopy.[253] Cytotoxicity assays on GRP/bombesin receptor-overexpressing human prostate cancer cells (PC-3) showed that **AuL12@P4**, bearing the bombesin-derived peptide on the surface, exhibited the highest cytotoxicity at 48 h (ca. 10 % viable cells compared with the control at dose = 10 μM eq of **AuL12**), whereas a loss of cell viability of ca. 80 % was observed with free **AuL12** or non-targeted **P4**.

In the same year, Che and co-workers[256] reported the use of **Au-1a**-loaded spherical mesoporous silica nanoparticles (MSPs; **P5** in Figure 15), for targeted anticancer therapy. The approximately 100 nm sized MSPs were loaded with the gold complex by an impregnation process, and afterwards, a biodegradable chitosan shell was constructed around the particles to prevent diffusion of the cargo from the mesopores. The chitosan polymer-shell was functionalized with the tumour-homing peptide Arg-Gly-Asp[257] (RGD, Figure 15a and b) for active targeting purposes, yielding **Au1a@P5(RGD)**.[256] Overall, a loading efficiency of 15 wt% was achieved (150.8 mg g^{-1} MSN) and the authors showed that integrin-expressing cells efficiently internalized **Au1a@P5(RGD)** (Figure 15c). Enhanced release of the gold complex was achieved when the NPs were exposed to cell lysates or taken up by A549 cells, as in both cases the NPs are exposed to hydrolytic enzymes that degrade the chitosan shell (Figure 15d).[256]

In 2020, a new formulation of **Au-1a** was proposed whereby the Au^{III} porphyrin was encapsulated into an interpenetrating network (IPN) platform containing chemi-

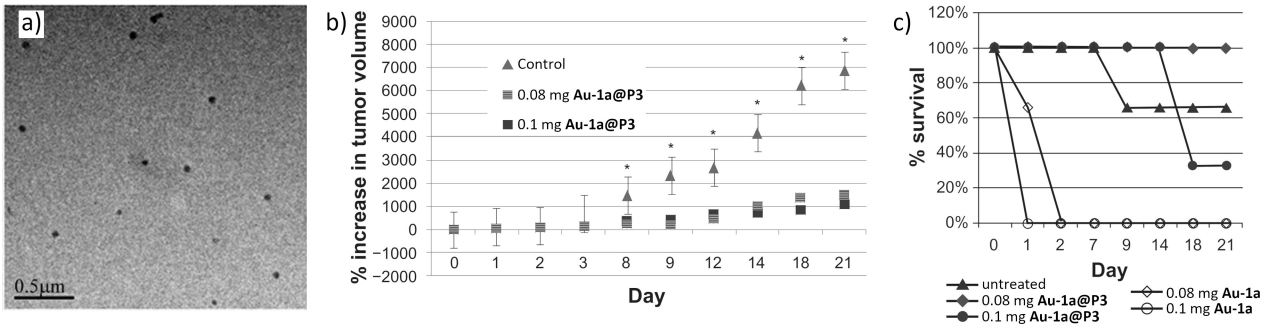

Figure 13. a) TEM image of 80 nm-sized **Au-1a@P3**. b) Tumour growth inhibition upon treatment with **Au-1a@P3.** c) Survival rate of neuroblastoma-bearing mice after **Au-1a@P3** treatment compared to the treatment using free **Au-1a** at different doses (number of mice = 6). Adapted with permission from ref. [185] copyright 2010 Dovepress.

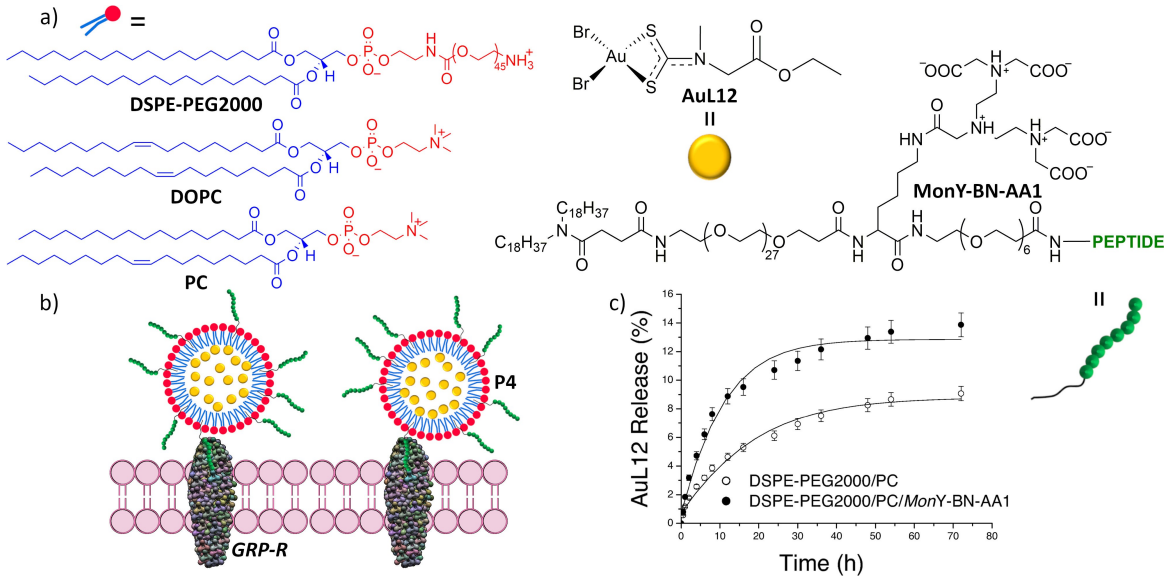

Figure 14. a) Chemical structure of phospholipids DSPE-PEG2000, PC, DOPC, gold compound **AuL12**, and the bombesin-derived peptide-based lipid MonY-BN-AA1. b) Bombesin functionalized and gold complex-loaded micelles (**P4**) bind to GRP-R receptors on the surface of cells, which in turn enables targeted drug delivery to GRP-R overexpressing cancer cells. c) Release profile of **AuL12** from micellar aggregates studied in serum. Adapted with permission from ref. [253] copyright 2010 SNMMI.

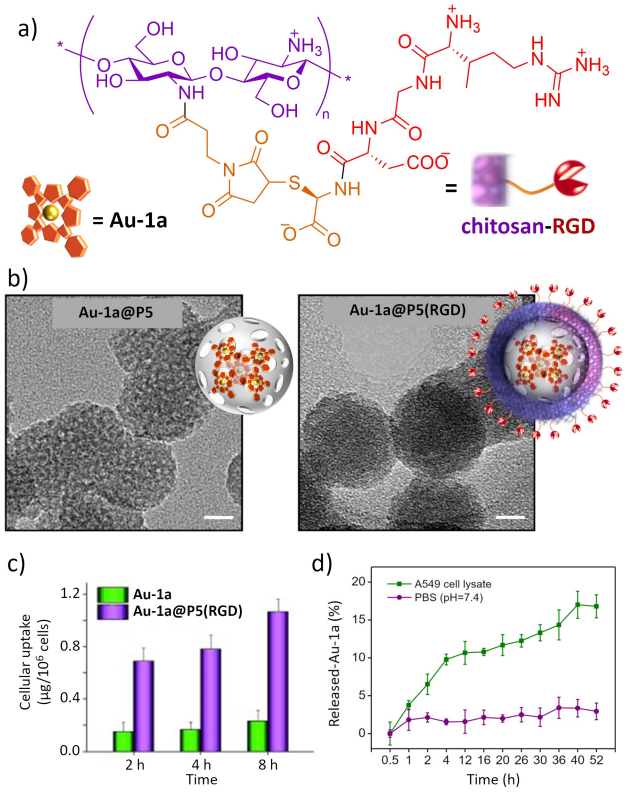

Figure 15. a) Chemical structure of the RGD-functionalized chitosan. b) TEM images of the mesoporous silica particles **Au1a@P5** (left) and **Au1a@P5(RGD)** (right). c) Quantitative analysis of cellular uptake in A549 cells after incubation with **Au-1a** and **Au1a@P5(RGD)** (each at 2.0 μM). d) *In vitro* release profiles of **Au-1a** from **Au1a@P5(RGD)** in A549 cell lysate and PBS (pH 7.4). Reproduced with permission from ref. [256] copyright 2014 Wiley-VCH.

cally-modified gelatin and polyethyleneglycol diacrylate (PEGdA), to favour systemic administration of the metallodrug.[258] Thus, Au-loaded IPN microparticles (**P6**) were obtained via a combination of UV exposure and sonication, which lead to spherical NPs in the range of 200–300 nm. Following lyophilization, the particle size exceeded 1500 nm which could be detrimental to their overall performance. It was hypothesized that the negatively charged gelatin moieties could interact with the cationic **Au-1a** also via strong electrostatic interactions, resulting in slow dissociation kinetic. **P6** maintained **Au-1a** bioactivity against lung cancer cells (NCI-H460). *In vivo* studies showed comparable anticancer effects of **P6** and **Au-1a** in nude mice bearing NCIH460 xenografts. Most notably, no observable systemic toxicity after intravenous injection of 6 mg kg^{-1} **P6** could be detected, while free **Au-1a** was markedly more toxic.[258]

Sun, Li, and co-workers reported a biocompatible and biodegradable Zn^{2+}-based metal–organic framework (Zn-MOF, **P7**) as a carrier for dinuclear NHC–Au^{I}-pyrrolidine-dithiocarbamato complexes (e.g. compound **1**, Figure 16).[259] These complexes exhibit potent anticancer activity against the A2780cis cell-line, with IC_{50} values ranging from 0.83 to 22 μM. Compound **1** (Figure 16a) was selected for further nano-formulation studies because of its 40-fold higher toxicity against A2780cis cells when compared with cisplatin. The MOF used in **P7** has been previously reported and consists of Zn^{2+}, adenine, and a benzene-1,3,5-tricarboxylic acid linker (Figure 16a).[260] The loading of **1** into Zn-MOF was achieved by an impregnation method, reaching a maximum loading of 2.049 mg g^{-1}, as was determined by inductively coupled plasma atomic emission spectroscopy (ICP-AES).[259] The carrier functions as an adsorbent capable of releasing the therapeutic gold complexes into

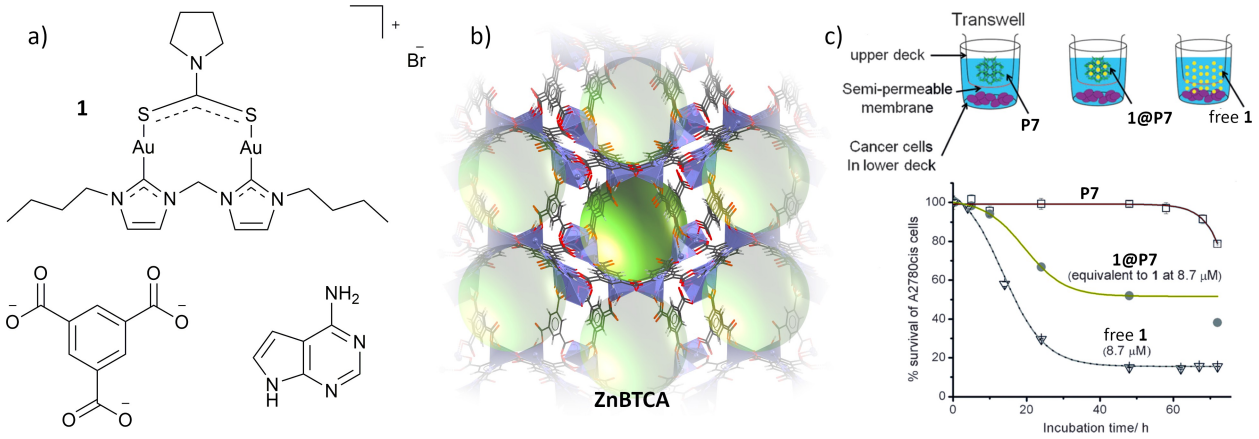

Figure 16. a) Chemical structures of the dinuclear NHC–Au^{I}-pyrrolidinedithiocarbamato complex **1** (top) and of benzene-1,3,5-tricarboxylic acid and adenine (bottom), which are the organic linkers in the Zn^{II}-based MOF. c) Perspective view of the ZnBTCA framework host (**P7**) displaying the channel regions highlighted with green spheres (Probe radio 1.0 Å, CCDC 1047851). c) Schematic representation of the trans-well assay-based cytotoxicity and antimigration studies of A2780cis cells and cytotoxic profiles with Zn-MOF and **1@P7**; time-dependent cytotoxicity of **1** at 8.7 μM is shown as a reference. Panel c) was adapted with permission from ref. [259]. copyright 2015 Wiley-VCH.

tissues for a prolonged period (up to 80 h, Figure 16c) – an interesting application when sustained drug release is aimed for the anti-proliferative activity of cis-platinum resistant carcinomas. However, direct intravenous administration is suboptimal for **1@P7**, as its size is too large for such applications (larger than 10 μm). Both **1** and **1@P7** exhibit anti-proliferative activity against cisplatin-resistant cancer cells, as was determined by trans-well assay-based *in vitro* experiments.[259] Although these Zn-MOFs are limited in terms of route of administration, their sustained release profile could firstly avoid the need for multiple administrations, thus, contributing to a reduction in unwanted chronic toxicity, and secondly, contribute to more stable absorption levels in tissues – all important factors when it comes to improving patient compliance.[261]

In the same year, Wang and co-workers[262] reported the use of pH-sensitive micelle-like NPs loaded with the potent TrRx inhibitor alkynyl phosphine Au^{I} compound (**AuI**, Figure 17). To prepare the micellar formulation (**P8**), mPEG-poly(amino ester) graft copolymers (Figure 17a) were first dissolved in a solution of **AuI** in DMSO and the formation of micelles was subsequently induced by the addition of PBS. The resulting gold complex-loaded micelles (**AuI@P8**, Figure 17b) have an average diameter of 50 nm (by DLS). ICP-AES was used to determine the **AuI** loading efficacy, which was found to be up to 47 %wt. The polymeric micelles are taken up by MCF-7 breast cancer cells and accumulate within the lysosome. In this acidic compartment of the cell, the ternary amines of the micellar aggregate are protonated, causing the micelles to disintegrate due to electrostatic repulsion forces. Furthermore, the formation of protonated amino groups in the acidic lysosomal milieu disrupts this cellular compartment, allowing cargo molecules to be transported more efficiently to the cytoplasm. In fact,

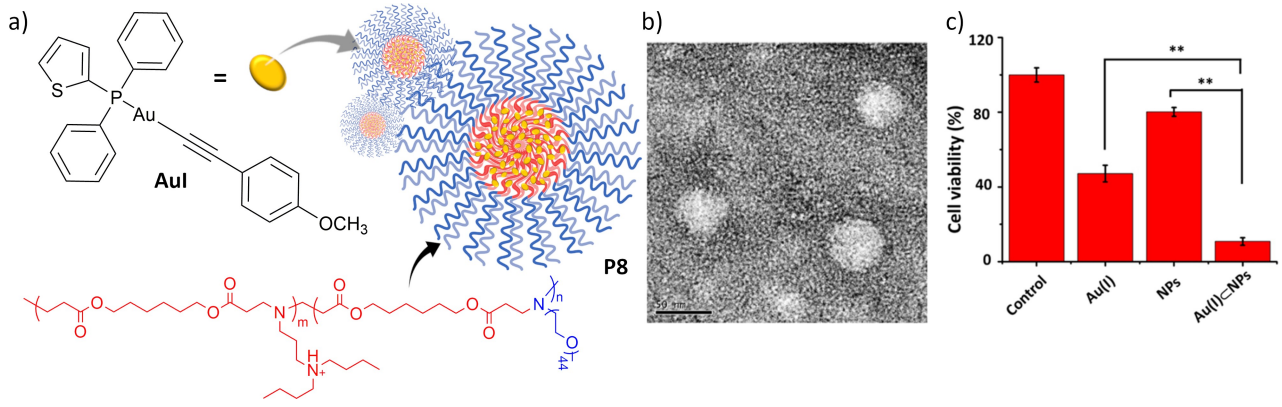

Figure 17. a) Schematic representation of **P8** and the chemical structures of **AuI** and mPEG-poly(amino ester) graft copolymer. b) TEM image of **AuI@P8**. Scale bar = 50 nm. c) Cell viabilities of MCF-7 treated with **AuI** (1.8 μg mL^{-1}), **P8** (64.7 μg mL^{-1}), and **AuI@P8** (66.5 μg mL^{-1}) for 24 h. Statistical significance: $p < 0.05$, and $p < 0.01$, one-way ANOVA for indicated comparison. Panels b) and c) reproduced with permission from ref. [262] copyright 2015 American Chemical Society.

AuI@P8 proved to be more effective than the empty nanocarrier or free **AuI** in killing cancer cells because the gold compound was more efficiently transfected into the cells (Figure 17c).[262] The principle of endosomal escape mechanism described in the latter example represents an important concept for the development of more effective metallodrug delivery systems to cancer cells.[263]

Inspired by the ability of ferritin proteins to act as containers that can store iron in a non-toxic form within the body (i.e. Fe^{III}), the Merlino group[264] used ferritin-based-cage-like structures (**P9**) to study the delivery of dinuclear gold complexes from the Auoxo family.[132,265] The loading of apoferritin (AFt) with $[Au_2(bipy^{Me})_2(\mu\text{-}O)_2][PF_6]_2$ ($bipy^{Me}$ = 6-methyl-2,2′-bipyridine), **Auoxo3** (see Figure 18a), was performed following a previously reported procedure.[266] In this example, the pH-dependent disassembly and reassembly of ferritin subunits in solution are exploited to entrap the cargo molecule into the AFt (**Auoxo3@P9** in Figure 18b).[264] The gold-loaded AFt cages have a size of about 13.8 ± 0.9 nm and can encapsulate **Auoxo3**, with ICP-MS measurements showing that there can be up to 420 gold atoms in a single cage. X-ray structure analysis showed that when located on the inner surface of the protein cage, the gold complex binds to the His and Cys residues of AFt in a linear geometry, which suggests its partial reduction and degradation. The anticancer activity of **Auoxo3@P9** was tested against three different human cancer cell lines (MCF-7, HeLa, and HepG2, Figure 18) and three non-tumourigenic cell lines (HRCE, HaCaT, and H9c2). **Auoxo3@P9** showed significant cytotoxicity to all cell lines (IC_{50} in MCF-7 cells: 41 ± 9 μg mL^{-1}), but to a lesser extent towards non-cancer cells (IC_{50} in HRCE cells: 61 ± 5 μg mL^{-1}), which contrasts with the toxicity of free **Auoxo3** (IC_{50} in MCF-7 cells: 8 ± 2 μg mL^{-1}; IC_{50} in HRCE cells: 2.2 ± 0.4 μg mL^{-1}). These results indicate that the acute toxicity of the gold complex is reduced when it is encapsulated in the protein carrier, probably due to its degradation. The enhanced anti-tumour properties can be explained by the fact that cancer cells overexpress transferrin receptor-1 (TfR1), which in turn allows enhanced uptake of **P9**.[267] The same group also reported the encapsulation of **Auoxo4** and **Au_2phen** (Figure 18a) in an AFt-cage and showed that their nanoformulations were more cytotoxic when compared with the previously reported **Auroxo3**-loaded ferritin-cage.[268]

In another work, the same group demonstrated that the Pt^{II}-Au^{I} heterobimetallic compound, [(PPh_3)Au(μ-pbi)Pt((Me)(DMSO)][PF_6] with pbi = 2-(2′-pyridyl)-benzimidazole (**4-PF$_6$** in Figure 19a), can be encapsulated within an AFt-cage (**P10**), which represents an interesting approach to Au- and Pt-based combination therapy.[269] Unfortunately, the compound degrades upon encapsulation inside the protein cage, whereby Au^{I} ions bind to the side chain of Cys126 (Figure 19b), while Pt^{II}-containing fragments are trapped in the bulk of the carrier. This degradation of the cargo is again an important aspect to be considered and addressed in the development of future AFt-based delivery vehicles. Cytotoxicity assays carried out for both **4-PF6** and **4-PF6@P10** indicate that **4-PF6** is more toxic than when encapsulated within the protein carrier. A comparison of cytotoxicity against two cancer cell lines (MCF-7 and HeLa cells) and two non-cancerous cell lines (H9c2 and HaCaT) revealed no significant selectivity between cancer and healthy cells.[269]

Recently, Yang, Liang, and co-workers described the use of AFt-based nanocarriers (**P11**) for the targeted delivery of

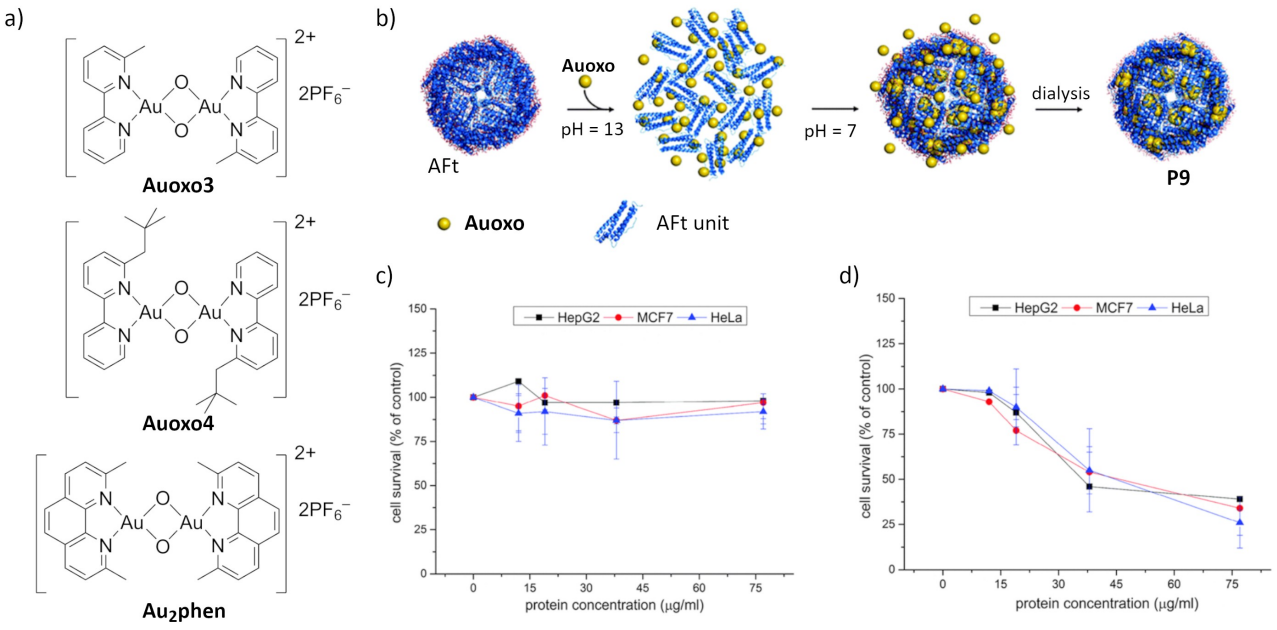

Figure 18. a) Chemical structure of the Auoxo complexes and Au2phen. b) Schematic representation of the encapsulation steps of **Auoxo3** within AFt (**P9**). c) Cell viability (MTT-assay) of non-loaded ferritin and d) of Au-AFt (**P9**) on three different cancer cell lines. Reproduced with permission from ref. [264] copyright 2016 The Royal Society of Chemistry.

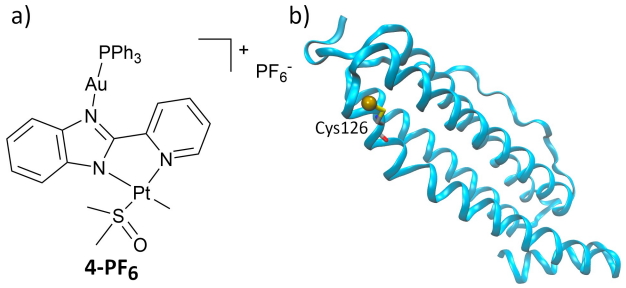

Figure 19. a) Chemical structure of the heterobimetallic complex [(PPh_3)Au(μ-pbi)Pt(Me)(DMSO)][PF_6] (**4-PF_6**). b) X-ray structure of the single Ft chain including the Au atom coordinated to Cys126 after encapsulation of **4-PF_6** in **P10** (PDB 6FX9).[269]

Au^{III} 3-(4-metylpiperidine)-thiosemicarbazide compounds against glioma.[270] Structural reactivity-based screening of selected gold compounds against glioma cells led to the identification of lead compound **C6** (Figure 20a) with an IC_{50} value of 0.66 ± 0.02 μM, which was used to load **P11**. AFt dissociates at both strongly basic and acidic media. In this example, AFt was first disassembled at acidic pH (pH 2.0). In a second step, the AFt subunits were mixed with the gold complex and reassembled by adjusting the pH to 7.5. The so-formed gold complex-loaded particles **P11** (Figure 20b) were spherical with an average size of 13 nm (by DLS) and possessed a ζ-potential value of approximately −18 mV, which is similar to the value on non-loaded AFt, indicating the successful encapsulation of the drug rather than simple surface adsorption. Differently from the previously discussed reports of the use of AFt as a carrier, in this work, the chosen gold complex did not undergo ligand exchange reactions with the carrier. Taking advantage of the pH-dependent assembly and disassembly behaviour of **P11**, the authors showed that although the particles were stable at pH 7.5, a particle half-life of 10 h was observed at pH 4.6. Thus, in acidic media **C6** is released, reaching a maximum release after 36 h. Targeted cellular uptake of **P11** toward glioma cells was observed, which may be explained by the AFt protein carrier itself, known to bind to the TfR1 receptor that is overexpressed by endothelial cells of the blood–brain barrier (BBB) or by glioma cells.[271] Indeed, **P11** accumulated more in TfR1-overexpressing U87MG cells and was localized in the lysosome.[270] **P11** was also able to cross the BBB *in vivo* when injected intravenously using healthy mouse models, and accumulation of the NPs in the brain region was higher in glioma-bearing mice between 6 to 12 h after injection (Figure 20d). Glioma tumour growth was effectively suppressed in mice treated with nano-formulation compared with free **C6** or temozolomide (Figure 20e).[270]

Rezaei and co-workers[272] reported magnetic-core and polymer shell NPs (**P12** in Figure 21a) capable of electrostatically adsorbing the Au^{III}-based anticancer drug, [7-$AuBr_3$(1,7-Phen)], on their surface. These 30 nm-sized magnetite-core and acrylic acid/PEG-shell NPs were loaded via impregnation in a solution of the gold complex, achieving a loading of about 9 % (by TGA and ICP-MS). Despite the possible coordination of carboxylate groups to the gold centre, according to the authors, gold complex adsorption occurs on the NPs because of electrostatic attraction between the carboxylate and the protonated phenanthroline at physiological pH. While only slow diffusion of the drug was observed at physiological pH values, acidic environment (pH < 5.6) can trigger enhanced release as the acrylamide moieties become protonated and

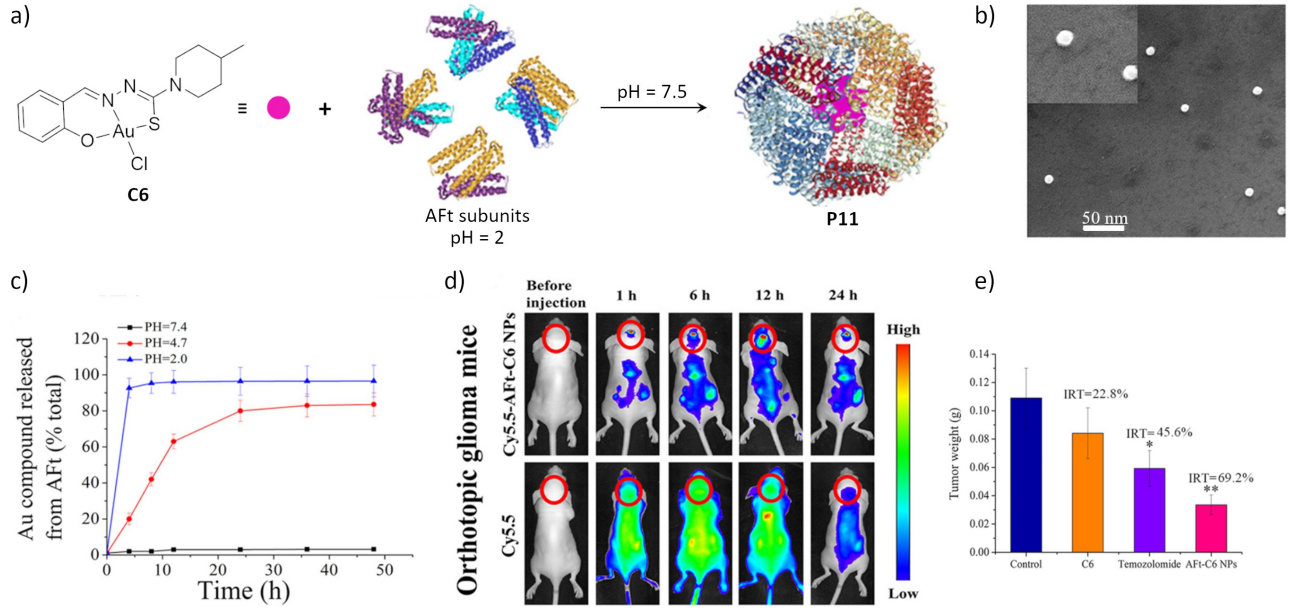

Figure 20. Chemical structure of the Au^{III} 3-(4-methyl piperidine)-thiosemicarbazide-based compound **C6** and the synthesis scheme for preparing **P11**. b) SEM image of **P11**. c) pH-dependent release study of C6 from **P11** in solution. d) *In vivo* fluorescence imaging of the brains of tumour-bearing mice intravenously injected with Cy5.5-AFt-**C6** NPs. e) Tumour weights measured 2 days after the last treatment. *p < 0.05, **p < 0.02. Reproduced with permission from ref. [270] copyright 2020 American Chemical Society.

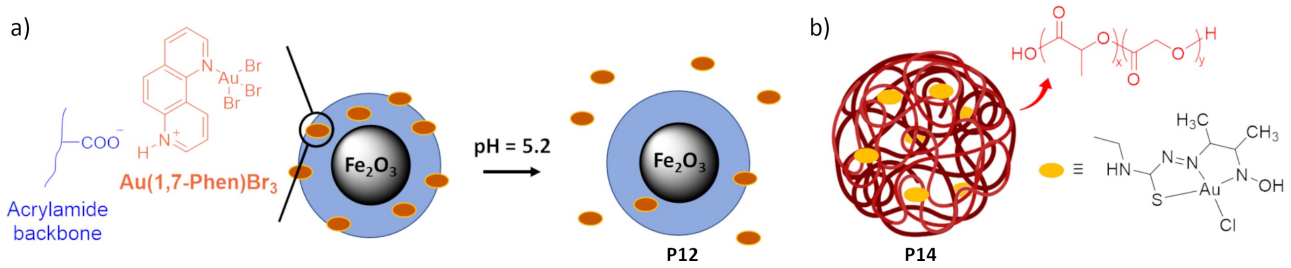

Figure 21. a) Chemical structure of Au(1,7-Phen)Br_3 and the schematic representation of the acid-mediated release of the gold complex from Fe_3O_4@PAA-PEG nanogels (**P12**). b) Poly(lactic-co-glycolic acid) (PLGA) nanoparticles (**P14**), loaded with a Au^{III} thiosemicarbazonate complex.

the attractive electrostatic interactions between the drug and the nanoparticle surface decrease. Moreover, when an external magnetic field was applied during *in vitro* experiments with HeLa cells, the gold-loaded **P12** showed slightly higher cytotoxicity on HeLa cells when compared with the free complex. This could be due to the magnetic field driving particle movement, promoting the translocation of the hydrophilic nanocarrier into the cells. However, the stability of these types of Au^{III} compounds in physiological media is not granted and has not been investigated in this study.

Amirghofran and co-workers[273] also reported the use of ca. 82 nm mesoporous silica particles for pH-dependent cellular delivery of the cyclometalated Au^{III} complex [Au(bzpy)Cl_2] (with bzpy = 2-benzylpyridine). Amino (**P13a**) and folic acid (**P13b**) functionalized NPs were prepared. The latter showed increased cytotoxicity ($IC_{50} = 18 \pm 3\ \mu g\,mL^{-1}$) against the folate-expressing MCF-7 human breast adenocarcinoma cell line compared to both the amino-functionalized NPs ($IC_{50} = 27 \pm 5\ \mu g\,mL^{-1}$) and the free gold compound ($IC_{50} = 32 \pm 2\ \mu g\,mL^{-1}$).[273]

Poly(lactic-co-glycolic acid) (PLGA) nanoparticles, loaded with an Au^{III} thiosemicarbazonate complex,[274] were reported by Maia and co-workers in 2020.[275] The 275 ± 5 nm PLGA NPs (**P14** in Figure 21b) were loaded with the gold complex via an impregnation method. The NPs showed a sustained release of the metallodrug (up to 200 h) controlled by diffusion processes. Although the use of **P14** for cancer treatment was not specifically investigated, PLGA-based NPs could be an interesting choice since PLGA is a biodegradable and biocompatible polymer already used for biomedical applications.[208,276]

Indeed, another PGLA-PEG-based NP (**P15**) used for the encapsulation of [Au(Et_3P)Cl] and its delivery to colorectal cancer cells was reported the same year by Pillozzi, Marzo, Cirri, and co-workers.[277] The particles were prepared by solubilizing the PLGA-PEG polymer ($PLGA_{7000\text{-}17.000Da}$–C=O–NH–$PEG_{3400Da}$–COOH) together with the Au^{I} complex in acetonitrile, whereas the subsequent addition of water triggered coacervation and the formation of spherical particles with an average size of 65 nm. Impressively, ICP-AES analysis indicated that 92.7 % of total added gold was encapsulated. The encapsulated gold complex was found to be less toxic ($IC_{50} = 274$ nM) compared to the free drug ($IC_{50} = 129$ nM), which can be explained by a shielding effect of the drug from the cells upon encapsulation. Drug-loaded **P15** significantly reduced cancer cell proliferation, which was accompanied by the downregulation of protein kinase B (Akt) phosphorylation—a signal transduction pathway critical for cell survival and growth.[278] In addition, it was found that loaded **P15** but not free [Au(Et_3P)Cl], affected the phosphorylation levels of extracellular signal-regulated kinases (ERK)—an important signalling pathway for cell division/proliferation.[279] The observed differences between **P15** and the free drug can be explained by the higher stability of the gold complex within the polymer matrix, the more efficient uptake of the lipophilic drug when present in PGLA-PEG particles, and the prolonged release profile of the cargo.

Galassi and co-workers recently reported the encapsulation of (4,5-dichloroimidazolyl-1H-1yl) (triphenylphosphine)gold(I) (**C-I**, Figure 22a) and (4,5 dicyanoimidazolyl-1H-1yl) (triphenylphosphine)gold(I) (**C-II**, Figure 22a), in lyotropic liquid crystalline lipid NPs (**P16**) composed of three different building blocks (Figure 22b): Monoolein (GMO), phytantriol (PHYT) and dioleoyl phosphatidylethanolamine (DOPE).[280] **C-I** and **C-II** were successfully encapsulated in **P16** formulations, as evidenced by the changes in the mesophase lattice parameters obtained from X-ray diffraction experiments, and by the spectral changes in the UV/Vis spectra of the gold complexes after loading, respectively. Since gold-phosphine complexes suffer from prompt ligand substitution reactions, their encapsulation is expected to enhance the stability and improve their

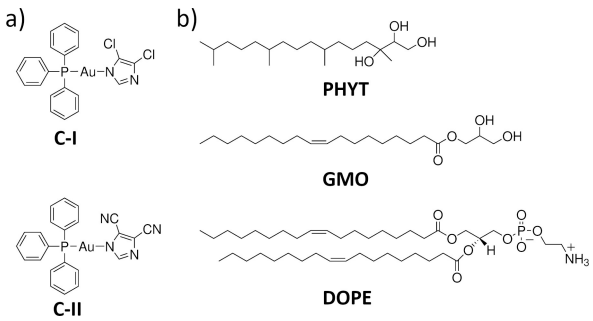

Figure 22. a) Chemical structures of (4,5-dichloroimidazolyl-1H-1yl) (triphenylphosphine)-gold(I) (C-I) and (4,5 dicyanoimidazolyl-1H-1yl) (triphenylphosphine)-gold(I) (C-II). b) Chemical structure of monoolein (GMO), phytantriol (PHYT) and dioleoyl phosphatidylethanolamine (DOPE), used for the preparation of lyotropic liquid crystalline lipid nano-systems (**P16**).

therapeutic properties,[281–283] future work on *in vitro* and *in vivo* characterization of these types of nano-formulations will be of great interest.

Recently, the group of Rouge[284] reported the encapsulation of the hydrophobic Au^{III}-dithiocarbamato complexes, [$AuBr_2$(SSC-Inp-OEt)] (**Ap228**) and [$AuBr_2$(SSC-Inp-GlcN1)] (**Ap209**) in a nucleic acid-bearing nano-capsule (NAN)[285] (**P17** in Figure 23). In addition, the nanocarrier was designed for the co-delivery of therapeutic siRNA (Bcl-2) that triggers the downregulation of the Bcl-2 gene, a regulator of apoptosis.[286,287] As depicted in Figure 23b, the micelles were prepared by first adding a tris-alkyne-containing ammonium surfactant to a solution of the corresponding metallodrug, **AP228** or **AP209**, with subsequent crosslinking of the resulting micelle via copper-catalysed azide-alkyne cycloaddition reaction using N_3-PEG-N_3. To render the NPs biodegradable, crosslinking via an alkyne-ene reaction using a short peptide with two cysteines (CGFLGGFLGGFLGC) was also investigated.[284] Following micelle crosslinking, the particles were functionalized with Bcl-2 using T4 DNA ligase, adapting a previously reported procedure.[288] The so-formed **P17** are spherical particles (Figure 23c) with a hydrodynamic diameter of 30–40 nm (Figure 23d). The packing of gold complexes within the nanocarrier was confirmed spectroscopically, as upon micelle formation a new absorption band at 500 nm emerged (Figure 23e).[284] Confocal microscopy showed that **P17** is taken up by HeLa cells and colocalizes with the endosome. Cytotoxicity towards HeLa cells was assessed by incubation with either **AP228** or **AP209** as a free drug or encapsulated within micelles. The results of these experiments showed that compared to 1 μM free drug, non-biodegradable **P17** with 500 nM of the drug performed only marginally better. Although ICP-MS analysis confirmed improved uptake of both metal drugs when loaded in **P17** by cells compared to the free drug formulation an inefficient release of the gold complex may explain these marginal differences. However, the biodegradable **P17** functionalized with Bcl-2 siRNA and loaded with **AP228** reduced cell viability more effectively than the free **AP228** drug. The latter observation can be explained by their intracellular degradation and the resulting enhanced release of their cytotoxic cargo.[284]

Recently, Marques, Fernandes and co-workers[289] reported the loading of the $[Au(cdc)_2]^-$ complex (cdc = cyanodithioimidocarbonate) in copolymer micelles (BCMs-$[Au(cdc)_2]^-$, **P18**) and tested their antitumour activity against ovarian cancer cells A2780 ($IC_{50} = 1.83 \pm 0.62$ μM) and A2780cisR ($IC_{50} = 1.69 \pm 0.43$). The nano-micelles have a size of 77 ± 27 nm and can encapsulate the hydrophobic drug with a good loading efficiency of 64 %. The beneficial effect of the micellar formulation is evidenced by the fact that the Au uptake in A2780 cells is about 17 % higher for BCMs-$[Au(cdc)_2]^-$ compared to $[Au(cdc)_2]^-$. In addition to anticancer activity, BCMs-$[Au(cdc)_2]^-$ also showed antibacterial properties.

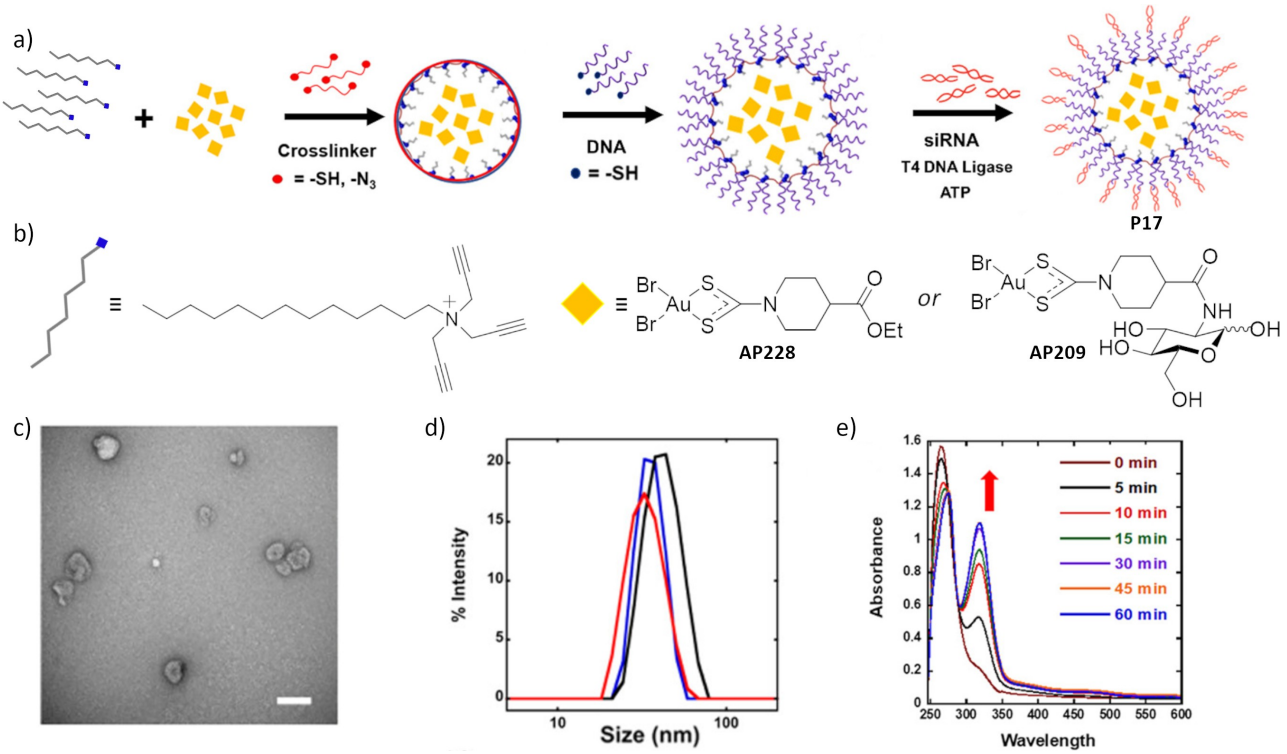

Figure 23. a) Schematic representation in the preparation of gold complex loaded NANs (**P17**). b) Chemical structure of the surfactant used to prepare NANs. Chemical structures of the gold complexes **AP228** and **AP209**. c) TEM image of **AP228** loaded NANs. Scale bar = 100 nm. d) Hydrodynamic diameter size distribution of AP 228 loaded NANs. e) UV–vis absorbance spectrum of AP228 in 50 % DMSO/PBS over 1 h. Reproduced with permission from ref. [284] copyright 2020 American Chemical Society.

Finally, the use of amphiphilic, protease-cleavable peptides to encapsulate hydrophobic metallodrugs was recently reported by Contel, Ulijn and co-workers.[290] Thus, two lipophilic [Au^{I}(NHC)Cl] complexes were encapsulated into amphiphilic decapeptides forming filamentous nano-structures with hydrophobic cores (**P19**), varying supramolecular packing arrangements and surface charge. Comparing the encapsulation efficiencies of anionic and cationic peptides, the presence of minimal gold is detected in the cationic peptides, possibly due to repulsions with the positively charged gold centre. *In vitro*, the gold-loaded peptide nanofilaments displayed enhanced cytotoxicity in comparison to the free Au^{I} compounds, when exposed to Caki-1 and MDA-MB-231 cancerous cell lines (overexpressing MMP-9), while no cytotoxicity was observed in non-cancerous lung fibroblasts (IMR-90). Such selective anti-proliferative effects were postulated to be due to the enhanced proteolytic activity in the vicinity of the cancer cells, leading to drug-bound peptide fragments with enhanced cellular uptake. The loss of the chlorido ligand, and subsequent coordination of the resulting [Au^{I}(NHC)]$^{+}$ fragment to peptides, may generate new bioconjugates that may be more cytotoxic and selective than the [AuCl(NHC)] precursors.

3.2. Particle Formulations Based on Covalently Tethered Gold Compounds

The covalent attachment of drugs on the surface of the nanocarriers enhances the stability of the cargo-carrier assembly, preventing premature release.[243,291] However, this strategy implies the chemical modification of the drugs, and thus important differences in the therapeutic activity can occur.[243,291] In the case of gold-based anticancer compounds two main grafting-based strategies have been used so far to produce nanomedicines. In the first case, gold compounds were chemically modified to become amphiphilic building blocks capable of self-assembling into nano-aggregates. In the second case, the conjugation of gold compounds with biomolecules was used to transport and protect the metal complex.

Pearson, Lu and Stenzel reported the use of glyocopolymer-based self-assembled nm-sized micelles (**P20** in Figure 24) as a delivery system of AF analogues against ovarian cancer cells (OVCAR-3 cells).[292] To this end, the authors prepared block copolymers based on oligo(ethylene glycol)methyl ether methacrylate and thioacethylglucose-acrylate by reversible addition-fragmentation chain-transfer (RAFT) polymerization (Figure 24). The advantage of using RAFT-polymerization to prepare the polymeric building blocks relies on the precise control over composition, molecular weight, and chemical functionality that can be obtained.[293] Thus, three different block copolymer systems were prepared: Poly(OEGMEMA)$_{34}$-b-poly(1-AuPEt$_3$)$_{47}$ (**P20a**) and the two shorter block copolymers Poly(F-OEGMEMA)$_{32}$-b-poly(1-AuPEt$_3$)$_{27}$ (**P20b**) and Poly(F-OEGMEMA)$_{32}$-b-poly(1-AuPEt$_3$)$_{7}$ (**P20c**, OEGMEMA = oligo(ethylene glycol) methyl ether methacrylate). Complexation yields of 54, 53, and 63 % for **a**, **b** and **c**, respectively were determined by TGA. While the self-assembly of polymer **a** resulted in the formation of 28 nm-sized micelles, the two shorter polymers **b** and **c** formed micelles with sizes of 23 and 9 nm, respectively (determined via DLS).[292] Cytotoxicity studies using OVCAR-3 cells were performed in cell media with or without the addition of fetal serum albumin to evaluate the stability of the micellar Au^{I} complexes. The gold-bearing block copolymers were toxic in both serum and serum-free media, although to a lesser extent than free AF. For example, the IC$_{50}$ of AF in a serum albumin-containing sample was ca. 1 μM, whereas the IC$_{50}$ of **P20b** and **P20c** was ca. 16 and 19 μM, respectively (the IC$_{50}$ for **P20a** was obtained only in serum albumin-free media and was 22 μM). In addition, the gold compound appears less susceptible to deactivation by biological species, because of the presence of a protective micelle. Cellular uptake studies on ovarian cancer cells (OVCAR-3 cells) showed that **P20c** was taken up via endocytosis, colocalizing in the lysosomes.[292] Although the latter finding indicates that the *in vitro* performance of **P20** is not optimal, further studies of the *in vivo* behaviour of this type of formulation are needed to determine its true potential, as a reduction of the acute is expected, with the possibility that some therapeutic effect will be maintained.

A similar strategy in using polymeric-glycol-based conjugates that exhibit toxicity toward hypoxic cells was reported by Narain and co-workers in 2013.[294] In this work, positively charged glycopolymer-based and dithiocarbamate-bearing acrylamide polymers were prepared by RAFT polymerization and functionalized in a second step with Au^{I} phosphine, by complexation with the dithiocarbamate groups (**P21** in Figure 25). Dispersions of the polymers in deionized water yielded particles of approximately 140 nm or 240 nm in size and positively charged (ζ-pot approximately +35 mV), depending on whether low (10 kDa) or high (30 kDa) weight polymers were used. Importantly, the NP dispersion formed stable colloids that can be stored at 4 °C for an extended period (up to 6 months). ICP-MS analysis showed that the gold content was higher for the smaller (140 nm) NPs (0.696 ppm/0.06 mg mL^{-1}) compared to the larger particles (0.438 ppm/0.06 mg mL^{-1}), which the authors attributed to the bulky chains of 30 kDa polymers that sterically hinder gold complexation by the dithiocarbamate groups. Both NPs showed significant cytotoxicity

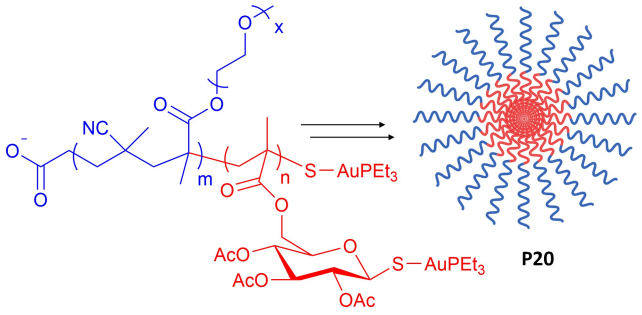

Figure 24. Micellar aggregates formed from AF-bearing oligo(ethylene glycol) methyl ether methacrylate block copolymers (**P20a-c**).[292]

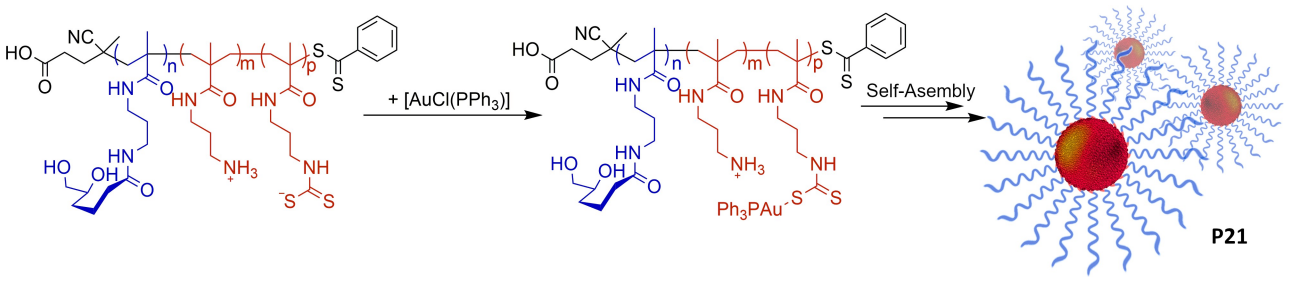

Figure 25. Chemical structure of the positively charged glyco-based and dithiocarbamate bearing acrylamide polymer and its complexation with [AuCl(PPh$_3$)]. The Au-functionalized polymers form self-assembled micelles in aqueous solutions, with a gold complex based core and a glyco-shell (**P21**).[294]

under hypoxic conditions against MCF-7 cells, which was not observed in normoxic MCF-7 cells. This selectivity in toxicity toward hypoxic cells was explained by a more complex interplay given by the known mitochondrial toxicity of Au^{I} compounds and the presence of abnormally enlarged mitochondria of hypoxic cells.[73,84]

In 2017, Che and co-workers[295] reported the preparation of amphiphilic covalent Au^{III}-porphyrin conjugates that can yield pH-responsive self-assembled micellar aggregates (**P22** in Figure 26) and were used for the delivery of gold complexes to HCT116 colon cancer cells. The amphiphilic gold complex-based polymer was prepared upon esterification of a mono-carboxylic acid analogue of **Au-1a** ([Au(TPP-COOH)]Cl (TPP-COOH = 5,10,15,20-tetraphenylporphyrin monocarboxylic acid), **Au-1a-COOH**) with H$_3$CO-PEG5000–OH, which, when dispersed in PBS, forms 120 nm-sized micelles (Figure 26b). The cellular uptake was studied using both cancer and non-tumourigenic cancer cells. The self-assembled micelles accumulated more efficiently in cancer cells, such as colorectal carcinoma (HCT116), human ovarian carcinoma (A2780), and its drug-resistant variant (A2780adr), compared to the non-PEGylated gold compound. Due to the presence of a hydrolysable ester bond between the hydrophobic headgroup of the gold complex and the hydrophilic PEG chain, **Au-1a-COOH** was released in lysosomes by acid-catalysed ester hydrolysis. The hydrolysis in living cells was detected by ultra-performance liquid chromatography coupled quadrupole time-of-flight mass spectrometry (UPLC-QTOF-MS) in colon cancer cells (HCT116). The *in vivo* anticancer activity of the micellar formulation was tested on HCT116 mice xenografts (intravenous injection; dose: 2 or 4 mg kg^{-1}) and a significant reduction in tumour volume (41 and 58 %, respectively) was found after 24 days of treatment compared to the control (Figure 26c). The authors did not comment on the survival rates of the experiments. Biodistribution studies on HCT116 mouse xenografts subjected to single-dose injection of **P22** showed a higher accumulation of gold in tumours than in the liver, spleen, lung, or kidney, suggesting an efficient transport system to diseased cells. This can most probably be explained by a combination of two factors: first, the presence of PEG chains of the NPs decreases the uptake by the RES system, which increases the blood-circulation lifetime of the NPs in the bloodstream;[204,296,297] second, the EPR effect may additionally contribute to a greater NP accumulation in the tumour.[298]

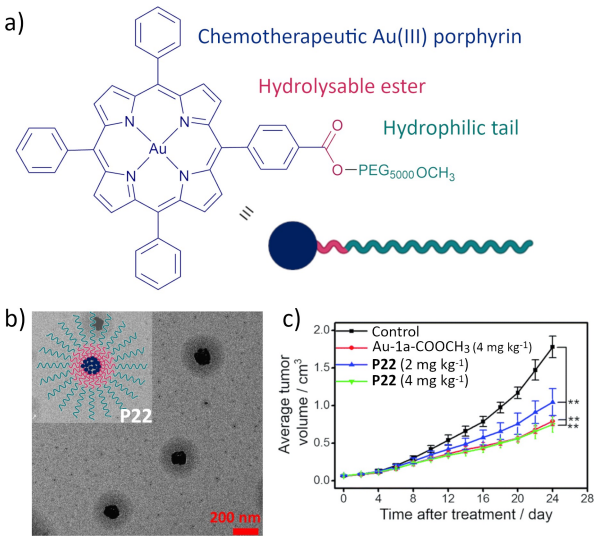

Figure 26. a) Chemical structure of the amphiphilic covalent Au^{III}-porphyrin surfactant (Au-1a-COOH). b) TEM image of self-assembled aggregates **P22** (size ca. 120 nm). c) Changes in tumour volume in mice ($n = 8$) after treatment with solvent control, ** denotes $p < 0.01$ vs. control. Reproduced with permission from ref. [295] copyright 2020 The Royal Society of Chemistry.

Most recently, Bai and co-workers[299] prepared a cRGD-functionalized, self-assembled Au^{III} porphyrin nano-drug (**P23** in Figure 27) that combines drug release with photothermal therapy (PTT) in one particle. Stimuli-triggered drug release was possible as **P23** disassembles in acidic media. Owing to the porphyrinic component of the released gold complex, PTT was used for anti-tumour treatment (Figure 27a). These tetra-(4-pyridyl) porphyrin Au^{III} (**AuT-PyP**)-based nano-aggregates had an average diameter of 65 nm (by TEM, Figure 27b). The aggregates were reported to maintain good colloidal stability for up to 5 days. Due to its pyridyl group, the compound is protonated in acidic environments (e.g., in the lysosome), triggering the degradation of the nanoparticle by electrostatic repulsive forces. Moreover, **P23** showed a dose- and irradiation-time-dependent photothermal effect, with random aggregation of the

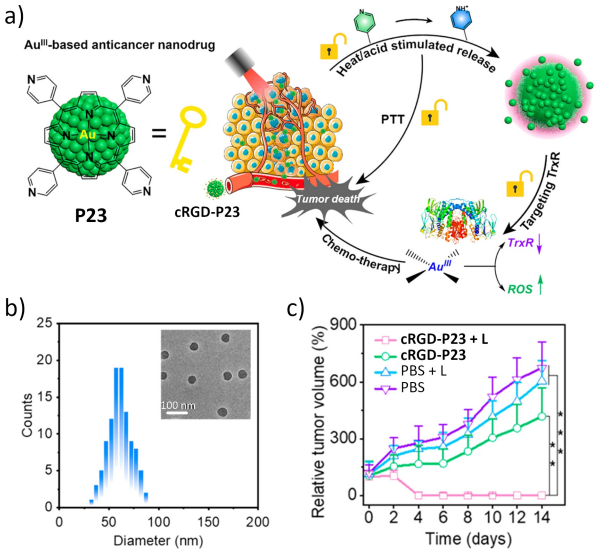

Figure 27. a) Schematic illustration of the heat/acid dual responsive behaviour of cRGD-AuPNSs (**P23**) for synergistic chemo-photothermal therapy. b) Size distribution and TEM image (inset) of AuPNSs. c) Relative tumour growth profiles and changes in body weight, respectively, during the therapy. "L" refers to the irradiation. Irradiation power (635 nm) = 0.8 W cm^{-2} (for 5 min); dose = 10 mg kg^{-1}. Reproduced with permission form ref. [299] copyright 2021 American Chemical Society.

gold complex within the nanocarrier increasing the PTT efficacy, which was ≈48.2 %. X-ray photoelectron spectroscopy (XPS) was used to demonstrate that the main oxidation state of the gold in the NPs was indeed Au^{III}. To test the possibility of active anticancer targeted therapy, **P23** was functionalized with the tumour-targeting peptide cRGD by first capping the NPs with bovine serum albumin (AuPNS-BSA) and then coupling the peptide, resulting in **cRGD-P23**. *In vitro* results showed that **cRGD-P23** accumulated in tumour cells, reaching a maximum at 6 h incubation. *In vivo* antitumour activity was investigated in HeLa tumour-bearing mice: remarkably, cotreatment of animals with **cRGD-P23** and PTT resulted in tumour inhibition rates of 100 %, while tumour inhibition with **cRGD-P23** without PTT was only 38 % (Figure 27c). All irradiation dosages (635 nm, 0.8 W cm^{-2}) lasted for 5 min and the dosage of the nano-formulation administered was 10 mg kg^{-1}.[299]

Bioconjugation of drugs to protein-based carriers (e.g., antibodies) has emerged as an interesting and promising strategy to improve the pharmacological properties of anticancer drugs and is successfully entering clinical practice.[300,301] For Au^{I} compounds, the affinity of Au for cysteine residues of serum proteins, especially human serum albumin (HSA), is considered a major reactivity problem that eventually leads to drug deactivation. Nevertheless, bioconjugation of metallodrugs with HSA has been proposed as a strategy to improve drug circulation[302] and accumulation in tumours.[303] Similarly, the conjugation of gold compounds to antibodies has been proposed as a strategy for targeted delivery.[102,103] Protein-metallodrug conjugates, while interesting systems for developing new nanomedicines, cannot solve the problem of delivering high payloads to diseased cells.

4. Summary and Outlook

In this review, we presented the advantages of gold-based compounds for anticancer treatment and described their peculiar and diverse biological activity. Further, we discussed the design, preparation, and performance of micro- and nanoparticles for the delivery of gold complexes in the search for new nanomedicines against cancer. Experimentally, translating compounds with excellent activity *in vitro* and possibly *in vivo* to the clinic is a challenge. Apart from the immense efforts in empirical synthetic work, the search for new hit compounds with better selectivity, solubility, and stability should also look for principles from emerging research areas to achieve improvements. For example, the advanced molecular designs combined with bioinformatics tools are enabling a better understanding of the structural factors that determine structure–activity relationships leading to new gold complexes with previously unknown MoAs, such as G4 s stabilization or UPS system modulation, which can be used to treat many types of drug-resistant cancers. We anticipate that, in the future, the use of big data libraries in combination with machine learning and artificial intelligence principles will play an important role in the development of superior gold compounds to fight cancer.[304,305]

In addition to molecular design, the use of NPs for the delivery of bioactive gold complexes has the potential to greatly improve the pharmacological properties of this class of metallodrugs. Some of the benefits of the partnership between gold metallodrugs and NPs have already become apparent in the early years of research in this field. First, the encapsulation of gold complexes in NPs can protect them from chemical degradation and reduces their undesirable and acute toxicity to healthy tissues and cells. Second, it has been shown that gold compounds can be targeted to cancer cells by exploiting the EPR effect or by functionalizing the surface of NPs with ligands that bind to cell surface receptors (e.g., exploiting transferrin receptor-1 or GRP receptors). Third, by tuning the chemical composition of the NPs, stimuli-triggered gold release can be obtained, enabling ideally a safe and effective spatial-temporal control over the drug release. Altogether, the use of NPs for gold delivery applications represents a promising alternative to promote their translation from the laboratory to clinical applications.

However, compared to a large number of existing nanomedicines based on organic compounds as anticancer drugs,[306–308] examples involving gold compounds are relatively rare. This is surprising, as it has been shown that the use of NPs can solve the typical drawbacks of these compounds for biological applications. Considering the first reported particle-based systems for gold delivery, there are recent examples that aim to improve important pharmacological properties by implementing stimuli-responsive drug release and active targeting of the nanocarrier towards cancer cells. Importantly, recent examples testing NP-based gold formulations in tumour-bearing mice demonstrated

tumour-suppressive activity while reducing acute drug toxicity.

The beneficial effects on the use of nanoparticles for the delivery of gold compounds are evident in the first reported examples (Table S2, Supporting Information). In general reduction of the systemic toxicity while maintaining the activity of the gold compound is consistently reported. However, the available evidence is still scarce and *in vivo* studies should carefully consider factors such as NP stability and drug release profiles. For example, it will be critical to work thoroughly on the ability to deliver a high payload of the drug to the diseased site while avoiding unwanted bioaccumulation of the nanocarrier. Fortunately, this does not appear to be a hopeless task, as many new nanocarriers have been reported capable of releasing the cargo in the presence of specific external stimuli that trigger the degradation of the particles and facilitate the clearance of the nanocarrier from the body. A major hurdle of NPs is active targeting toward cancer as so far, the effects reported *in vitro* studies have not been as evident in clinical trials, and there is increasing evidence that the influence of the protein corona may play a crucial role in this regard.[309–312] Despite these recent efforts to develop "smart" nanomedicines, more intensive research in this area has the potential to develop safer and less toxic gold-based cancer therapies that could enter clinical trials.

Acknowledgements

G.M.-A thanks the funding by the Carl Friedrich von Siemens Research Fellowship of the Alexander von Humboldt Foundation. Support from TUM Innovation Network "Artificial Intelligence Powered Multifunctional Materials Design" (ARTEMIS) is gratefully acknowledged. Open Access funding enabled and organized by *Projekt DEAL. Open Access funding enabled and organized by Projekt DEAL.*

Conflict of Interest

The authors declare no conflict of interest.

Keywords: Anticancer · Gold Compounds · Nano-Formulation · Nanomedicine · Nanoparticles

[1] H. Sung, J. Ferlay, R. L. Siegel, M. Laversanne, I. Soerjomataram, A. Jemal, F. Bray, *CA Cancer J. Clin.* **2021**, *71*, 209–249.
[2] S. Reardon, *Science* **2011**, *333*, 558–559.
[3] S. Pilleron, D. Sarfati, M. Janssen-Heijnen, J. Vignat, J. Ferlay, F. Bray, I. Soerjomataram, *Int. J. Cancer* **2019**, *144*, 49–58.
[4] World Health Organization, WHO, *WHO Report on Cancer: Setting Priorities, Investing Wisely and Providing Care for All.*, World Health Organization, Geneva, **2020**.
[5] B. Rosenberg, *Interdiscip. Sci. Rev.* **1978**, *3*, 134–147.
[6] S. Rottenberg, C. Disler, P. Perego, *Nat. Rev. Cancer* **2021**, *21*, 37–50.
[7] L. Kelland, *Nat. Rev. Cancer* **2007**, *7*, 573–584.
[8] I. Pötsch, D. Baier, B. K. Keppler, W. Berger, in *Met. Anticancer Agents*, The Royal Society Of Chemistry, Cambridge, **2019**, pp. 308–347.
[9] B. Oronsky, C. M. Ray, A. I. Spira, J. B. Trepel, C. A. Carter, H. M. Cottrill, *Med. Oncol.* **2017**, *34*, 103.
[10] A. Bamias, C. Bamia, F. Zagouri, E. Kostouros, K. Kakoyianni, A. Rodolakis, G. Vlahos, D. Haidopoulos, N. Thomakos, A. Antsaklis, M. A. Dimopoulos, *Oncology* **2013**, *84*, 158–165.
[11] *Metal-Based Anticancer Agents* (Eds.: A. Casini, A. Vessières, S. M. Meier-Menches), Royal Society Of Chemistry, Cambridge, **2019**.
[12] T. Lazarević, A. Rilak, Ž. D. Bugarčić, *Eur. J. Med. Chem.* **2017**, *142*, 8–31.
[13] E. J. Anthony, E. M. Bolitho, H. E. Bridgewater, O. W. L. Carter, J. M. Donnelly, C. Imberti, E. C. Lant, F. Lermyte, R. J. Needham, M. Palau, P. J. Sadler, H. Shi, F. -X. Wang, W. -Y. Zhang, Z. Zhang, *Chem. Sci.* **2020**, *11*, 12888–12917 .
[14] L. Zhang, N. Montesdeoca, J. Karges, H. Xiao, *Angew. Chem. Int. Ed.* **2023**, *2023*, e202300662 .
[15] S. Nobili, E. Mini, I. Landini, C. Gabbiani, A. Casini, L. Messori, *Med. Res. Rev.* **2010**, *30*, 550–580.
[16] B. Bertrand, A. Casini, *Dalton Trans.* **2014**, *43*, 4209–4219.
[17] C. Nardon, G. Boscutti, D. Fregona, *Anticancer Res.* **2014**, *34*, 487–492.
[18] P. I. Da Silva Maia, V. M. Deflon, U. Abram, *Future Med. Chem.* **2014**, *6*, 1515–1536.
[19] T. Zou, C. T. Lum, C.-N. N. Lok, J.-J. J. Zhang, C.-M. M. Che, *Chem. Soc. Rev.* **2015**, *44*, 8786–8801.
[20] A. Casini, R. W. Y. Sun, I. Ott, in *Met. Dev. Action Anticancer Agents* (Eds.: S. Astrid, S. Helmut, F. Eva, K. O. S. Roland), De Gruyter, Amsterdam, **2018**, pp. 199–217.
[21] G. G. Graham, M. W. Whitehouse, G. R. Bushell, *Inflammopharmacology* **2008**, *16*, 126–132.
[22] J. M. Madeira, D. L. Gibson, W. F. Kean, A. Klegeris, *Inflammopharmacology* **2012**, *20*, 297–306.
[23] A. Casini, A. Guerri, C. Gabbiani, L. Messori, *J. Inorg. Biochem.* **2008**, *102*, 995–1006.
[24] C. L. Ventola, *P&T* **2017**, *42*, 742–755.
[25] K. Riehemann, S. W. Schneider, T. A. Luger, B. Godin, M. Ferrari, H. Fuchs, *Angew. Chem. Int. Ed.* **2009**, *48*, 872–897; *Angew. Chem.* **2009**, *121*, 886–913.
[26] A. Akinc, M. A. Maier, M. Manoharan, K. Fitzgerald, M. Jayaraman, S. Barros, S. Ansell, X. Du, M. J. Hope, T. D. Madden, B. L. Mui, S. C. Semple, Y. K. Tam, M. Ciufolini, D. Witzigmann, J. A. Kulkarni, R. van der Meel, P. R. Cullis, *Nat. Nanotechnol.* **2019**, *14*, 1084–1087.
[27] Y. H. Chung, V. Beiss, S. N. Fiering, N. F. Steinmetz, *ACS Nano* **2020**, *14*, 12522–12537.
[28] M. Vert, Y. Doi, K. H. Hellwich, M. Hess, P. Hodge, P. Kubisa, M. Rinaudo, F. Schué, *Pure Appl. Chem.* **2012**, *84*, 377–410.
[29] European Commission (E.C), "Environment: Questions and Answers on the Commission Recommendation on the definition of Nanomaterial," can be found under http://ec.europa.eu/environment/chemicals/nanotech/faq/questions answers en.htm#4, **2016**.
[30] V. Wagner, A. Dullaart, A. K. Bock, A. Zweck, *Nat. Biotechnol.* **2006**, *24*, 1211–1217.
[31] J. Wolfram, M. Ferrari, *Nano Today* **2019**, *25*, 85–98.
[32] M. J. Mitchell, M. M. Billingsley, R. M. Haley, M. E. Wechsler, N. A. Peppas, R. Langer, *Nat. Rev. Drug Discovery* **2021**, *20*, 101–124.
[33] J. I. Hare, T. Lammers, M. B. Ashford, S. Puri, G. Storm, S. T. Barry, *Adv. Drug Delivery Rev.* **2017**, *108*, 25–38.

[34] G. Pillai, *SOJ Pharm. Pharm. Sci.* **2014**, *1*, 13.
[35] A. A. Halwani, *Pharmaceutics* **2022**, *14*, 106.
[36] Q. Peña, A. Wang, O. Zaremba, Y. Shi, H. W. Scheeren, J. M. Metselaar, F. Kiessling, R. M. Pallares, S. Wuttke, T. Lammers, *Chem. Soc. Rev.* **2022**, *51*, 2544–2582.
[37] E. S. Kim, C. Lu, F. R. Khuri, M. Tonda, B. S. Glisson, D. Liu, M. Jung, W. K. Hong, R. S. Herbst, *Lung Cancer* **2001**, *34*, 427–432.
[38] T. C. Johnstone, K. Suntharalingam, S. J. Lippard, *Chem. Rev.* **2016**, *116*, 3436–3486.
[39] R. M. Crist, J. H. Grossman, A. K. Patri, S. T. Stern, M. A. Dobrovolskaia, P. P. Adiseshaiah, J. D. Clogston, S. E. McNeil, *Integr. Biol.* **2013**, *5*, 66–73.
[40] C. N. Lok, T. Zou, J. J. Zhang, I. W. S. Lin, C. M. Che, *Adv. Mater.* **2014**, *26*, 5550–5557.
[41] Z. R. Goddard, M. J. Marín, D. A. Russell, M. Searcey, *Chem. Soc. Rev.* **2020**, *49*, 8774–8789.
[42] M. Fan, Y. Han, S. Gao, H. Yan, L. Cao, Z. Li, X. J. Liang, J. Zhang, *Theranostics* **2020**, *10*, 4944–4957.
[43] S. Siddique, J. C. L. Chow, *Appl. Sci.* **2020**, *10*, 3824.
[44] K. Sztandera, M. Gorzkiewicz, B. Klajnert-Maculewicz, *Mol. Pharmaceutics* **2019**, *16*, 1–23.
[45] S. Kumar, A. Diwan, P. Singh, S. Gulati, D. Choudhary, A. Mongia, S. Shukla, A. Gupta, *RSC Adv.* **2019**, *9*, 23894–23907.
[46] E. Spyratou, M. Makropoulou, E. Efstathopoulos, A. Georgakilas, L. Sihver, *Cancers* **2017**, *9*, 173.
[47] S. Jain, D. G. Hirst, J. M. O'Sullivan, *Br. J. Radiol.* **2012**, *85*, 101–113.
[48] J. B. Vines, J. H. Yoon, N. E. Ryu, D. J. Lim, H. Park, *Front. Chem.* **2019**, *7*, 167.
[49] S. R. Thomas, A. Casini, *J. Organomet. Chem.* **2021**, *938*, 121743.
[50] B. Bertrand, M. R. M. Williams, M. Bochmann, *Chem. Eur. J.* **2018**, *24*, 11840–11851.
[51] C. I. Yeo, K. K. Ooi, E. R. T. Tiekink, *Molecules* **2018**, *23*, 1410.
[52] R. P. Herrera, M. C. Gimeno, *Chem. Rev.* **2021**, *121*, 8311–8363.
[53] C. Nardon, N. Pettenuzzo, D. Fregona, *Curr. Med. Chem.* **2016**, *23*, 3374–3403.
[54] E. E. Langdon-Jones, S. J. A. A. Pope, *Chem. Commun.* **2014**, *50*, 10343–10354.
[55] G. Faa, C. Gerosa, D. Fanni, J. I. Lachowicz, V. M. Nurchi, *Curr. Med. Chem.* **2018**, *25*, 75–84.
[56] N. Mirzadeh, T. S. Reddy, S. K. Bhargava, *Coord. Chem. Rev.* **2019**, *388*, 343–359.
[57] C. K. Adokoh, *RSC Adv.* **2020**, *10*, 2975–2988.
[58] D. Buac, S. Schmitt, G. Ventro, F. Rani Kona, Q. Ping Dou, *Mini-Rev. Med. Chem.* **2012**, *12*, 1193–1201.
[59] E. Márta Nagy, L. Ronconi, C. Nardon, D. Fregona, *Mini-Rev. Med. Chem.* **2012**, *12*, 1216–1229.
[60] S. Jurgens, F. E. Kuhn, A. Casini, *Curr. Med. Chem.* **2018**, *25*, 437–461.
[61] K.-C. C. Tong, D. Hu, P.-K. K. Wan, C.-N. N. Lok, C.-M. M. Che, *Front. Chem.* **2020**, *8*, 587207.
[62] M. Porchia, M. Pellei, M. Marinelli, F. Tisato, F. Del Bello, C. Santini, *Eur. J. Med. Chem.* **2018**, *146*, 709–746.
[63] T. Zou, C. N. Lok, P. K. Wan, Z. F. Zhang, S. K. Fung, C. M. Che, *Curr. Opin. Chem. Biol.* **2018**, *43*, 30–36.
[64] C. Hu, X. Li, W. Wang, R. Zhang, L. Deng, *Curr. Med. Chem.* **2014**, *21*, 1220–1230.
[65] M. Mora, M. C. Gimeno, R. Visbal, *Chem. Soc. Rev.* **2019**, *48*, 447–462. .
[66] A. Tialiou, J. Chin, B. K. Keppler, M. R. Reithofer, *Biomedicine* **2022**, *10*, 1417.
[67] Z. Yang, G. Jiang, Z. Xu, S. Zhao, W. Liu, *Coord. Chem. Rev.* **2020**, *423*, 213492.
[68] Y. Sun, Y. Lu, M. Bian, Z. Yang, X. Ma, W. Liu, *Eur. J. Med. Chem.* **2021**, *211*, 113098.
[69] M. Zaki, S. Hairat, E. S. Aazam, *RSC Adv.* **2019**, *9*, 3239–3278.
[70] B. Glišić, U. Rychlewska, M. I. Djuran, *Dalton Trans.* **2012**, *41*, 6887–6901.
[71] V. Fernández-Moreira, R. P. Herrera, M. C. Gimeno, *Pure Appl. Chem.* **2019**, *91*, 247–269.
[72] Y. Lu, X. Ma, X. Chang, Z. Liang, L. Lv, M. Shan, Q. Lu, Z. Wen, R. Gust, W. Liu, *Chem. Soc. Rev.* **2022**, *51*, 5518–5556.
[73] A. Bindoli, M. P. Rigobello, G. Scutari, C. Gabbiani, A. Casini, L. Messori, *Coord. Chem. Rev.* **2009**, *253*, 1692–1707.
[74] S. Radisavljević, B. Petrović, *Front. Chem.* **2020**, *8*, 379.
[75] S. Parveen, F. Arjmand, S. Tabassum, *Eur. J. Med. Chem.* **2019**, *175*, 269–286.
[76] S. Jürgens, A. Casini, *Chimia* **2017**, *71*, 92.
[77] J. Ceramella, A. Mariconda, D. Iacopetta, C. Saturnino, A. Barbarossa, A. Caruso, C. Rosano, M. S. Sinicropi, P. Longo, *Bioorg. Med. Chem. Lett.* **2020**, *30*, 126905.
[78] M. G. Karaaslan, A. Aktaş, C. Gürses, Y. Gök, B. Ateş, *Bioorg. Chem.* **2020**, *95*, 103552.
[79] A. Casini, S. R. Thomas, *Chem. Lett.* **2021**, *50*, 1516–1522. .
[80] S. Yue, M. Luo, H. Liu, S. Wei, *Front. Chem.* **2020**, *8*, 543.
[81] M. A. Carvajal, J. J. Novoa, S. Alvarez, *J. Am. Chem. Soc.* **2004**, *126*, 1465–1477.
[82] A. Laguna, *Modern Supramolecular Gold Chemistry*, Wiley-VCH, Weinheim, **2008**.
[83] R. G. Pearson, *J. Am. Chem. Soc.* **1963**, *85*, 3533–3539.
[84] M. P. Rigobello, G. Scutari, A. Folda, A. Bindoli, *Biochem. Pharmacol.* **2004**, *67*, 689–696.
[85] S. Tian, F. M. Siu, C. N. Lok, Y. M. E. Fung, C. M. Che, *Metallomics* **2019**, *11*, 1925–1936.
[86] K. Yan, C. N. Lok, K. Bierla, C. M. Che, *Chem. Commun.* **2010**, *46*, 7691–7693.
[87] S. A. Pérez, C. De Haro, C. Vicente, A. Donaire, A. Zamora, J. Zajac, H. Kostrhunova, V. Brabec, D. Bautista, J. Ruiz, *ACS Chem. Biol.* **2017**, *12*, 1524–1537.
[88] B. Yu, Y. Liu, X. Peng, S. Hua, G. Zhou, K. Yan, Y. Liu, *Metallomics* **2020**, *12*, 104–113.
[89] N. S. Jamaludin, Z. J. Goh, Y. K. Cheah, K. P. Ang, J. H. Sim, C. H. Khoo, Z. A. Fairuz, S. N. B. A. Halim, S. W. Ng, H. L. Seng, E. R. T. Tiekink, *Eur. J. Med. Chem.* **2013**, *67*, 127–141.
[90] S. Urig, K. Fritz-Wolf, R. Réau, C. Herold-Mende, K. Tóth, E. Davioud-Charvet, K. Becker, *Angew. Chem. Int. Ed.* **2006**, *45*, 1881–1886; *Angew. Chem.* **2006**, *118*, 1915–1920.
[91] K. Fritz-Wolf, S. Kehr, M. Stumpf, S. Rahlfs, K. Becker, *Nat. Commun.* **2011**, *2*, 383.
[92] D. Parsonage, F. Sheng, K. Hirata, A. Debnath, J. H. McKerrow, S. L. Reed, R. Abagyan, L. B. Poole, L. M. Podust, *J. Struct. Biol.* **2016**, *194*, 180–190.
[93] T. Marzo, L. Massai, A. Pratesi, M. Stefanini, D. Cirri, F. Magherini, M. Becatti, I. Landini, S. Nobili, E. Mini, O. Crociani, A. Arcangeli, S. Pillozzi, T. Gamberi, L. Messori, *ACS Med. Chem. Lett.* **2019**, *10*, 656–660.
[94] M. J. McKeage, L. Maharaj, S. J. Berners-Price, *Coord. Chem. Rev.* **2002**, *232*, 127–135.
[95] J. H. Sze, P. V. Raninga, K. Nakamura, M. Casey, K. K. Khanna, S. J. Berners-Price, G. Di Trapani, K. F. Tonissen, *Redox. Biol.* **2020**, *28*, 101310.
[96] M. P. Rigobello, G. Scutari, R. Boscolo, A. Bindoli, *Br. J. Pharmacol.* **2002**, *136*, 1162–1168.
[97] P. J. Barnard, S. J. Berners-Price, *Coord. Chem. Rev.* **2007**, *251*, 1889–1902.
[98] J. H. Kim, E. Reeder, S. Parkin, S. G. Awuah, *Sci. Rep.* **2019**, *9*, 12335.

[99] O. Florès, D. Velic, N. Mabrouk, A. Bettaïeb, C. Tomasoni, J. M. Robert, C. Paul, C. Goze, C. Roussakis, E. Bodio, *ChemBioChem* **2019**, *20*, 2255–2261.

[100] M. A. Grin, S. I. Tikhonov, A. S. Petrova, V. A. Pogorilyy, A. N. Noev, V. V. Tatarskiy, D. B. Shpakovsky, E. R. Milaeva, E. V. Kalinina, N. N. Chernov, A. A. Shtil, A. F. Mironov, A. D. Kaprin, E. V. Filonenko, *Anti-Cancer Agents Med. Chem.* **2019**, *20*, 49–58.

[101] J. Zhang, H. Zou, J. Lei, B. He, X. He, H. H. Y. Sung, R. T. K. Kwok, J. W. Y. Lam, L. Zheng, B. Z. Tang, *Angew. Chem. Int. Ed.* **2020**, *59*, 7097–7105; *Angew. Chem.* **2020**, *132*, 7163–7171.

[102] M. J. Matos, C. Labão-Almeida, C. Sayers, O. Dada, M. Tacke, G. J. L. Bernardes, *Chem. Eur. J.* **2018**, *24*, 12250–12253.

[103] N. Curado, G. Dewaele-Le Roi, S. Poty, J. S. Lewis, M. Contel, *Chem. Commun.* **2019**, *55*, 1394–1397.

[104] R. T. Mertens, W. C. Jennings, S. Ofori, J. H. Kim, S. Parkin, G. F. Kwakye, S. G. Awuah, *JACS Au* **2021**, *1*, 439–449.

[105] S. K. Goetzfried, C. M. Gallati, M. Cziferszky, R. A. Talmazan, K. Wurst, K. R. Liedl, M. Podewitz, R. Gust, *Inorg. Chem.* **2020**, *59*, 15312–15323.

[106] P. J. Barnard, M. V. Baker, S. J. Berners-Price, D. A. Day, *J. Inorg. Biochem.* **2004**, *98*, 1642–1647.

[107] J. L. Hickey, R. A. Ruhayel, P. J. Barnard, M. V. Baker, S. J. Berners-Price, A. Filipovska, *J. Am. Chem. Soc.* **2008**, *130*, 12570–12571.

[108] T. Zou, C. T. Lum, C. N. Lok, W. P. To, K. H. Low, C. M. Che, *Angew. Chem. Int. Ed.* **2014**, *53*, 5810–5814; *Angew. Chem.* **2014**, *126*, 5920–5924.

[109] S. Sen, M. W. Perrin, A. C. Sedgwick, E. Y. Dunsky, V. M. Lynch, X. P. He, J. L. Sessler, J. F. Arambula, *Chem. Commun.* **2020**, *56*, 7877–7880.

[110] S. Sen, Y. Li, V. Lynch, K. Arumugam, J. L. Sessler, J. F. Arambula, *Chem. Commun.* **2019**, *55*, 10627–10630.

[111] I. Ott, in *Adv. Inorg. Chem.* (Eds.: P. J. Sadler, R. van Eldik), Academic Press, San Diego, **2020**, pp. 121–148.

[112] C. M. Gallati, S. K. Goetzfried, M. Ausserer, J. Sagasser, M. Plangger, K. Wurst, M. Hermann, D. Baecker, B. Kircher, R. Gust, *Dalton Trans.* **2020**, *49*, 5471–5481.

[113] B. Dominelli, C. H. G. Jakob, J. Oberkofler, P. J. Fischer, E. M. Esslinger, R. M. Reich, F. Marques, T. Pinheiro, J. D. G. Correia, F. E. Kühn, *Eur. J. Med. Chem.* **2020**, *203*, 112576.

[114] C. H. G. Jakob, B. Dominelli, E. M. Hahn, T. O. Berghausen, T. Pinheiro, F. Marques, R. M. Reich, J. D. G. Correia, F. E. Kühn, *Chem. Asian J.* **2020**, *15*, 2754–2762.

[115] D. Curran, H. Müller-Bunz, S. I. Bär, R. Schobert, X. Zhu, M. Tacke, *Molecules* **2020**, *25*, 3474.

[116] N. Casares, M. O. Pequignot, A. Tesniere, F. Ghiringhelli, S. Roux, N. Chaput, E. Schmitt, A. Hamai, S. Hervas-Stubbs, M. Obeid, F. Coutant, D. Métivier, E. Pichard, P. Aucouturier, G. Pierron, C. Garrido, L. Zitvogel, G. Kroemer, *J. Exp. Med.* **2005**, *202*, 1691–1701.

[117] O. Kepp, L. Senovilla, G. Kroemer, *Oncotarget* **2014**, *5*, 5190–5191.

[118] S. Sen, S. Hufnagel, E. Y. Maier, I. Aguilar, J. Selvakumar, J. E. Devore, V. M. Lynch, K. Arumugam, Z. Cui, J. L. Sessler, J. F. Arambula, *J. Am. Chem. Soc.* **2020**, *142*, 20536–20541.

[119] M. T. Proetto, K. Alexander, M. Melaimi, G. Bertrand, N. C. Gianneschi, *Chem. Eur. J.* **2021**, *27*, 3772–3778.

[120] M. Altaf, M. Monim-Ul-Mehboob, A. A. A. Seliman, A. A. Isab, V. Dhuna, G. Bhatia, K. Dhuna, *J. Organomet. Chem.* **2014**, *765*, 68–79.

[121] C. H. Chui, R. S. M. Wong, R. Gambari, G. Y. M. Cheng, M. C. W. Yuen, K. W. Chan, S. W. Tong, F. Y. Lau, P. B. S. Lai, K. H. Lam, C. L. Ho, C. W. Kan, K. S. Y. Leung, W. Y. Wong, *Bioorg. Med. Chem.* **2009**, *17*, 7872–7877.

[122] E. Ortega, A. Zamora, U. Basu, P. Lippmann, V. Rodríguez, C. Janiak, I. Ott, J. Ruiz, *J. Inorg. Biochem.* **2020**, *203*, 110910.

[123] M. S. Alsaeedi, B. A. Babgi, M. A. Hussien, M. H. Abdellattif, M. G. Humphrey, *Molecules* **2020**, *25*, 1033.

[124] H. Zou, J. Zhang, C. Wu, B. He, Y. Hu, H. H. Y. Sung, R. T. K. Kwok, J. W. Y. Lam, L. Zheng, B. Z. Tang, *ACS Nano* **2021**, *15*, 9176–9185.

[125] D. Śmiłowicz, J. C. Slootweg, N. Metzler-Nolte, *Mol. Pharmaceutics* **2019**, *16*, 4572–4581.

[126] S. A. Sousa, J. H. Leitão, R. A. L. Silva, D. Belo, I. C. Santos, J. F. Guerreiro, M. Martins, D. Fontinha, M. Prudêncio, M. Almeida, D. Lorcy, F. Marques, *J. Inorg. Biochem.* **2020**, *202*, 110904.

[127] L. Brustolin, N. Pettenuzzo, C. Nardon, S. Quarta, L. Marchiò, B. Biondi, P. Pontisso, D. Fregona, *Dalton Trans.* **2019**, *48*, 16017–16025.

[128] S. Gukathasan, S. Parkin, S. G. Awuah, *Inorg. Chem.* **2019**, *58*, 9326–9340.

[129] T. M. Khan, N. S. Gul, X. Lu, J. H. Wei, Y. C. Liu, H. Sun, H. Liang, C. Orvig, Z. F. Chen, *Eur. J. Med. Chem.* **2019**, *163*, 333–343.

[130] D. van der Westhuizen, C. A. Slabber, M. A. Fernandes, D. F. Joubert, G. Kleinhans, C. J. van der Westhuizen, A. Stander, O. Q. Munro, D. I. Bezuidenhout, *Chem. Eur. J.* **2021**, *27*, 8295–8307.

[131] R. D. Teo, H. B. Gray, P. Lim, J. Termini, E. Domeshek, Z. Gross, *Chem. Commun.* **2014**, *50*, 13789–13792.

[132] A. Casini, M. A. Cinellu, G. Minghetti, C. Gabbiani, M. Coronnello, E. Mini, L. Messori, *J. Med. Chem.* **2006**, *49*, 5524–5531.

[133] G. Gorini, F. Magherini, T. Fiaschi, L. Massai, M. Becatti, A. Modesti, L. Messori, T. Gamberi, *Biomedicine* **2021**, *9*, 871.

[134] L. Ronconi, L. Giovagnini, C. Marzano, F. Bettìo, R. Graziani, G. Pilloni, D. Fregona, *Inorg. Chem.* **2005**, *44*, 1867–1881.

[135] N. Pettenuzzo, L. Brustolin, E. Coltri, A. Gambalunga, F. Chiara, A. Trevisan, B. Biondi, C. Nardon, D. Fregona, *ChemMedChem* **2019**, *14*, 1162–1172.

[136] C. Nardon, F. Chiara, L. Brustolin, A. Gambalunga, F. Ciscato, A. Rasola, A. Trevisan, D. Fregona, *ChemistryOpen* **2015**, *4*, 183–191.

[137] L. Ronconi, D. Fregona, *Dalton Trans.* **2009**, 10670.

[138] M. F. Tomasello, C. Nardon, V. Lanza, G. Di Natale, N. Pettenuzzo, S. Salmaso, D. Milardi, P. Caliceti, G. Pappalardo, D. Fregona, *Eur. J. Med. Chem.* **2017**, *138*, 115–127.

[139] A. P. Martins, A. Marrone, A. Ciancetta, A. G. Cobo, M. Echevarría, T. F. Moura, N. Re, A. Casini, G. Soveral, *PLoS One* **2012**, *7*, e37435.

[140] A. De Almeida, A. F. Mósca, D. Wragg, M. Wenzel, P. Kavanagh, G. Barone, S. Leoni, G. Soveral, A. Casini, *Chem. Commun.* **2017**, *53*, 3830–3833.

[141] B. Aikman, A. De Almeida, S. M. Meier-Menches, A. Casini, *Metallomics* **2018**, *10*, 696–712.

[142] A. P. Martins, A. Ciancetta, A. deAlmeida, A. Marrone, N. Re, G. Soveral, A. Casini, *ChemMedChem* **2013**, *8*, 1086–1092.

[143] C.-M. Che, R. W.-Y. Sun, W.-Y. Yu, C.-B. Ko, N. Zhu, H. Sun, *Chem. Commun.* **2003**, 1718–1719.

[144] D. Hu, Y. Liu, Y. T. Lai, K. C. Tong, Y. M. Fung, C. N. Lok, C. M. Che, *Angew. Chem. Int. Ed.* **2016**, *55*, 1387–1391; *Angew. Chem.* **2016**, *128*, 1409–1413.

[145] K. C. Tong, C. N. Lok, P. K. Wan, D. Hu, Y. M. E. Fung, X. Y. Chang, S. Huang, H. Jiang, C. M. Che, *Proc. Natl. Acad. Sci. USA* **2020**, *117*, 1321–1329.

[146] R. V. Parish, J. Mack, L. Hargreaves, J. P. Wright, R. G. Buckley, A. M. Elsome, S. P. Fricker, B. R. C. Theobald, *J. Chem. Soc. Dalton Trans.* **1996**, 69–74.
[147] M. R. M. Williams, B. Bertrand, D. L. Hughes, Z. A. E. Waller, C. Schmidt, I. Ott, M. O'Connell, M. Searcey, M. Bochmann, *Metallomics* **2018**, *10*, 1655–1666.
[148] R. T. Mertens, S. Parkin, S. G. Awuah, *Chem. Sci.* **2020**, *11*, 10465–10482.
[149] M. Cassandri, A. Smirnov, F. Novelli, C. Pitolli, M. Agostini, M. Malewicz, G. Melino, G. Raschellà, *Cell Death Dis.* **2017**, *3*, 17071.
[150] J. Jen, Y.-C. Wang, *J. Biomed. Sci.* **2016**, *23*, 53.
[151] C. Abbehausen, *Metallomics* **2019**, *11*, 15–28.
[152] M. A. Franzman, A. M. Barrios, *Inorg. Chem.* **2008**, *47*, 3928–3930.
[153] A. Laskay, C. Garino, Y. O. Tsybin, L. Salassa, A. Casini, *Chem. Commun.* **2015**, *51*, 1612–1615.
[154] C. Abbehausen, R. E. F. De Paiva, R. Bjornsson, S. Q. Gomes, Z. Du, P. P. Corbi, F. A. Lima, N. Farrell, *Inorg. Chem.* **2018**, *57*, 218–230.
[155] A. Jacques, C. Lebrun, A. Casini, I. Kieffer, O. Proux, J.-M. Latour, O. Sénèque, *Inorg. Chem.* **2015**, *54*, 4104–4113.
[156] F. Mendes, M. Groessl, A. A. Nazarov, Y. O. Tsybin, G. Sava, I. Santos, P. J. Dyson, A. Casini, *J. Med. Chem.* **2011**, *54*, 2196–2206.
[157] M. F. Langelier, J. L. Planck, S. Roy, J. M. Pascal, *J. Biol. Chem.* **2011**, *286*, 10690–10701.
[158] A. Citta, V. Scalcon, P. Göbel, B. Bertrand, M. Wenzel, A. Folda, M. P. Rigobello, E. Meggers, A. Casini, *RSC Adv.* **2016**, *6*, 79147–79152.
[159] M. N. Wenzel, S. M. Meier-Menches, T. L. Williams, E. Rämisch, G. Barone, A. Casini, *Chem. Commun.* **2018**, *54*, 611–614.
[160] M. N. Wenzel, R. Bonsignore, S. R. Thomas, D. Bourissou, G. Barone, A. Casini, *Chem. Eur. J.* **2019**, *25*, 7628–7634.
[161] S. R. Thomas, R. Bonsignore, J. Sánchez Escudero, S. M. Meier-Menches, C. M. Brown, M. O. Wolf, G. Barone, L. Y. P. Luk, A. Casini, *ChemBioChem* **2020**, *21*, 3071–3076.
[162] C. Schmidt, M. Zollo, R. Bonsignore, A. Casini, S. M. Hacker, *Chem. Commun.* **2022**, *58*, 5526–5529.
[163] A. S. Arojojoye, R. T. Mertens, S. Ofori, S. R. Parkin, S. G. Awuah, *Molecules* **2020**, *25*, 5735.
[164] J. H. Kim, S. Ofori, S. Parkin, H. Vekaria, P. G. Sullivan, S. G. Awuah, *Chem. Sci.* **2021**, *12*, 7467–7479.
[165] R. H. Shoemaker, *Nat. Rev. Cancer* **2006**, *6*, 813–823.
[166] C. K. L. Li, R. W. Y. Sun, S. C. F. Kui, N. Zhu, C. M. Che, *Chem. Eur. J.* **2006**, *12*, 5253–5266.
[167] R. W. Y. Sun, C. N. Lok, T. T. H. Fong, C. K. L. Li, Z. F. Yang, A. F. M. Siu, C. M. Che, *Chem. Sci.* **2013**, *4*, 1979–1988.
[168] S. K. Fung, T. Zou, B. Cao, P. Y. Lee, Y. M. E. Fung, D. Hu, C. N. Lok, C. M. Che, *Angew. Chem. Int. Ed.* **2017**, *56*, 3892–3896; *Angew. Chem.* **2017**, *129*, 3950–3954.
[169] L. Messori, G. Marcon, M. A. Cinellu, M. Coronnello, E. Mini, C. Gabbiani, P. Orioli, *Bioorg. Med. Chem.* **2004**, *12*, 6039–6043.
[170] T. Gamberi, L. Massai, F. Magherini, I. Landini, T. Fiaschi, F. Scaletti, C. Gabbiani, L. Bianchi, L. Bini, S. Nobili, G. Perrone, E. Mini, L. Messori, A. Modesti, *J. Proteomics* **2014**, *103*, 103–120.
[171] H. Luo, B. Cao, A. S. C. Chan, R. W. Y. Sun, T. Zou, *Angew. Chem. Int. Ed.* **2020**, *59*, 11046–11052; *Angew. Chem.* **2020**, *132*, 11139–11145.
[172] I. Ott, X. Qian, Y. Xu, D. H. W. Vlecken, I. J. Marques, D. Kubutat, J. Will, W. S. Sheldrick, P. Jesse, A. Prokop, C. P. Bagowski, *J. Med. Chem.* **2009**, *52*, 763–770.
[173] A. Meyer, C. P. Bagowski, M. Kokoschka, M. Stefanopoulou, H. Alborzinia, S. Can, D. H. Vlecken, W. S. Sheldrick, S. Wölfl, I. Ott, *Angew. Chem. Int. Ed.* **2012**, *51*, 8895–8899; *Angew. Chem.* **2012**, *124*, 9025–9030.
[174] T. Srinivasa Reddy, S. H. Privér, N. Mirzadeh, R. B. Luwor, V. Ganga Reddy, S. Ramesan, S. K. Bhargava, *Inorg. Chem.* **2020**, *59*, 5662–5673.
[175] T. S. Reddy, D. Pooja, S. H. Privér, R. B. Luwor, N. Mirzadeh, S. Ramesan, S. Ramakrishna, S. Karri, M. Kuncha, S. K. Bhargava, *Chem. Eur. J.* **2019**, *25*, 14089–14100.
[176] Ö. Karaca, S. M. Meier-Menches, A. Casini, F. E. Kühn, *Chem. Commun.* **2017**, *53*, 8249–8260.
[177] R. Hänsel-Hertsch, M. Di Antonio, S. Balasubramanian, *Nat. Rev. Mol. Cell Biol.* **2017**, *18*, 279–284.
[178] D. Varshney, J. Spiegel, K. Zyner, D. Tannahill, S. Balasubramanian, *Nat. Rev. Mol. Cell Biol.* **2020**, *21*, 459–474.
[179] J. Spiegel, S. Adhikari, S. Balasubramanian, *Trends Chem.* **2020**, *2*, 123–136.
[180] E. Y. N. Lam, D. Beraldi, D. Tannahill, S. Balasubramanian, *Nat. Commun.* **2013**, *4*, 1796.
[181] A. K. Todd, S. M. Haider, G. N. Parkinson, S. Neidle, *Nucleic Acids Res.* **2007**, *35*, 5799–5808.
[182] A. Rangan, O. Y. Fedoroff, L. H. Hurley, *J. Biol. Chem.* **2001**, *276*, 4640–4646.
[183] A. Awadasseid, X. Ma, Y. Wu, W. Zhang, *Biomed. Pharmacother.* **2021**, *139*, 111550.
[184] N. Kosiol, S. Juranek, P. Brossart, A. Heine, K. Paeschke, *Mol. Cancer* **2021**, *20*, 40.
[185] P. Lee, Y. Zhu, J. J. Yan, R. W. Y. Sun, W. Hao, X. Liu, C. M. Che, K. K. Y. Wong, *Nanotechnol. Sci. Appl.* **2010**, *3*, 23–28.
[186] B. Bertrand, L. Stefan, M. Pirrotta, D. Monchaud, E. Bodio, P. Richard, P. Le Gendre, E. Warmerdam, M. H. De Jager, G. M. M. Groothuis, M. Picquet, A. Casini, *Inorg. Chem.* **2014**, *53*, 2296–2303.
[187] A. Arola, R. Vilar, *Curr. Top. Med. Chem.* **2008**, *8*, 1405–1415.
[188] A. Arola-Arnal, J. Benet-Buchholz, S. Neidle, R. Vilar, *Inorg. Chem.* **2008**, *47*, 11910–11919.
[189] T. Kench, R. Vilar, in *Annu. Rep. Med. Chem.* (Ed.: S. Neidle), Academic Press, San Diego, **2020**, pp. 485–515.
[190] S. M. Meier-Menches, B. Neuditschko, K. Zappe, M. Schaier, M. C. Gerner, K. G. Schmetterer, G. Del Favero, R. Bonsignore, M. Cichna-Markl, G. Koellensperger, A. Casini, C. Gerner, *Chem. Eur. J.* **2020**, *26*, 15528–15537.
[191] S. M. Meier-Menches, B. Aikman, D. Döllerer, W. T. Kloosterman, S. J. Coles, N. Santi, L. Luk, A. Casini, R. Bonsignore, *J. Inorg. Biochem.* **2020**, *202*, 110844.
[192] C. Kaußler, D. Wragg, C. Schmidt, G. Moreno-Alcántar, C. Jandl, J. Stephan, R. A. Fischer, S. Leoni, A. Casini, R. Bonsignore, *Inorg. Chem.* **2022**, *61*, 20405–20423.
[193] A. C. Anselmo, S. Mitragotri, *Bioeng. Transl. Med.* **2019**, *4*, e10143.
[194] A. K. Pearce, R. K. O'Reilly, *Bioconjugate Chem.* **2019**, *30*, 2300–2311.
[195] J. G. Croissant, Y. Fatieiev, A. Almalik, N. M. Khashab, *Adv. Healthcare Mater.* **2018**, *7*, 1700831.
[196] N. Kamaly, B. Yameen, J. Wu, O. C. Farokhzad, *Chem. Rev.* **2016**, *116*, 2602–2663.
[197] W. Poon, Y. N. Zhang, B. Ouyang, B. R. Kingston, J. L. Y. Wu, S. Wilhelm, W. C. W. Chan, *ACS Nano* **2019**, *13*, 5785–5798.
[198] T. Sun, Y. S. Zhang, B. Pang, D. C. Hyun, M. Yang, Y. Xia, *Angew. Chem. Int. Ed.* **2014**, *53*, 12320–12364; *Angew. Chem.* **2014**, *126*, 12520–12568.
[199] P. Decuzzi, B. Godin, T. Tanaka, S. Y. Lee, C. Chiappini, X. Liu, M. Ferrari, *J. Controlled Release* **2010**, *141*, 320–327.
[200] L. Talamini, M. B. Violatto, Q. Cai, M. P. Monopoli, K. Kantner, Ž. Krpetić, A. Perez-Potti, J. Cookman, D. Garry,

C. P. Silveira, L. Boselli, B. Pelaz, T. Serchi, S. Cambier, A. C. Gutleb, N. Feliu, Y. Yan, M. Salmona, W. J. Parak, K. A. Dawson, P. Bigini, *ACS Nano* **2017**, *11*, 5519–5529.
[201] P. Dogra, N. L. Adolphi, Z. Wang, Y. S. Lin, K. S. Butler, P. N. Durfee, J. G. Croissant, A. Noureddine, E. N. Coker, E. L. Bearer, V. Cristini, C. J. Brinker, *Nat. Commun.* **2018**, *9*, 4551.
[202] L. E. Van Vlerken, T. K. Vyas, M. M. Amiji, *Pharm. Res.* **2007**, *24*, 1405–1414.
[203] Q. Dai, C. Walkey, W. C. W. Chan, *Angew. Chem. Int. Ed.* **2014**, *53*, 5093–5096; *Angew. Chem.* **2014**, *126*, 5193–5196.
[204] S. Schöttler, G. Becker, S. Winzen, T. Steinbach, K. Mohr, K. Landfester, V. Mailänder, F. R. Wurm, *Nat. Nanotechnol.* **2016**, *11*, 372–377.
[205] J. Simon, L. K. Müller, M. Kokkinopoulou, I. Lieberwirth, S. Morsbach, K. Landfester, V. Mailänder, *Nanoscale* **2018**, *10*, 10731–10739.
[206] M. Cristofanilli, "SGT-53, Carboplatin, and Pembrolizumab for the Treatment of Metastatic Triple Negative Inflammatory Breast Cancer," can be found under https://clinicaltrials.gov/ct2/show/NCT05093387, **2022**.
[207] S. Mura, J. Nicolas, P. Couvreur, *Nat. Mater.* **2013**, *12*, 991–1003.
[208] C. I. C. Crucho, *ChemMedChem* **2015**, *10*, 24–38.
[209] M. Kanamala, W. R. Wilson, M. Yang, B. D. Palmer, Z. Wu, *Biomaterials* **2016**, *85*, 152–167.
[210] J. Wen, K. Yang, F. Liu, H. Li, Y. Xu, S. Sun, *Chem. Soc. Rev.* **2017**, *46*, 6024–6045.
[211] T. T. H. Thi, E. J. A. Suys, J. S. Lee, D. H. Nguyen, K. D. Park, N. P. Truong, *Vaccine* **2021**, *9*, 359.
[212] R. Savla, J. Browne, V. Plassat, K. M. Wasan, E. K. Wasan, *Drug Dev. Ind. Pharm.* **2017**, *43*, 1743–1758.
[213] T. M. Allen, P. R. Cullis, *Adv. Drug Delivery Rev.* **2013**, *65*, 36–48.
[214] M. Elsabahy, K. L. Wooley, *Chem. Soc. Rev.* **2012**, *41*, 2545–2561.
[215] N. Rohani, L. Hao, M. S. Alexis, B. A. Joughin, K. Krismer, M. N. Moufarrej, A. R. Soltis, D. A. Lauffenburger, M. B. Yaffe, C. B. Burge, S. N. Bhatia, F. B. Gertler, *Cancer Res.* **2019**, *79*, 1952–1966.
[216] S. Ohkuma, B. Poole, *Proc. Natl. Acad. Sci. USA* **1978**, *75*, 3327–3331.
[217] E. Miele, G. P. Spinelli, E. Miele, F. Tomao, S. Tomao, *Int. J. Nanomed.* **2009**, *4*, 99–105.
[218] D. Belletti, F. Pederzoli, F. Forni, M. A. Vandelli, G. Tosi, B. Ruozi, *Expert Opin. Drug Delivery* **2017**, *14*, 825–840.
[219] L. Schoonen, J. C. M. Van Hest, *Nanoscale* **2014**, *6*, 7124–7141.
[220] J. Neburkova, A. M. Rulseh, S. L. Y. Chang, H. Raabova, J. Vejpravova, M. Dracinsky, J. Tarabek, J. Kotek, M. Pingle, P. Majer, J. Vymazal, P. Cigler, *Nanoscale Adv.* **2020**, *2*, 5567–5571.
[221] M. Manzano, M. Vallet-Regí, M. Manzano, M. Vallet-Regí, *Adv. Funct. Mater.* **2020**, *30*, 1902634.
[222] T. I. Janjua, Y. Cao, C. Yu, A. Popat, *Nat. Rev. Mater.* **2021**, *6*, 1072–1074.
[223] V. Poscher, Y. Salinas, *Materials* **2020**, *13*, 3668.
[224] X. Du, X. Li, L. Xiong, X. Zhang, F. Kleitz, S. Z. Qiao, *Biomaterials* **2016**, *91*, 90–127.
[225] S. Quignard, S. Masse, G. Laurent, T. Coradin, *Chem. Commun.* **2013**, *49*, 3410–3412.
[226] L. Maggini, I. Cabrera, A. Ruiz-Carretero, E. A. Prasetyanto, E. Robinet, L. De Cola, *Nanoscale* **2016**, *8*, 7240–7247.
[227] L. Talamini, P. Picchetti, L. M. Ferreira, G. Sitia, L. Russo, M. B. Violatto, L. Travaglini, J. Fernandez Alarcon, L. Righelli, P. Bigini, L. De Cola, *ACS Nano* **2021**, *15*, 9701–9716.
[228] D. Shao, M. Li, Z. Wang, X. Zheng, Y. H. Lao, Z. Chang, F. Zhang, M. Lu, J. Yue, H. Hu, H. Yan, L. Chen, W. fei Dong, K. W. Leong, *Adv. Mater.* **2018**, *30*, 1801198.
[229] L. Maggini, L. Travaglini, I. Cabrera, P. Castro-Hartmann, L. De Cola, *Chem. Eur. J.* **2016**, *22*, 3697–3703.
[230] J. G. Croissant, Y. Fatieiev, K. Julfakyan, J. Lu, A. H. Emwas, D. H. Anjum, H. Omar, F. Tamanoi, J. I. Zink, N. M. Khashab, *Chem. Eur. J.* **2016**, *22*, 14806–14811.
[231] Z. Gao, S. P. H. Moghaddam, H. Ghandehari, I. Zharov, *RSC Adv.* **2018**, *8*, 4914–4920.
[232] L. Travaglini, P. Picchetti, R. Totovao, E. A. Prasetyanto, L. De Cola, *Mater. Chem. Front.* **2019**, *3*, 111–119.
[233] H. Soo Choi, W. Liu, P. Misra, E. Tanaka, J. P. Zimmer, B. Itty Ipe, M. G. Bawendi, J. V. Frangioni, *Nat. Biotechnol.* **2007**, *25*, 1165–1170.
[234] H. Furukawa, K. E. Cordova, M. O'Keeffe, O. M. Yaghi, *Science* **2013**, *341*, 974.
[235] A. Casini, R. A. Fischer, G. Moreno-Alcántar, *2.22 - Supramolecular metal-based molecules and materials for biomedical applications in Comprehensive Inorganic Chemistry III*, Elsevier, Amsterdam, **2023**, pp. 714–743, https://doi.org/10.1016/B978-0-12-823144-9.00047-9.
[236] P. Horcajada, C. Serre, M. Vallet-Regí, M. Sebban, F. Taulelle, G. Férey, *Angew. Chem. Int. Ed.* **2006**, *45*, 5974–5978; *Angew. Chem.* **2006**, *118*, 6120–6124.
[237] S. Haddad, I. A. Lázaro, M. Fantham, A. Mishra, J. Silvestre-Albero, J. W. M. Osterrieth, G. S. K. Schierle, C. F. Kaminski, R. S. Forgan, D. Fairen-Jimenez, *J. Am. Chem. Soc.* **2020**, *142*, 6661–6674.
[238] A. Sangtani, O. K. Nag, L. D. Field, J. C. Breger, J. B. Delehanty, *Wiley Interdiscip. Rev. Nanomed. Nanobiotechnol.* **2017**, *9*, e1466.
[239] E. K. Lim, T. Kim, S. Paik, S. Haam, Y. M. Huh, K. Lee, *Chem. Rev.* **2015**, *115*, 327–394.
[240] Y. Xue, H. Bai, B. Peng, B. Fang, J. Baell, L. Li, W. Huang, N. H. Voelcker, *Chem. Soc. Rev.* **2021**, *50*, 4872–4931.
[241] J. Zhou, L. Rao, G. Yu, T. R. Cook, X. Chen, F. Huang, *Chem. Soc. Rev.* **2021**, *50*, 2839–2891.
[242] N. Wang, X. Cheng, N. Li, H. Wang, H. Chen, *Adv. Healthcare Mater.* **2019**, *8*, 1801002.
[243] S. Shen, Y. Wu, Y. Liu, D. Wu, *Int. J. Nanomed.* **2017**, *12*, 4085–4109.
[244] R. R. Davis, D. T. Hobbs, R. Khashaba, P. Sehkar, F. N. Seta, R. L. W. Messer, J. B. Lewis, J. C. Wataha, *J. Biomed. Mater. Res. Part A* **2010**, *93*, 864–869.
[245] J. J. Yan, R. W. Y. Sun, P. Wu, M. C. M. Lin, A. S. C. Chan, C. M. Che, *Dalton Trans.* **2010**, *39*, 7700–7705.
[246] M. Nyman, D. T. Hobbs, *Chem. Mater.* **2006**, *18*, 6425–6435.
[247] D. T. Hobbs, R. L. W. Messer, J. B. Lewis, D. R. Click, P. E. Lockwood, J. C. Wataha, *J. Biomed. Mater. Res. Part B* **2006**, *78*, 296–301.
[248] A. E. Nel, L. Mädler, D. Velegol, T. Xia, E. M. V. Hoek, P. Somasundaran, F. Klaessig, V. Castranova, M. Thompson, *Nat. Mater.* **2009**, *8*, 543–557.
[249] R. Singh, J. W. Lillard, *Exp. Mol. Pathol.* **2009**, *86*, 215–223.
[250] S. A. Kulkarni, S. S. Feng, *Pharm. Res.* **2013**, *30*, 2512–2522.
[251] M. Simionescu, D. Popov, A. Sima, *Cell Tissue Res.* **2009**, *335*, 27–40.
[252] P. Lee, R. Zhang, V. Li, X. Liu, R. W. Y. Sun, C. M. Che, K. K. Y. Wong, *Int. J. Nanomed.* **2012**, *7*, 731–737.
[253] P. Ringhieri, R. Iannitti, C. Nardon, R. Palumbo, D. Fregona, G. Morelli, A. Accardo, *Int. J. Pharm.* **2014**, *473*, 194–202.
[254] A. Krishnadas, I. Rubinstein, H. Önyüksel, *Pharm. Res.* **2003**, *20*, 297–302.
[255] L. Baratto, H. Duan, H. Mäcke, A. Iagaru, *J. Nucl. Med.* **2020**, *61*, 792–798.

[256] L. He, T. Chen, Y. You, H. Hu, W. Zheng, W. L. Kwong, T. Zou, C. M. Che, *Angew. Chem. Int. Ed.* **2014**, *53*, 12532–12536; *Angew. Chem.* **2014**, *126*, 12740–12744.
[257] U. K. Marelli, F. Rechenmacher, T. R. A. Sobahi, C. Mas-Moruno, H. Kessler, *Front. Oncol.* **2013**, *3*, 222.
[258] P. Y. Lee, C.-N. Lok, C.-M. Che, W. J. Kao, *Pharm. Res.* **2020**, *37*, 220.
[259] R. W. Y. Sun, M. Zhang, D. Li, Z. F. Zhang, H. Cai, M. Li, Y. J. Xian, S. W. Ng, A. S. T. Wong, *Chem. Eur. J.* **2015**, *21*, 18534–18538.
[260] H. Cai, M. Li, X. R. Lin, W. Chen, G. H. Chen, X. C. Huang, D. Li, *Angew. Chem. Int. Ed.* **2015**, *54*, 10454–10459; *Angew. Chem.* **2015**, *127*, 10600–10605.
[261] J. V. Natarajan, C. Nugraha, X. W. Ng, S. Venkatraman, *J. Controlled Release* **2014**, *193*, 122–138.
[262] Y. X. Lin, Y. J. Gao, Y. Wang, Z. Y. Qiao, G. Fan, S. L. Qiao, R. X. Zhang, L. Wang, H. Wang, *Mol. Pharmaceutics* **2015**, *12*, 2869–2878.
[263] S. A. Smith, L. I. Selby, A. P. R. Johnston, G. K. Such, *Bioconjugate Chem.* **2019**, *30*, 263–272.
[264] G. Ferraro, D. M. Monti, A. Amoresano, N. Pontillo, G. Petruk, F. Pane, M. A. Cinellu, A. Merlino, *Chem. Commun.* **2016**, *52*, 9518–9521.
[265] C. Gabbiani, A. Guerri, M. A. Cinellu, L. Messori, *Open Crystallogr. J.* **2010**, *3*, 29–40.
[266] X. T. Ji, L. Huang, H. Q. Huang, *J. Proteomics* **2012**, *75*, 3145–3157.
[267] M. Truffi, L. Fiandra, L. Sorrentino, M. Monieri, F. Corsi, S. Mazzucchelli, *Pharmacol. Res.* **2016**, *107*, 57–65.
[268] D. M. Monti, G. Ferraro, G. Petruk, L. Maiore, F. Pane, A. Amoresano, M. A. Cinellu, A. Merlino, *Dalton Trans.* **2017**, *46*, 15354–15362.
[269] G. Ferraro, G. Petruk, L. Maiore, F. Pane, A. Amoresano, M. A. Cinellu, D. M. Monti, A. Merlino, *Int. J. Biol. Macromol.* **2018**, *115*, 1116–1121.
[270] J. Zhang, Z. Zhang, M. Jiang, S. Li, H. Yuan, H. Sun, F. Yang, H. Liang, *J. Med. Chem.* **2020**, *63*, 13695–13708.
[271] T. Moos, E. H. Morgan, *Cell. Mol. Neurobiol.* **2000**, *20*, 77–95.
[272] S. J. T. Rezaei, K. Norouzi, A. Hesami, A. M. Malekzadeh, A. Ramazani, V. Amani, R. Ahmadi, *Appl. Organomet. Chem.* **2018**, *32*, e4303.
[273] S. Malekmohammadi, H. Hadadzadeh, Z. Amirghofran, *J. Mol. Liq.* **2018**, *265*, 797–806.
[274] A. C. R. Gonçalves, Z. A. Carneiro, C. G. Oliveira, A. Danuello, W. Guerra, R. J. Oliveira, F. B. Ferreira, L. L. W. Veloso-Silva, F. A. H. Batista, J. C. Borges, S. de Albuquerque, V. M. Deflon, P. I. S. Maia, *Eur. J. Med. Chem.* **2017**, *141*, 615–631.
[275] R. T. C. Silva, L. F. Dalmolin, J. A. Moreto, C. G. Oliveira, A. E. H. Machado, R. F. V. Lopez, P. I. S. Maia, *J. Nanopart. Res.* **2020**, *22*, 339.
[276] J. M. Lü, X. Wang, C. Marin-Muller, H. Wang, P. H. Lin, Q. Yao, C. Chen, *Expert Rev. Mol. Diagn.* **2009**, *9*, 325–341.
[277] A. Menconi, T. Marzo, L. Massai, A. Pratesi, M. Severi, G. Petroni, L. Antonuzzo, L. Messori, S. Pillozzi, D. Cirri, *Biometals* **2021**, *34*, 867–879.
[278] K. D. Freeman-Cook, C. Autry, G. Borzillo, D. Gordon, E. Barbacci-Tobin, V. Bernardo, D. Briere, T. Clark, M. Corbett, J. Jakubczak, S. Kakar, E. Knauth, B. Lippa, M. J. Luzzio, M. Mansour, G. Martinelli, M. Marx, K. Nelson, J. Pandit, F. Rajamohan, S. Robinson, C. Subramanyam, L. Wei, M. Wythes, J. Morris, *J. Med. Chem.* **2010**, *53*, 4615–4622.
[279] S. Yoon, R. Seger, *Growth Factors* **2006**, *24*, 21–44.
[280] P. Astolfi, M. Pisani, E. Giorgini, B. Rossi, A. Damin, F. Vita, O. Francescangeli, L. Luciani, R. Galassi, *Nanomaterials* **2020**, *10*, 1851.
[281] V. Gambini, M. Tilio, E. W. Maina, C. Andreani, C. Bartolacci, J. Wang, M. Iezzi, S. Ferraro, A. T. Ramadori, O. C. Simon, S. Pucciarelli, G. Wu, Q. P. Dou, C. Marchini, R. Galassi, A. Amici, *Eur. J. Med. Chem.* **2018**, *155*, 418–427.
[282] E. Vergara, E. Cerrada, A. Casini, O. Zava, M. Laguna, P. J. Dyson, *Organometallics* **2010**, *29*, 2596–2603.
[283] I. Mármol, P. Castellnou, R. Alvarez, M. C. Gimeno, M. J. Rodríguez-Yoldi, E. Cerrada, *Eur. J. Med. Chem.* **2019**, *183*, 111661.
[284] A. K. Hartmann, S. Gudipati, A. Pettenuzzo, L. Ronconi, J. L. Rouge, *Bioconjugate Chem.* **2020**, *31*, 1063–1069.
[285] J. K. Awino, S. Gudipati, A. K. Hartmann, J. J. Santiana, D. F. Cairns-Gibson, N. Gomez, J. L. Rouge, *J. Am. Chem. Soc.* **2017**, *139*, 6278–6281.
[286] J. Kale, E. J. Osterlund, D. W. Andrews, *Cell Death Differ.* **2018**, *25*, 65–80.
[287] G. Kroemer, *Nat. Med.* **1997**, *3*, 614–620.
[288] J. L. Rouge, L. Hao, X. A. Wu, W. E. Briley, C. A. Mirkin, *ACS Nano* **2014**, *8*, 8837–8843.
[289] M. Pérez Colodrero, K. E. Papathanasiou, A. Sousa, J. F. Santos, F. Silva, S. A. Sousa, J. H. Leitão, A. P. Matos, T. Pinheiro, R. A. L. Silva, D. Belo, M. Almeida, F. Marques, C. Fernandes, *Pharmaceutica* **2023**, *15*, 564.
[290] Y. Marciano, V. Del Solar, N. Nayeem, D. Dave, J. Son, M. Contel, R. V. Ulijn, *J. Am. Chem. Soc.* **2023**, *145*, 234–246.
[291] C. Li, J. Wang, Y. Wang, H. Gao, G. Wei, Y. Huang, H. Yu, Y. Gan, Y. Wang, L. Mei, H. Chen, H. Hu, Z. Zhang, Y. Jin, *Acta Pharm. Sin. B* **2019**, *9*, 1145–1162.
[292] S. Pearson, H. Lu, M. H. Stenzel, *Macromolecules* **2015**, *48*, 1065–1076.
[293] D. J. Keddie, *Chem. Soc. Rev.* **2014**, *43*, 496–505.
[294] M. Ahmed, S. Mamba, X. H. Yang, J. Darkwa, P. Kumar, R. Narain, *Bioconjugate Chem.* **2013**, *24*, 979–986.
[295] C. Y.-S. Chung, S.-K. Fung, K.-C. Tong, P.-K. Wan, C.-N. Lok, Y. Huang, T. Chen, C.-M. Che, *Chem. Sci.* **2017**, *8*, 1942–1953.
[296] D. Bazile, C. Prud'homme, M. Bassoullet, M. Marlard, G. Spenlehauer, M. Veillard, *J. Pharm. Sci.* **1995**, *84*, 493–498.
[297] F. F. Davis, *Adv. Drug Delivery Rev.* **2002**, *54*, 457–458.
[298] H. Maeda, J. Wu, T. Sawa, Y. Matsumura, K. Hori, *J. Controlled Release* **2000**, *65*, 271–284.
[299] X. Wang, J. Wang, J. Wang, Y. Zhong, L. Han, J. Yan, P. Duan, B. Shi, F. Bai, *Nano Lett.* **2021**, *21*, 3418–3425.
[300] I. Pysz, P. J. M. Jackson, D. E. Thurston, in *Cytotoxic Payloads Antib. – Drug Conjug.*, The Royal Society Of Chemistry, Cambridge, **2019**, https://doi.org/10.1039/9781788012898-00001.
[301] J. Feld, S. K. Barta, C. Schinke, I. Braunschweig, Y. Zhou, A. K. Verma, *Oncotarget* **2013**, *4*, 397–412.
[302] M. Liu, Z. J. Lim, Y. Y. Gwee, A. Levina, P. A. Lay, *Angew. Chem. Int. Ed.* **2010**, *49*, 1661–1664; *Angew. Chem.* **2010**, *122*, 1705–1708.
[303] A. Wunder, G. Stehle, H. Sinn, H. H. Schrenk, D. Hoff-Biederbeck, F. Bader, E. A. Friedrich, P. Peschke, W. Maier-Borst, D. L. Heene, *Int. J. Oncol.* **1997**, *11*, 497–507.
[304] M. H. S. Segler, T. Kogej, C. Tyrchan, M. P. Waller, *ACS Cent. Sci.* **2018**, *4*, 120–131.
[305] F. Gentile, J. C. Yaacoub, J. Gleave, M. Fernandez, A. T. Ton, F. Ban, A. Stern, A. Cherkasov, *Nat. Protoc.* **2022**, *17*, 672–697.
[306] M. Alavi, A. Nokhodchi, *Crit. Rev. Ther. Drug Carrier Syst.* **2020**, *37*, 591–611.
[307] Q. Gu, J. Z. Xing, M. Huang, X. Zhang, J. Chen, *J. Biomater. Appl.* **2013**, *28*, 298–307.
[308] A. Bertucci, E. A. Prasetyanto, D. Septiadi, A. Manicardi, E. Brognara, R. Gambari, R. Corradini, L. De Cola, *Small* **2015**, *11*, 5687–5695.

[309] A. Salvati, A. S. Pitek, M. P. Monopoli, K. Prapainop, F. B. Bombelli, D. R. Hristov, P. M. Kelly, C. Åberg, E. Mahon, K. A. Dawson, *Nat. Nanotechnol.* **2013**, *8*, 137–143.
[310] K. E. Wheeler, A. J. Chetwynd, K. M. Fahy, B. S. Hong, J. A. Tochihuitl, L. A. Foster, I. Lynch, *Nat. Nanotechnol.* **2021**, *16*, 617–629.
[311] S. Wilhelm, A. J. Tavares, Q. Dai, S. Ohta, J. Audet, H. F. Dvorak, W. C. W. Chan, *Nat. Rev. Mater.* **2016**, *1*, 16014.
[312] D. Walczyk, F. B. Bombelli, M. P. Monopoli, I. Lynch, K. A. Dawson, *J. Am. Chem. Soc.* **2010**, *132*, 5761–5768.
[313] W. Humphrey, A. Dalke, K. Schulten, *J. Mol. Graphics* **1996**, *14*, 33–38.
[314] C. F. MacRae, I. Sovago, S. J. Cottrell, P. T. A. Galek, P. McCabe, E. Pidcock, M. Platings, G. P. Shields, J. S. Stevens, M. Towler, P. A. Wood, *J. Appl. Crystallogr.* **2020**, *53*, 226–235.

Manuscript received: December 19, 2022
Accepted manuscript online: February 27, 2023
Version of record online: March 15, 2023